AGU100 ADVANCING EARTH AND SPACE SCIENCE

Reviews of Geophysics

REVIEW ARTICLE
10.1029/2019RG000670

**Key Points:**
- Ozone dry deposition through pathways other than plant stomata is critical for describing the total terrestrial ozone sink
- Process-level knowledge of ozone deposition pathways is missing from the models used to quantify deposition impacts on the Earth system
- Long-term ozone flux and related measurements are key for establishing relative importance of individual pathways

**Correspondence to:**
O. E. Clifton,
oclifton@ucar.edu

**Citation:**
Clifton, O. E., Fiore, A. M., Massman, W. J., Baublitz, C. B., Coyle, M., Emberson, L., et al. (2020). Dry deposition of ozone over land: processes, measurement, and modeling. *Reviews of Geophysics*, *58*, e2019RG000670. https://doi.org/10.1029/2019RG000670

Received 24 OCT 2019
Accepted 24 JAN 2020
Accepted article online 3 FEB 2020



# Dry Deposition of Ozone Over Land: Processes, Measurement, and Modeling

**Olivia E. Clifton[1], Arlene M. Fiore[2], William J. Massman[3], Colleen B. Baublitz[2], Mhairi Coyle[4,5], Lisa Emberson[6], Silvano Fares[7], Delphine K. Farmer[8], Pierre Gentine[9], Giacomo Gerosa[10], Alex B. Guenther[11], Detlev Helmig[12], Danica L. Lombardozzi[1], J. William Munger[13], Edward G. Patton[1], Sally E. Pusede[14], Donna B. Schwede[15], Sam J. Silva[16], Matthias Sörgel[17], Allison L. Steiner[18], and Amos P. K. Tai[19]**

[1]National Center for Atmospheric Research, Boulder, CO, USA, [2]Department of Earth and Environmental Sciences, Columbia University, New York, NY, USA and Lamont-Doherty Earth Observatory of Columbia University, Palisades, NY, USA, [3]USDA Forest Service, Rocky Mountain Research Station, Fort Collins, CO, USA, [4]United Kingdom Centre for Ecology and Hydrology, Edinburgh, Midlothian, UK, [5]The James Hutton Institute, Aberdeen, UK, [6]Stockholm Environment Institute, Environment Department, University of York, York, UK, [7]Council of Agricultural Research and Economics, Research Centre for Forestry and Wood, and National Research Council, Institute of Bioeconomy, Rome, Italy, [8]Department of Chemistry, Colorado State University, Fort Collins, CO, USA, [9]Department of Earth and Environmental Engineering, Columbia University, New York, NY, USA, [10]Dipartimento di Matematica e Fisica, Università Cattolica del Sacro Cuore, Brescia, Italy, [11]Department of Earth System Science, University of California, Irvine, CA, USA, [12]Institute of Alpine and Arctic Research, University of Colorado Boulder, Boulder, CO, USA, [13]School of Engineering and Applied Sciences and Department of Earth and Planetary Sciences, Harvard University, Cambridge, MA, USA, [14]Department of Environmental Sciences, University of Virginia, Charlottesville, VA, USA, [15]U.S. Environmental Protection Agency, National Exposure Research Laboratory, Research Triangle Park, NC, USA, [16]Department of Civil and Environmental Engineering, Massachusetts Institute of Technology, Cambridge, MA, USA, [17]Atmospheric Chemistry Department, Max Plank Institute for Chemistry, Mainz, Germany, [18]Department of Atmospheric, Oceanic and Space Sciences, University of Michigan, Ann Arbor, MI, USA, [19]Earth System Science Programme, Faculty of Science, and State Key Laboratory of Agrobiotechnology, The Chinese University of Hong Kong, Hong Kong

**Abstract** Dry deposition of ozone is an important sink of ozone in near-surface air. When dry deposition occurs through plant stomata, ozone can injure the plant, altering water and carbon cycling and reducing crop yields. Quantifying both stomatal and nonstomatal uptake accurately is relevant for understanding ozone's impact on human health as an air pollutant and on climate as a potent short-lived greenhouse gas and primary control on the removal of several reactive greenhouse gases and air pollutants. Robust ozone dry deposition estimates require knowledge of the relative importance of individual deposition pathways, but spatiotemporal variability in nonstomatal deposition is poorly understood. Here we integrate understanding of ozone deposition processes by synthesizing research from fields such as atmospheric chemistry, ecology, and meteorology. We critically review methods for measurements and modeling, highlighting the empiricism that underpins modeling and thus the interpretation of observations. Our unprecedented synthesis of knowledge on deposition pathways, particularly soil and leaf cuticles, reveals process understanding not yet included in widely used models. If coordinated with short-term field intensives, laboratory studies, and mechanistic modeling, measurements from a few long-term sites would bridge the molecular to ecosystem scales necessary to establish the relative importance of individual deposition pathways and the extent to which they vary in space and time. Our recommended approaches seek to close knowledge gaps that currently limit quantifying the impact of ozone dry deposition on air quality, ecosystems, and climate.

**Plain Language Summary** The removal of tropospheric ozone at Earth's surface (often called dry deposition) is important for our understanding of air pollution, ecosystem health, and climate. Several processes contribute to dry deposition of ozone. While we have basic knowledge of these processes, we lack the ability to robustly estimate changes in ozone dry deposition through time and from one place to another. Here we review ozone deposition processes, measurements, and modeling and propose steps necessary to close gaps in understanding. A major conclusion revealed by our review is that most deposition processes can be fairly well described from a theoretical standpoint, but the relative importance of the various processes remains uncertain. We suggest that progress can be made by establishing multiyear measurements

of ozone dry deposition at a limited set of sites around the world and coordinating these measurements with laboratory and field experiments that can be integrated with theory through carefully designed modeling studies.

## 1. Introduction

Dry deposition, or removal at the Earth's surface, is a primary sink of ozone in the troposphere where ozone is an air pollutant, greenhouse gas, and central to the atmospheric oxidative capacity. Ozone dry deposition occurring through plant stomata (the pores on leaves controlling gas exchange) damages plants. While the potential for ozone dry deposition to influence air quality, ecosystems, and crop yields has been recognized for decades (e.g., Hosker & Lindberg, 1982; Reich, 1987; Rich, 1964; Turner et al., 1973), mechanistic understanding of ozone dry deposition is incomplete. Figure 1 illustrates processes contributing to ozone dry deposition and how changes in ozone dry deposition impact tropospheric chemistry, air quality, ecosystems, and climate. In this review, we synthesize knowledge of controlling processes, review measurement and modeling approaches, and recommend approaches to close knowledge gaps.

To undergo dry deposition, atmospheric turbulence transports ozone close to a given surface and then ozone must move through the quasi-laminar boundary layer around that surface. The rate of ozone uptake by a particular surface depends on the surface's properties. Ozone dry deposition occurs not only through stomatal uptake (Rich et al., 1970) but also through other nonstomatal deposition pathways including uptake by leaf cuticles (Rondón et al., 1993; S. Sun, Moravek, Trebs, et al., 2016), soil (Garland & Penkett, 1976; Turner et al., 1974), snow (Helmig, Bocquet, et al., 2007; Helmig, Ganzeveld, et al., 2007), water (Gallagher et al., 2001; Helmig et al., 2012), and man-made surfaces (Shen & Gao, 2018). Both surfaces with high-destruction rates (e.g., vegetation) and spatially extensive surfaces with low destruction rates (e.g., snow and water) are relevant to the tropospheric ozone budget and large-scale ozone pollution (Clifton, 2018; Ganzeveld et al., 2009; Hardacre et al., 2015; Helmig, Ganzeveld, et al., 2007).

Quantifying stomatal ozone uptake is not only important for estimating ozone removal but also for understanding the plant response to ozone. Stomatal ozone uptake injures plants by generating reactive oxygen species that can induce cell death and lesions and thus accelerate senescence (Ainsworth et al., 2012; Fiscus et al., 2005). Reactive oxygen species also impair photosynthetic enzyme activities, enhance respiration, and interfere with carbon allocation (Ainsworth et al., 2012; Fiscus et al., 2005). Ozone injury to plants alters terrestrial carbon and water cycling (Arnold et al., 2018; Franz et al., 2017; Hoshika et al., 2015; Lombardozzi et al., 2015; Oliver et al., 2018; Sadiq et al., 2017; G. Sun et al., 2012; Yue & Unger, 2014), which influences boundary-layer meteorology (J. Li et al., 2016, Li, Mahalov, et al., 2018; Sadiq et al., 2017; Super et al., 2015) and climate (Kvalevåg & Myhre, 2013; Sitch et al., 2007) and increases surface ozone due to a reduced stomatal ozone sink (J. Li et al., 2016, Li, Mahalov, & Hyde, 2018; Sadiq et al., 2017; S. S. Zhou et al., 2018).

Numerical simulations of tropospheric ozone, including high ozone pollution episodes and background ozone levels, are sensitive to model descriptions of ozone dry deposition (Anav et al., 2018; Beddows et al., 2017; Bela et al., 2015; Campbell et al., 2019; Clifton, 2018; Emberson et al., 2013; Falk & Søvde Haslerud, 2019; Helmig, Ganzeveld, et al., 2007; Hogrefe et al., 2018; Huang et al., 2016; J.-T. Lin et al., 2008; M. Lin et al., 2017, 2019; Matichuk et al., 2017; Silva & Heald, 2018; Solberg et al., 2008; Tang et al., 2011; Val Martin et al., 2014; Vautard et al., 2005; Vieno et al., 2010; Walker, 2014; Wild, 2007; A. Y. H. Wong et al., 2019). However, many widely used ozone dry deposition schemes do not represent processes mechanistically or capture observed spatiotemporal variations (Clifton et al., 2017; Kavassalis & Murphy, 2017; Pleim & Ran, 2011; Silva et al., 2019; Silva & Heald, 2018; Travis & Jacob, 2019). Among models, differences are twofold to threefold in estimates of ozone dry deposition for a given location (Hardacre et al., 2015; Schwede et al., 2011; Z. Wu et al., 2018; A. Y. H. Wong et al., 2019) and in estimates of the global annual tropospheric ozone loss through dry deposition (Hardacre et al., 2015; Stevenson et al., 2006; Wild, 2007; Young et al., 2013, 2018). Understanding of the contribution of individual deposition pathways to ozone dry deposition is incomplete but key for building mechanistic representation in the large-scale models used to quantify the effects of ozone dry deposition across Earth systems from hourly to centennial time scales.

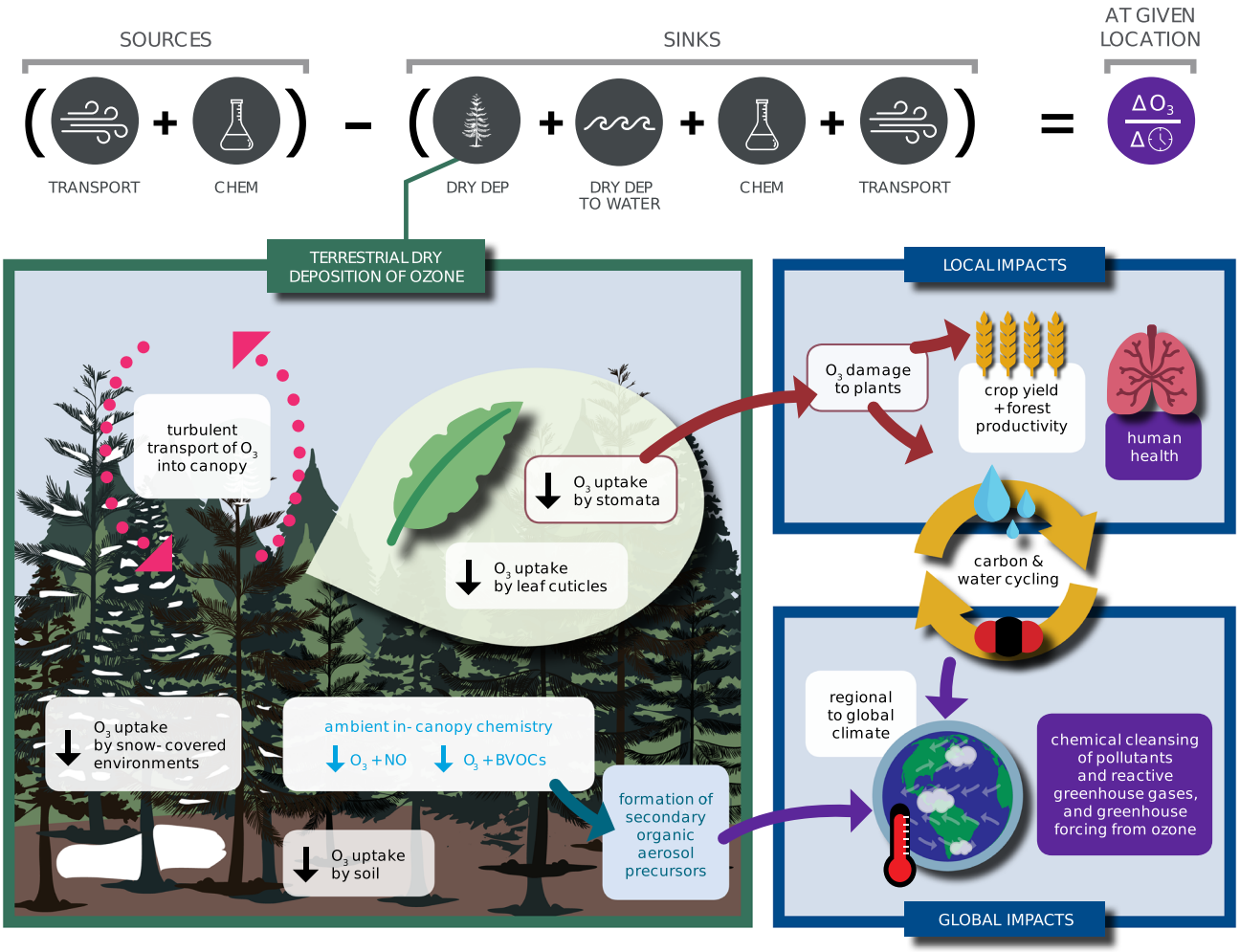


**Figure 1.** Processes contributing and related to terrestrial ozone dry deposition and its impacts on tropospheric chemistry, air pollution, ecosystems, and climate, both directly (red and blue arrows) and indirectly (purple boxes and arrows; e.g., through changes in tropospheric ozone). Yellow arrows indicate that carbon and water cycling connect the local impact of ozone plant damage to global impacts on climate. Processes included on the left-hand panel in white boxes are reviewed in this paper; downward black arrows represent ozone deposition pathways. Figure illustrated by Simmi Sinha.

Below, we address the following questions:

1. What approaches are currently used to measure and model ozone dry deposition?
2. What is current understanding of the processes controlling ozone dry deposition based on theory, observations, and modeling?
3. What major knowledge gaps and uncertainties exist with respect to (1) and (2)?
4. How can we most rapidly advance knowledge of ozone dry deposition and its impacts on air quality, vegetation, and climate?

We examine stomatal, leaf cuticular, soil, and snow deposition pathways, as well as turbulent transport and fast ozone loss through ambient chemistry. Not only is fast chemistry important for building understanding of ozone dry deposition from ozone flux measurements, but it also leads to formation of secondary aerosol precursors (e.g., Bouvier-Brown et al., 2009; Kurpius & Goldstein, 2003). To limit the scope of our review, we do not cover transport through the quasi-laminar boundary layer adjacent to surfaces. However, the magnitude of quasi-laminar transport can widely vary among model parameterizations, and thus, uncertainty in this process may be nonnegligible (e.g., Brutsaert, 1979; Massman, 1999, 2004; Schuepp, 1993). Differences across models (e.g., Choudhury & Monteith, 1988; Jensen & Hummelshøj, 1995, 1997; Massman, 1999; Wesely & Hicks, 1977), the impacts of canopy structure, turbulence, and leaf properties (e.g.,

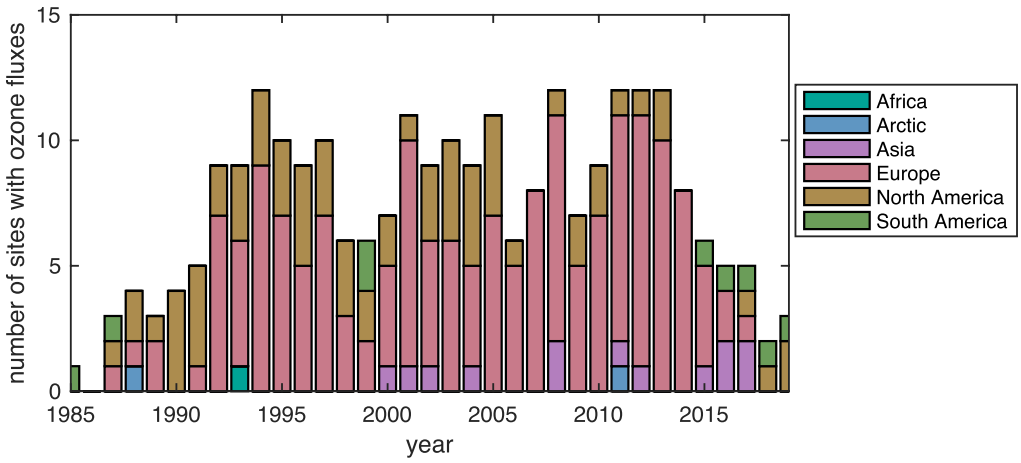


**Figure 2.** No growth in the number of sites that measure ozone fluxes since the mid-1990s as shown by the number of sites per year with ozone flux measurements from 1985 to 2019. Table A1 in Appendix A contains the full list of ozone flux data sets and relevant details. In brief, included data sets are for terrestrial surfaces and represent the ecosystem scale (both flux gradient and eddy covariance fluxes). Not all data sets reported are in the peer-reviewed literature, some are included following personal communication. Most sites included do not have a full year of data for a given year (e.g., 57 out of 114 sites have two months of data or less). Very low numbers after 2014 may reflect the time needed to report and analyze data.

aerodynamics, morphology, and presence of water) on transport (e.g., Cook & Viskanta, 1968; Daudet et al., 1999; Stokes et al., 2006), and scaling from leaf to canopy should be emphasized in future research. While in this review we discuss the deposition pathways considered to be most important for terrestrial ozone dry deposition impacts on tropospheric chemistry, air quality, and vegetation, we emphasize that better understanding of ozone dry deposition to other terrestrial surfaces, such as urban surfaces, lakes, rivers, branches, and leaf litter, is needed.

## 2. Measuring Ozone Dry Deposition

### 2.1. History of Measurements and Survey of Current Data Sets

Methods for field measurement of ozone dry deposition have been available since the 1950s (e.g., Regener, 1957). In the 1950s and 1960s, ozone dry deposition was typically measured using gradient methods during short campaigns (e.g., Galbally, 1971). By the 1970s, the eddy covariance (EC) approach—the preferred approach for measuring turbulent fluxes (Hicks et al., 1989; Meyers & Baldocchi, 2005)—became possible with fast ozone analyzers deployed on masts and towers (e.g., Wesely et al., 1978) and aircraft (e.g., Lenschow et al., 1980). Growing recognition of the importance of biogeochemical cycles led to workshops in the late 1970s and 1980s recommending research priorities for fluxes of ozone, carbon dioxide, and other constituents (Georgii, 1989; Hicks et al., 1980; Hosker & Lindberg, 1982; Lenschow & Hicks, 1989). In particular, a 1987 workshop on trace gas and particle fluxes recommended that future studies "span both diurnal and seasonal cycles" and investigate "surfaces of importance to global budgets" (Lenschow & Hicks, 1989).

Likely as the result of momentum in the research community and support from funding agencies, the number of sites with ecosystem-scale ozone fluxes increased from the late 1980s into the next decade (Figure 2). The first annual record of continuous hourly ozone and carbon dioxide EC fluxes began in the early 1990s at Harvard Forest in the northeastern United States (Munger et al., 1996; Wofsy et al., 1993). However, emphasis on ozone dry deposition in the community waned around the millennium, as evident from stabilizing number of sites with measurements after the mid-1990s (very low numbers after 2014 may reflect the time needed to report and analyze data).

Sites with ozone fluxes primarily reside in Europe and North America (Figure 2), indicating a paucity of knowledge on ozone dry deposition for most parts of the world. More consistent emphasis on ozone fluxes in Europe (Figure 2) may reflect regional initiatives to quantify the impact of ozone on ecosystems. While the observational record captures a variety of land use/land cover (LULC) types, most data are for crops and

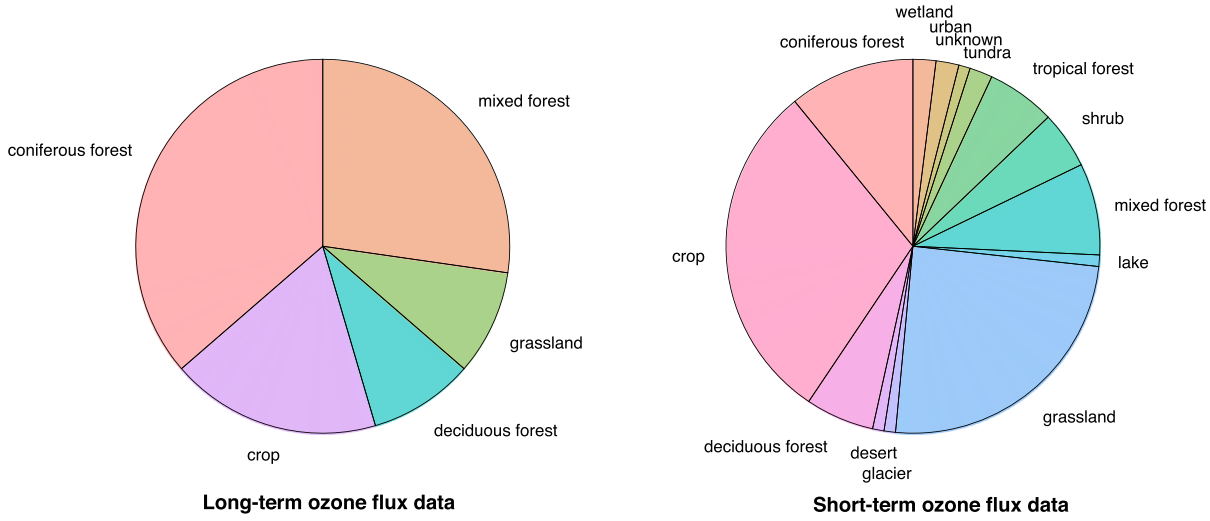


**Figure 3.** Land use/land cover types represented in ozone flux data sets. Long-term data are defined as more than 5 years of annual records. Table A1 contains the full list of data sets.

forests (Figure 3), and the data sets for particularly undersampled LULC types tend to be very short term (i.e., days) (Table A1 in Appendix A).

Advancing understanding of ozone dry deposition requires synthesizing knowledge and testing hypotheses across ozone flux data sets. However, current knowledge does not reflect a meta-analysis of all, or even the majority, of data sets in Table A1. While Table A1 provides a record for future studies to identify potentially available ozone flux data, the lack of a central archive limits efforts to analyze multiple records. Differences in instrumentation, a lack of coordinated protocols across data sets, and in some cases missing complementary measurements also limit the utility of older data and meaningful syntheses across records.

Despite the common emphasis in the 1970s and 1980s on the need to establish long-term flux observations for gases like ozone and carbon dioxide, ozone flux data lag far behind carbon dioxide flux data in the number, data set length, and diversity of sites. Carbon dioxide fluxes are available for around 900 sites for over 7,000 combined site years of data, including many sites with more than a decade of data (Chu et al., 2017). In contrast, only 114 sites have ozone fluxes, only 11 sites have more than 5 years of data, and none exceed 15 years (Table A1). There are likely different needs in terms of carbon dioxide versus ozone flux data, but gaining a robust understanding of interannual variability and trends in ozone dry deposition and accurately interpreting the observational anomalies challenging current understanding require long-term data. The recent National Academies of Sciences, Engineering, and Medicine (NASEM, 2016) report on *The Future of Atmospheric Chemistry Research* also emphasizes the need for long-term fluxes of reactive gases and aerosols.

One issue impeding ozone EC measurements is the fast ozone analyzers meeting the stringent criteria of the EC technique are generally resource intensive to operate. The lack of simple reliable analyzers may in part explain why ozone EC measurements have been limited to research groups with atmospheric chemistry and physics expertise while the ecological community widely adopted carbon dioxide EC, catalyzing the development of a larger network. Motivating the development of new measurement techniques and an observational network is also challenging for an interdisciplinary subject such as ozone dry deposition.

A misconception that the mechanisms controlling ozone dry deposition are well understood may have also contributed to ozone flux measurements losing luster. While the literature widely states that stomatal uptake governs ozone dry deposition over physiologically active vegetation (e.g., Baldocchi et al., 1987; Bauer et al., 2000; Erisman et al., 1994; Mills et al., 2018; Potier et al., 2015), observationally based estimates of the stomatal fraction of ozone dry deposition show a codominant role for deposition through nonstomatal pathways (Figure 4) with stomatal uptake as 45% of the total on average.

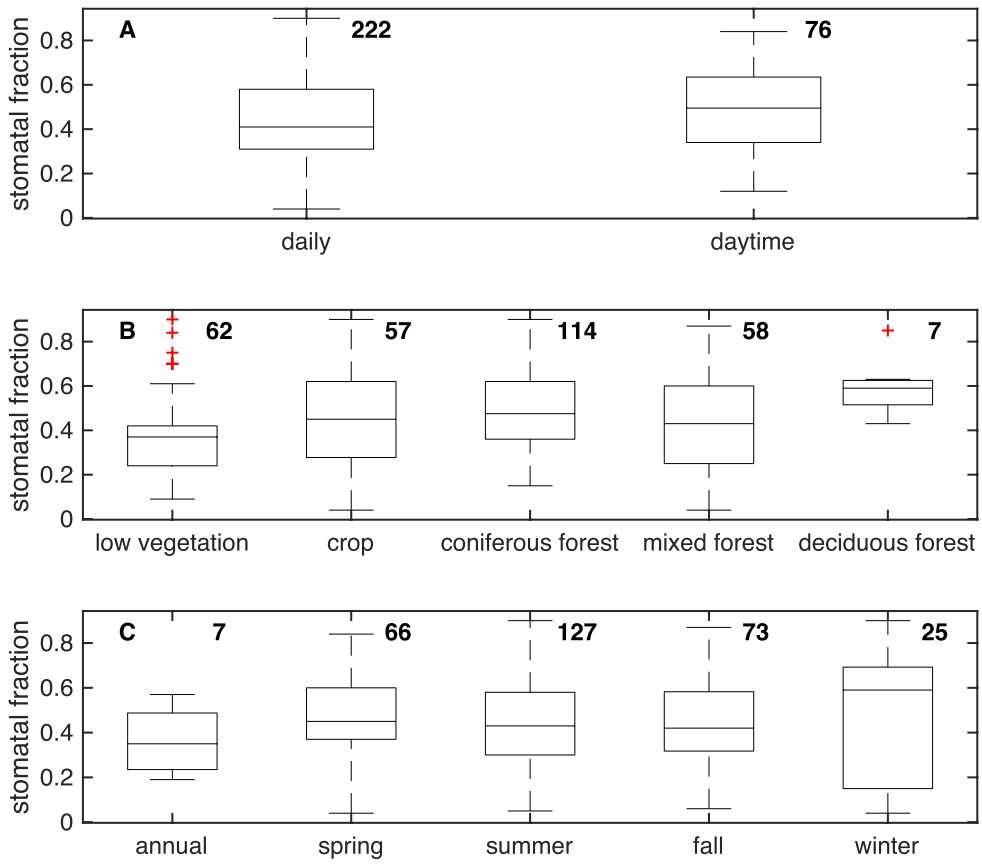


**Figure 4.** The stomatal fraction of ozone dry deposition aggregated from estimates from field sites in previous literature. The number of data points in each composite is to the right of the respective box and whiskers plot. Not all data sets reporting spring, summer, fall, or winter stomatal fraction estimates provide an annual estimate, and thus, the annual estimate is lower than the estimate for each season. The bottom of the box is the 25th percentile of the data, middle is the median, and the top is the 75th percentile. The error bars indicate maximum and minimum values not considering outliers (red symbols). Outliers are defined as values >1.5× the interquartile range of the 25th to 75th percentiles. Sites and references included are Auchencorth Moss (Fowler et al., 2001), Bergamo (Gerosa et al., 2003), Bily Kriz (Juráň et al., 2019; Zapletal et al., 2011), Blodgett Forest (Ducker et al., 2018; Fares, McKay, et al., 2010; Goldstein, 2003; Kurpius & Goldstein, 2003), Bondville (L. Zhang et al., 2006), Braunscheig (Mészáros, Horváth, et al., 2009), Bugacpuszta (Horváth et al., 2017), Burriana (Cieslik, 2004), Cadenazzo (Bassin et al., 2004), Cala Violina (Cieslik, 2009), Camp Borden (Fuentes et al., 1992), Castelporziano (Cieslik, 2004, 2009; Gerosa et al., 2005; Gerosa, Finco, Mereu, Vitale, et al., 2009,Gerosa, Finco, Mereu, Marzuoli, et al., 2009; Fares et al., 2014; Hoshika et al., 2017; Savi & Fares, 2014), California Ozone Deposition Experiment cotton (Grantz et al., 1997), California Ozone Deposition Experiment vineyard (Grantz et al., 1995), Comun Nuovo (Bassin et al., 2004; Cieslik, 2009), Cuatro Vientos (Cieslik, 2004), Diepoholz (El-Madany et al., 2017), Flanders (Neirynck et al., 2012), Gilchriston Farm (Coyle et al., 2009), GLEES Brooklyn Lake (Zeller & Nikolov, 2000), Grignon (Stella, Personne, et al., 2011; Stella et al., 2013), Hartheim (Joss & Graber, 1996), Harvard Forest (Clifton et al., 2017; Ducker et al., 2018), Hyytiälä (Altimir et al., 2006; Ducker et al., 2018; Launiainen et al., 2013; Rannik et al., 2012; P. T. Zhou et al., 2017), Ispra (Cieslik, 2004), Kaamanen (Tuovinen et al., 1998), Kane Experimental Forest (L. Zhang et al., 2006), Klippeneck (Cieslik, 2004), Kranzberger Forst (Nunn et al., 2010), La Cape Sud (Stella, Personne, et al., 2011), Le Dézert (Cieslik, 2004), Les Landes (Lamaud et al., 2002), Lincove (Fares et al., 2012), Lochristi (Zona et al., 2014), Central Plains Experimental Range (Massman, 1993), Nashville (L. Zhang et al., 2006), Niwot Ridge (Turnipseed et al., 2009), Polder Piloto de Sarazola (Pio et al., 2000), Ramat Hanadiv Nature Park (Q. Li, Gabay, et al., 2018), Rhineland-Palatinate (Plake, Stella, et al., 2015), Rivox (Coe et al., 1995), S. Pietro Capofiume (Cieslik, 2004, 2009), San Rossore (Hoshika et al., 2017), Sand Flats State Forest (L. Zhang et al., 2006), Sand Mountain (L. Zhang et al., 2006), Sinderhoeve (Van Pul & Jacobs, 1994), Speulderbos (Dorsey et al., 2004), Ulborg (Mikkelsen et al., 2004), UMBS Prophet (Hogg, 2007; Hogg et al., 2007), Viols-en-Laval (Cieslik, 2004), and Voghera (Cieslik, 2004, 2009; Gerosa et al., 2007).

Not only is nonstomatal uptake nonnegligible, but it is also highly variable. Observationally based studies illustrate unexpected variations in nonstomatal deposition in diel cycles (Coe et al., 1995; Rondón et al., 1993) including over soil and snow (Fumagalli et al., 2016; Helmig, Cohen, et al., 2009; Stella, Loubet,

et al., 2011; Stella et al., 2019), year-to-year variability (Clifton et al., 2017; Rannik et al., 2012), after rain and dew (Fuentes et al., 1992; Potier et al., 2015), and spatially (Clifton et al., 2019; Godowitch, 1990; Lenschow et al., 1981; Mahrt et al., 1995; Wolfe et al., 2015). Measurements also show that ambient chemistry with unmeasured biogenic volatile organic compounds (BVOCs) influences ozone flux observations (Goldstein et al., 2004; Kurpius & Goldstein, 2003; Wolfe et al., 2011).

Unconstrained variations in ozone dry deposition challenge the ability to attribute changes in tropospheric ozone to other processes (e.g., sources) accurately. Capturing unexpected variability with ozone flux records allows the community to build hypotheses about controlling processes, target laboratory and field measurements (Altimir et al., 2006; Fuentes & Gillespie, 1992; Fumagalli et al., 2016; Pleijel et al., 1995; Potier et al., 2017; S. Sun, Moravek, Trebs, et al., 2016; S. Sun, Moravek, von der Heyden, et al., 2016) and build mechanistic models (e.g., Potier et al., 2015).

Mechanistic modeling is fundamental for interpreting observed ozone fluxes because the ozone flux integrates many different processes, and techniques to isolate individual processes are limited. For example, isolating nonstomatal deposition and fast in-canopy chemistry from the ozone flux strongly relies on residual analysis, leading to uncertainty in variations and the relative importance of a given process. Together with the statistical power provided by long-term data, mechanistic modeling also informs ozone dry deposition schemes, which currently rely on poorly constrained empirical relationships (e.g., Tuovinen et al., 2004; Wesely, 1989; L. Zhang et al., 2002).

### 2.2. Measurement Techniques

Here we review approaches for measuring ozone dry deposition. We discuss EC, flux gradient, modified Bowen Ratio, chamber, and isotopic methods. We detail the fast ozone analyzers needed for EC because their cost, maintenance requirements, and limited availability may thwart efforts to measure dry deposition through ozone EC, the most fundamental and direct method for measuring turbulent exchange (e.g., Hicks et al., 1989; Meyers & Baldocchi, 2005).

#### 2.2.1. Micrometeorological Approaches

We start with the Reynolds-averaged mass continuity equation for ozone at a given location under turbulent conditions (e.g., Stull, 1988) to elucidate the strengths and limitations of a vertical turbulent ozone flux measurement representing ozone dry deposition.

$$\frac{\partial \overline{O_3}}{\partial t} = -\left(\overline{u}\frac{\partial \overline{O_3}}{\partial x} + \overline{v}\frac{\partial \overline{O_3}}{\partial y} + \overline{w}\frac{\partial \overline{O_3}}{\partial z}\right) - \left(\frac{\partial \overline{u' O_3'}}{\partial x} + \frac{\partial \overline{v' O_3'}}{\partial y} + \frac{\partial \overline{w' O_3'}}{\partial z}\right) + \overline{P}_{O_3} - \overline{L}_{O_3} - \overline{Dep}_{O_3}. \quad (1)$$

$\overline{O_3}$ is ozone concentration; $u$, $v$, and $w$ are wind velocity in longitudinal ($x$), lateral ($y$), and vertical ($z$) directions; $\overline{P}_{O_3}$ is chemical production of ozone; $\overline{L}_{O_3}$ is chemical loss of ozone; and $\overline{Dep}_{O_3}$ is dry deposition of ozone. Overbars represent temporal averages, and primes represent fluctuations from the temporal average.

In the absence of both subsidence ($\overline{w} = 0$) and horizontal advection of ozone $\left(\overline{u}\frac{\partial \overline{O_3}}{\partial x} = \overline{v}\frac{\partial \overline{O_3}}{\partial y} = 0\right)$, equation (1) simplifies to

$$\frac{\partial \overline{O_3}}{\partial t} = -\frac{\partial F_{O_{3,z}}}{\partial z} + \overline{P}_{O_3} - \overline{L}_{O_3} - \overline{Dep}_{O_3}. \quad (2)$$

We now refer to the vertical turbulent flux of ozone ($\overline{w'O_3'}$) as $F_{O_3,z}$. Integrating equation (2) from the ground to the height of measurement ($h$) yields

$$\int_0^h \frac{\partial \overline{O_3}}{\partial t} dz = -\int_0^h \frac{\partial F_{O_{3,z}}}{\partial z} dz + \int_0^h \overline{P}_{O_3} dz - \int_0^h \overline{L}_{O_3} dz - \int_0^h \overline{Dep}_{O_3} dz, \quad (3)$$

where

$$\int_0^h \frac{\partial F_{O_{3,z}}}{\partial z} dz = F^h{}_{O_3,z} - F^0{}_{O_3,z}.$$

$F^h{}_{O_3,z}$ represents the ozone flux at $h$, and $F^0{}_{O_3,z}$ represents ozone flux at the ground. The community frequently assumes that $F^h{}_{O_3,z}$ represents ozone dry deposition beneath $h$:

$$F^h{}_{O_3,z} = F^0{}_{O_3,z} - \int_0^h \overline{Dep}_{O_3} dz. \quad (4)$$

For this assumption to be valid, equation (3) demonstrates two additional conditions need to be satisfied (or the contributions from each term quantified adequately).

The first condition is negligible ambient ozone chemistry below $h$ $\left(\int_0^h \overline{P}_{O_3} dz = \int_0^h \overline{L}_{O_3} dz = 0\right)$. This is not always true; we further discuss this in section 4.5.

The second condition is stationary ozone concentration on the time frame of the averaging operator $\left(\int_0^h \frac{\partial \overline{O_3}}{\partial t} dz = 0\right)$. Storage, or ozone temporarily accumulating within the canopy (i.e., between the ground surface and $h$), violates this condition. Estimating storage requires ozone concentration measurements at different heights in the canopy (the number of heights needed depends on how much ozone changes vertically). An assumption inherent to using one concentration profile is that the location represents the ecosystem sampled by the vertical turbulent flux measurement. This assumption has been shown to be limited for carbon dioxide (e.g., Nicolini et al., 2018).

Storage is considered to be nonnegligible in forest canopies. Not many studies give estimates of ozone storage, but storage tends to overestimate ozone dry deposition in forests during morning and underestimate during evening, with the influence averaging out over a day (e.g., Finco et al., 2018; Munger et al., 1996; Rummel et al., 2007). Specifically, the bias is <20% at Harvard Forest (Munger et al., 1996) and Bosco Fontana in Italy (Finco et al., 2018) but may be ~50% at a tropical forest in Reserva Biológica Jarú (Rummel et al., 2007).

#### 2.2.1.1. Eddy Covariance

Ozone EC systems are usually custom built by research groups and require atmospheric chemistry and physics expertise (e.g., Weinheimer, 2006). Because there is no formal recipe for their design, we present necessary considerations for ozone and refer the reader to previous reviews on EC (e.g., Aubinet et al., 2012; Lee et al., 2004).

A first consideration is to measure the vertical wind velocity and ozone concentration at a frequency high enough to resolve the full range of eddies contributing to vertical transport. In particular, the ozone analyzer has to be sufficiently accurate to resolve concentration variability due to turbulence (10–60 Hz) but also ambient chemistry, which may require a faster measurement. Instrument frequency responses can be evaluated by comparing spectra and cospectra for ozone with those for heat and momentum. Derivation of transfer functions based on the cospectra enables correction for any loss of high-frequency contributions (e.g., Aubinet et al., 2012; Lee et al., 2004).

Current ozone analyzers used for EC are based on chemiluminescence, or light production via chemical reaction, due to their fast response times. While there is a method to correct ozone fluxes measured with an ultraviolet (UV) photometric ozone analyzer, the empirical correction is large, and random uncertainty in the daytime ozone flux is 60% (Wohlfahrt, Hörtnagl, et al., 2009). Reported frequency response corrections from fast ozone analyzers typically range from 5% to 30% (Bauer et al., 2000; Keronen et al., 2003; Horváth et al., 2017; Munger et al., 1996; Plake, Stella, et al., 2015; Zhu et al., 2015).

A second consideration is that duration of the averaging interval must be long enough to sample the slowest turbulent eddies contributing to exchange but short enough that ozone concentration remains stationary. Sampling or random error may be an important contribution to uncertainty in ozone EC. For example, the sampling error ranges from 23% to 33% for one analyzer during different time periods at five sites in the eastern United States (Finkelstein & Sims, 2001) and from 10% to 20% with another analyzer at Hyytiälä in southern Finland (Keronen et al., 2003; Rannik et al., 2009).

Third, there are not currently open-path fast-response ozone analyzers. High instrument flow rates are thus needed to minimize residence time in measurement volumes and ozone loss in the sample stream due to reaction with walls or other compounds, as well as achieve a turbulent flow, which reduces attenuation in the tubing (Lenschow & Raupach, 1991). When the required flow rate is too high for the analyzer to

**Table 1**
*Commercially Available Fast Ozone Analyzers*

| Manufacturer or research group | Model | Type | Response time (approximate) (Hz) | References |
|---|---|---|---|---|
| Enviscope GmbH | Schnelle Ozon Sonde | Solid | 10 | Zahn et al. (2012) and Zhu et al. (2015) |
| Sextant | FOS | Solid | 10 | Stella et al. (2012) and Q. Li, Gabay et al. (2018) |
| Ecometrics | Chemiluminescence Ozone Fast Analyser | Solid | 10 | (GFAS clone) https://www.ecometrics.it/cosa-facciamo/338-2/, date of access 10 July 2019 |
| Ecophysics | CLD88 | Gas (NO) | 10 | https://www.ecophysics-us.com/atmospheric-research-products, date of access 10 July 2019 |

accommodate, excess flow can be pulled through a bypass pump. For pressure-sensitive analyzers (e.g., when the reaction required to detect ozone is sensitive to pressure), linking the bypass flow to a pressure controller may be necessary to maintain constant pressure at the analyzer inlet.

Chemiluminescence analyzers vary by reagent phase: gas, solid ("dry"), and liquid ("wet"). While chemiluminescence analyzers have fast response times and high sensitivity, they can be expensive (gas) or need frequent maintenance and calibration (dry and wet), adding labor costs and down time. Gas chemiluminescence leverages the reactions between ozone and ethene (e.g., Desjardins et al., 1995; Droppo, 1985; Duyzer et al., 1983; Munger et al., 1996) or nitric oxide (NO) (e.g., Bariteau et al., 2010; Eastman & Stedman, 1977; Pearson, 1990; Stedman et al., 1972). While several gas chemiluminescence analyzers were commercially available in the past, to our knowledge, there is only one currently available (Table 1).

Dry chemiluminescence uses a solid dye that emits light upon reaction with ozone. Not requiring toxic (e.g., NO) or flammable (e.g., ethene) compressed gases, dry chemiluminescence is advantageous over gas chemiluminescence. Dry analyzers also can be smaller and only require low power due to the physical configuration of their electronic components and the pumps or fans used to sample air. A coumarin solid dye, which emits a blue light upon reaction with ozone, is typically used for dry chemiluminescence (e.g., Muller et al., 2010). The photomultiplier tubes for detection of blue light are less expensive than the ones for red light needed for other common gas or dry chemiluminescence techniques. A dry analyzer used to be offered by Gesellschaft Für Angewandte Systemtechnik (GFAS) (Güsten et al., 1992; Güsten & Heinrich, 1996). Several groups made or used GFAS clones (e.g., Bauer et al., 2000; Coyle, 2005; Coyle et al., 2009; Cros et al., 2000; Finco et al., 2018; Kurpius et al., 2002; Mészáros, Horváth, et al., 2009). Currently, there are three dry analyzers commercially available, including one GFAS clone (Table 1).

Disadvantages of dry chemiluminescence include degradation of dye-impregnated discs (i.e., loss of ozone sensitivity) such that they need regular replacement (e.g., every few days). There is a 12% daily mean difference between ozone fluxes from a GFAS and a GFAS clone at Easter Bush in southern Scotland (Muller et al., 2010), suggesting analyzer performance and disc stability may be sources of uncertainty in ozone flux data. A new disc preparation method extending disc field stability is described in Ermel et al. (2013) who show high ozone sensitivity can be maintained over threefold more disc ozone uptake. An extended disc stability means measurements can proceed either for longer without maintenance or in higher ozone environments with similar maintenance.

A second ozone analyzer, which can be a commonly used UV absorbance instrument, is always necessary in dry chemiluminescence setups to account for the changing disc sensitivity. Different techniques to calculate an absolute signal can lead to substantially different ozone fluxes, as shown by measurements at Easter Bush (Muller et al., 2010) and a Chinese wheat field (Zhu et al., 2015).

Wet chemiluminescence employs organic liquid dye that emits light upon reaction with ozone (e.g., Drummond et al., 1991; Keronen et al., 2003; Ray et al., 1986; Zona et al., 2014). In principle, wet chemiluminescence is a relative measurement (because the dye degrades), but with a substantial amount of liquid reagent in the bottle used for measurement, it can be considered absolute. The dye does need to recirculate (usually via a peristaltic pump), however, and recirculation often fails when the bottle is not close to full (Keronen et al., 2003). Depending on ozone concentration at the site, the bottle may only need to be refilled every few months to keep it near full though (Keronen et al., 2003).

The need for long-term ambient ozone concentration measurements not requiring much maintenance has driven the market toward instruments inherently too slow for EC. More robust and economical fast analyzers not requiring frequent maintenance or involving toxic or flammable consumables or compressed gases will enable more ozone EC measurements and thus faster progress toward improved understanding of ozone dry deposition.

#### 2.2.1.2. Flux Gradient

The flux gradient technique requires determining the eddy diffusivity for ozone and the ozone concentration at two heights above a surface. Commonly used slower ozone instruments (e.g., UV absorbance) are adequate for this technique, likely making the technique more affordable and simpler than ozone EC. However, the flux gradient method has several limiting assumptions. For example, it assumes K-theory and often eddy diffusivity for ozone ($K_{o_3}$) equals eddy diffusivity for sensible heat. K-theory (or first-order closure; e.g., Stull, 1988) assumes transport only occurs down the local mean gradient, but organized turbulent motions can transport material up-gradient (or countergradient).

$$F_{O_3}^h = -K_{o_3} \frac{\partial \overline{O_3}}{\partial z}. \tag{5}$$

The eddy diffusivity for sensible heat can be calculated by employing Monin-Obukhov Similarity Theory (MOST) (Businger et al., 1971; Högström, 1988). However, MOST does not hold in the roughness sublayer above vegetation (Raupach, 1979), which can extend higher than double the vegetation height (e.g., Cellier & Brunet, 1992; Harman & Finnigan, 2007; Thom, 1975). Most observed gradients are located below this height. Additionally, ozone is reactive, and ambient chemistry may perturb the ozone gradient so assuming the eddy diffusivity for ozone is equal to that for heat is not always valid (Fitzjarrald & Lenschow, 1983; Lenschow, 1982; Vilá-Guerau de Arellano & Duynkerke, 1992).

Using a single analyzer with switching or moveable inlets to sequentially sample concentrations at different heights for the ozone gradient measurement is preferred over separate analyzers for the different heights because the latter requires effort to eliminate biases between the analyzers. However, when the measurements are not simultaneous (i.e., one analyzer is used at multiple heights), then the gradient needs to be stable over the time required to obtain measurements at both heights. Otherwise, there needs to be a correction for sequential sampling.

Inferring accurate ozone fluxes using the flux gradient technique is also challenging because ozone differences between the two heights may be very small and challenge the resolution and accuracy of the instrument (Businger, 1986). Maximizing the vertical distance between top and bottom heights to get larger differences helps (Arya, 2001), but both measurements must be in the surface layer with comparable footprints. Comparison of ozone EC and gradient fluxes over several ecosystems suggests fluxes and $v_d$ from the flux gradient technique may be biased and not represent variations accurately (Duyzer & Westrate, 1995; Loubet et al., 2013; Mikkelsen et al., 2000; Muller et al., 2009; Z. Y. Wu et al., 2015).

#### 2.2.1.3. Modified Bowen Ratio

The approach commonly called the modified Bowen Ratio technique (Businger, 1986) is also used to infer ozone fluxes from an ozone concentration gradient (e.g., Leuning et al., 1979; Leuning, Unsworth, et al., 1979; Mayer et al., 2011). The Bowen Ratio approach assumes similar turbulent diffusivities of ozone and of a reference quantity (i.e., another scalar, such as carbon dioxide), so the ozone flux can be calculated by a simple scaling of the flux of the reference quantity ("ref"):

$$F_{O_3}^h = F_{\mathrm{Ref}}^h \frac{\frac{\partial \overline{O_3}}{\partial z}}{\frac{\partial \overline{C_{\mathrm{ref}}}}{\partial z}}. \tag{6}$$

The concentrations of ozone and the reference quantity $\left(\overline{C_{\mathrm{ref}}}\right)$ are from measurements at the same heights in the surface layer. The modified Bowen Ratio technique may be advantageous over the flux gradient technique because the modified Bowen Ratio technique does not directly require turbulent diffusivity estimates. While commonly used ozone UV absorbance instruments are likely adequate for this technique, this

method requires detection of likely small gradients in ozone and the reference quantity. Previous work suggests substantial biases (50–100%) in ozone fluxes estimated with the modified Bowen Ratio technique with carbon dioxide fluxes relative to ozone EC at Harvard Forest (Z. Y. Wu et al., 2015).

#### 2.2.2. Chamber Methods

Chamber methods are employed to isolate ozone uptake to foliage, soil, water, and other surfaces in the field (Almand-Hunter et al., 2015; Altimir et al., 2002; Fumagalli et al., 2016; Gut et al., 2002; Horváth et al., 2006; Kaplan et al., 1988; Kirkman et al., 2002; Meixner et al., 1997; Pilegaard, 2001; Remde et al., 1993; Tong et al., 2011; Unsworth et al., 1984; Wieser et al., 2012). However, previous work largely focuses on soil NO emissions (e.g., Gut et al., 2002; Horváth et al., 2006; Kaplan et al., 1988; Kirkman et al., 2002; Meixner et al., 1997; Remde et al., 1993) or plant responses to ozone (e.g., Tong et al., 2011; Wieser et al., 2012) rather than ozone deposition processes.

For an open chamber, air is generally drawn into the chamber, and the ozone concentration difference between the inlet and outlet is measured with a slow ozone instrument. The uptake rate to the surface is determined from the concentration difference, the known flow rate into the chamber, and volume of the chamber.

We emphasize the value of chamber methods for gaining mechanistic understanding of ozone dry deposition (e.g., Altimir et al., 2006; Fumagalli et al., 2016). However, we note that chamber footprint is small (i.e., on the order of a meter or less), chambers modify microclimate, and ozone chemistry may occur in the chamber air or with chamber walls and tubing (Breuninger et al., 2012; Pape et al., 2009). In the field, multiple chambers are necessary to account for inhomogeneity across a wider area (e.g., the footprint of a flux tower) as well as understand the robustness of observed dependencies on environmental conditions.

The strength in using chamber measurements to separate the canopy portion of the ozone flux from the ground ozone uptake (see equation (4)) (e.g., Duyzer et al., 2004; Finco et al., 2018; Rummel et al., 2007) or to serve as a surrogate to ozone EC (Almand-Hunter et al., 2015; Plake, Stella, et al., 2015) hinges on the ability to obtain an estimate spatially representative of the ecosystem, to remove the effects of turbulent transport modified by the chamber, and to estimate in-canopy turbulent transport and the contribution from fast ambient chemistry to the ecosystem-scale ozone fluxes.

#### 2.2.3. Isotopic Methods

Isotopic experiments in the laboratory and field may be able to pinpoint the primary sites of ozone surface reactions and thus improve understanding of ozone deposition pathways (Subke et al., 2009; Toet et al., 2009). Subke et al. (2009) present a method for adding $^{18}O$ into an electric discharge ozone generator and using a silica gel to separate $^{18}O$ ozone from $^{18}O$ $O_2$. However, $^{18}O$ from the generated ozone leads to $^{18}O$ enriched water vapor as well as other gases (e.g., $O_2$) that do not necessarily remain on a surface, complicating estimates of deposited ozone (Toet et al., 2009). The authors conclude that better understanding of the reactions determining loss of $^{18}O$ ozone into other gases is needed for this technique to be useful for constraining ozone deposition pathways.

## 3. Modeling Ozone Dry Deposition Using Resistance Networks

We present common resistance network approaches for parameterizing ozone dry deposition in models considering vegetation as one big leaf and in models considering vertical variation in plant canopy structure. In general, resistance network approaches have many strengths. For example, resistance approaches are appropriate for modeling at different scales, simple, and adaptable, and allow for representing individual processes.

For big-leaf models, we describe both single- and dual-surface models. Dividing the negative ozone flux at height $h$ $\left(F^h_{O_3}\right)$ by the ozone concentration at that height ($O_{3h}$) gives the ozone deposition velocity ($v_d$), a simple measure of the efficiency of ozone dry deposition:

$$v_d = -\frac{F^h{}_{O_3}}{O_{3h}}. \tag{7}$$

The simplest possible resistance network for $v_d$ is the single-surface big-leaf model (Figure 5a), which lumps all surfaces to which ozone deposits into a single surface:

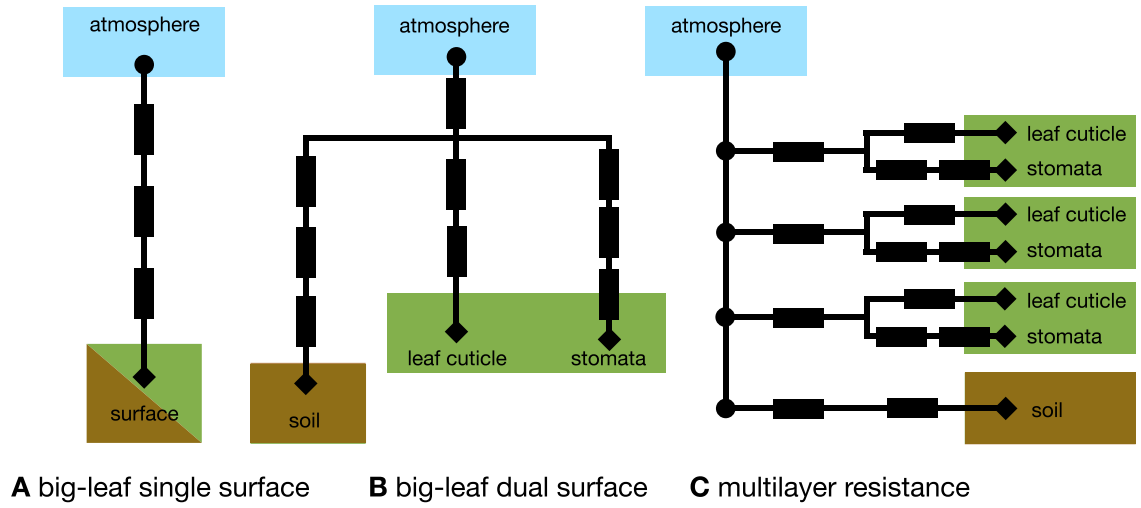


**Figure 5.** Resistance networks for modeling ozone dry deposition. Circles and diamonds show where ozone concentration is needed as input for a given network. For the diamonds, the ozone concentration is typically assumed to be zero. Rectangles indicate resistances. (a) shows a big-leaf single surface model, (b) shows a big-leaf dual surface model, and (c) shows a multilayer resistance model.

$$v_d = (r_a + r_b + r_c)^{-1}. \tag{8}$$

$r_a$ is the bulk aerodynamic resistance; $r_b$ is the bulk quasi-laminar boundary-layer resistance; and $r_c$ is the bulk surface resistance for the single-surface model. Due to the need to separate stomatal from nonstomatal deposition for modeling ozone impacts on plants, $r_c$ in a single-surface big-leaf model is typically modeled in the following way, with the assumption that stomatal and the bulk nonstomatal surfaces are at the same height in the canopy:

$$r_c = \left(\frac{1}{r_{\text{stom}} + r_{\text{meso}}} + \frac{1}{r_{\text{ns}}}\right)^{-1}. \tag{9}$$

$r_{\text{stom}}$ is the resistance to uptake of ozone through diffusion into stomata; $r_{\text{meso}}$ is the resistance to ozone reaction inside the leaf; $r_{\text{ns}}$ is the resistance to all nonstomatal deposition pathways. Often, a residual $r_{\text{ns}}$ is inferred using ozone fluxes and complementary micrometeorological measurements (i.e., to infer $r_a$, $r_b$, and $r_{\text{stom}}$) with this single-surface big-leaf approach.

The dual-surface big-leaf model (Figure 5b) considers two surfaces for dry deposition. In the context of a plant canopy, the two surfaces represented are typically leaves and soil, with all leaves considered to be at one height.

$$v_d = \left(r_a + \left(\frac{1}{r_{b,\text{leaf}} + r_{\text{stom}} + r_{\text{meso}}} + \frac{1}{r_{b,\text{leaf}} + r_{\text{cut}}} + \frac{1}{r_{\text{ac}} + r_{b,\text{soil}} + r_{\text{soil}}}\right)^{-1}\right)^{-1}. \tag{10}$$

$r_{b,\text{leaf}}$ is the resistance associated with transfer in the quasi-laminar boundary layer around leaves; $r_{\text{stom}}$ and $r_{\text{meso}}$ are as defined for the single-surface big-leaf model; $r_{\text{cut}}$ is the leaf cuticular resistance to ozone uptake; $r_{\text{ac}}$ is the resistance associated with atmospheric transport through the canopy air space; $r_{b,\text{soil}}$ is the resistance in the quasi-laminar boundary layer around soil; and $r_{\text{soil}}$ is the resistance to ozone uptake by soil.

The big-leaf resistance network structure varies across different dry deposition schemes. For example, Wesely (1989) consider a bulk quasi-laminar boundary layer resistance for soil and leaves, which is added in series with the bulk $r_a$, whereas Massman (2004) consider different quasi-laminar boundary layer resistances for soil versus leaves.

One big-leaf modeling shortcoming is that there is no consideration of vertical variation in leaf properties and functioning (e.g., in response to canopy attenuation of solar radiation). Multilayer resistance models (Figure 5c)—where surface resistance ($r_{\text{surf}}$) is calculated at each level of the canopy ($z$) below canopy height ($h_c$)—are designed to address this issue:

$$r_{\mathrm{surf}}(z) = \left(\frac{1}{r_{b,\mathrm{leaf}}(z) + r_{\mathrm{stom}}(z) + r_{\mathrm{meso}}(z)} + \frac{1}{r_{b,\mathrm{leaf}}(z) + r_{\mathrm{cut}}(z)}\right)^{-1} \text{ if } z \leq h_{\mathrm{c}}, \tag{11}$$

$$r_{\mathrm{surf}}(z) = \left(\frac{1}{r_{b,\mathrm{soil}} + r_{\mathrm{soil}}}\right)^{-1} \text{ if } z = 0. \tag{12}$$

To calculate $v_d$ with this approach, the above $r_{\mathrm{surf}}$ parameterization needs to be embedded into a model considering ozone turbulent transport among canopy layers and between $h_{\mathrm{c}}$ and $h$. Turbulent transport could be simulated with a resistance approach or more explicitly.

Most ozone dry deposition schemes deployed in regional and global models use big-leaf approaches. Multilayer resistance approaches exist (e.g., Duyzer et al., 2004; Fares et al., 2019; Ganzeveld et al., 2002; Launiainen et al., 2013; Meyers et al., 1998; Potier et al., 2015; Wolfe & Thornton, 2011; P. T. Zhou et al., 2017) but mostly are used in single-point models for interpreting field observations rather than modeling regional-to-global ozone dry deposition. An advantage of the multilayer approach is that the ozone continuity equation can be calculated at every height and thus the influence of in-canopy chemistry (e.g., Ashworth et al., 2015; Wolfe et al., 2011) or turbulence (e.g., Chang et al., 2018; Patton et al., 2016; Pyles et al., 2000) explicitly resolved. We refer to the approach where the ozone mass continuity equation is solved at each height as a multilayer canopy model. To our knowledge, in-canopy chemistry has never been explicitly considered in a big-leaf framework although empiricism in model development may have led to implicit inclusion (Wolfe et al., 2011).

## 4. Theory, Models, and Observations of Terrestrial Ozone Deposition Pathways and Related Processes

We review ozone dry deposition to plant stomata (section 4.1), leaf cuticles (section 4.2), soil (section 4.3), and snow-covered surfaces (section 4.6). We also review turbulent transport (section 4.4) and ambient chemistry (section 4.5), presenting these sections before the section on deposition to snow-covered surfaces due to our focus on turbulence and chemistry in plant canopies. In all sections, we discuss modeling and measurement techniques. For sections on deposition to cuticles, soil, and snow-covered surfaces, we synthesize understanding of these processes based on laboratory and field observations and theory. For sections on stomatal deposition, turbulence, and fast ambient chemistry, we highlight advances in understanding pioneered by the fields of plant physiology/ecology, boundary-layer meteorology, and atmospheric chemistry, respectively, and identify steps needed to advance knowledge of the process as related to ozone dry deposition.

### 4.1. Stomata

Stomata are the pores on plant leaves regulating gas exchange between the atmosphere and vegetation. Accurate estimates of the stomatal ozone flux ($F_{\mathrm{stom}}$) are key for interpreting ozone flux observations and assessing ozone plant damage. $F_{\mathrm{stom}}$ is estimated by dividing the ambient ozone concentration outside the leaf ($O_{3\mathrm{leaf}}$) by the sum of several resistances:

$$F_{\mathrm{stom}} = \frac{-O_{3\mathrm{leaf}}}{r_{b,\mathrm{leaf}} + r_{\mathrm{stom}} + r_{\mathrm{meso}}}. \tag{13}$$

$r_{b,\mathrm{leaf}}$ is the resistance to transport through the quasi-laminar boundary layer between the leaf and outside air; $r_{\mathrm{stom}}$ is the resistance to gaseous diffusion through stomatal pores; and $r_{\mathrm{meso}}$ is the resistance to ozone reaction inside the leaf. The inverse of $r_{\mathrm{stom}}$ is stomatal conductance ($g_s$). While a mesophyll resistance (i.e., $r_{\mathrm{meso}}$) is the conventional way of describing that reactions destroying ozone within the leaf may limit $F_{\mathrm{stom}}$, ozone is not primarily destroyed inside the leaf by reactions with the mesophyll tissue. Despite $r_{\mathrm{meso}}$ being a misnomer, we retain the terminology for consistency with previous work (e.g., Wesely, 1989).

Observational approaches and prognostic models for $r_{\mathrm{stom}}$ are typically for water vapor. To obtain an estimate of the resistance to ozone diffusion through stomatal pores, $r_{\mathrm{stom}}$ for water vapor is multiplied by the ratio of the diffusivity of water vapor in air to the diffusivity of ozone in air. The current estimate of this ratio is 1.61 (Massman, 1998). The assumption inherent to this approach is proportionality between ozone diffusing inward through stomata and water vapor diffusing outward. One limitation of this assumption is

that collisions between ozone and water vapor molecules may lead to an error of 4–10% in estimates of the stomatal ozone flux (Uddling et al., 2012).

A widely used assumption is that reactions inside the leaf do not limit stomatal ozone uptake (i.e., negligible $r_{meso}$). While some laboratory studies (Laisk et al., 1989; Omasa et al., 2000; S. Sun, Moravek, von der Heyden, et al., 2016; Wang et al., 1995) and the modeling study of Plöchl et al. (2000) suggest this assumption holds, the findings of other laboratory studies and the modeling study of Tuzet et al. (2011) suggest otherwise. In particular, laboratory findings of nonlinear relationships between stomatal uptake of water vapor and stomatal uptake of ozone (Eller & Sparks, 2006; Fares et al., 2007; Fares, Park, et al., 2010; Loreto & Fares, 2007; Tuzet et al., 2011) may imply nonnegligible resistance to ozone reaction inside the leaf. Nonetheless, separating ozone destruction inside the leaf from $g_s$, cuticular ozone uptake, and gas-phase ozone loss is challenging. We recommend future studies further investigate ozone destruction inside the leaf and its influence on stomatal ozone uptake.

In the rest of this section, we highlight common observational constraints on $g_s$ (section 4.1.1) and prognostic $g_s$ models (section 4.1.2). We discuss leaf, tree, and ecosystem-scale observational approaches. Note we say observational constraints or approaches because $g_s$ is not typically measured directly. For prognostic $g_s$ modeling, common mechanistic and empirical approaches are highlighted. We also review how the stomatal ozone sink may influence itself through ozone plant damage (section 4.1.3).

#### 4.1.1. Measuring Stomatal Conductance at Leaf, Tree, and Ecosystem Scales

Leaf-level observational constraints typically inform mechanistic and empirical prognostic $g_s$ models. Leaf-level $g_s$ is inferred from a leaf diffusion porometer or gas exchange system, which record changes in humidity or maintain constant water vapor to infer transpiration. To obtain $g_s$, transpiration is divided by the vapor pressure deficit between the substomatal cavity of the leaf and porometer chamber. To calculate vapor pressure deficit, the air inside the leaf is assumed to be saturated. A recent study using carbon and water isotopes challenges this assumption, finding subsaturation in two conifer species under moderate to high atmospheric vapor pressure deficit and a resulting bias in the inferred $g_s$ (Cernusak et al., 2018). Whether subsaturation inside the leaf occurs more broadly is unknown.

Ecosystem-scale observational $g_s$ constraints are often used for directly interpreting ozone turbulent flux measurements and estimate the ecosystem-scale stomatal ozone uptake. We discuss multiple methods of inferring ecosystem-scale $g_s$ because we recommend using multiple independent approaches to quantify ecosystem-scale $g_s$ due to uncertainties across approaches. Ideally, agreement among approaches would be used to draw robust conclusions.

The first ecosystem-scale method employs water vapor EC fluxes and is the most popular method for estimating the ecosystem-scale stomatal ozone uptake. In this method, water vapor fluxes are inverted assuming Fick's law to obtain a surface conductance for water vapor. The intricacies of this method, described below, result in several ways of applying it (e.g., Gerosa et al., 2007).

The surface conductance for water vapor is not exactly $g_s$ because surface conductance includes contributions from in-canopy turbulent transport of water vapor (Baldocchi et al., 1987; Baldocchi et al., 1991; Paw U & Meyers, 1989; Raupach & Finnigan, 1987) and evaporation from soil and vegetation (Baldocchi et al., 1987; Baldocchi & Meyers, 1998; Raupach & Finnigan, 1987) in addition to $g_s$. The contribution of evaporation is undesirable in estimating stomatal ozone uptake because evaporation is not directly related to ozone dry deposition. While advances with respect to the ecosystem-scale transpiration fraction of evapotranspiration (e.g., Stoy et al., 2019) will help estimates of surface conductance more strictly represent $g_s$, there is still the issue that surface conductance includes the contribution of turbulent transport of water vapor through the canopy. Assuming similar in-canopy concentration profiles of ozone and water vapor, the contribution of in-canopy turbulence to the surface conductance may be desirable in an ecosystem-scale estimate of $g_s$. However, the safety of the assumption of similar ozone and water vapor in-canopy profiles and thus transport needs to be evaluated.

Inverting the water vapor EC flux via Fick's law for surface conductance requires an ecosystem-scale estimate of water vapor inside the leaf. The assumption for estimating this is that leaf air is saturated, which may be problematic as suggested by leaf level measurements (e.g., Cernusak et al., 2018), and requires an estimate of ecosystem-scale leaf temperature (more commonly, canopy skin temperature). Because canopy

skin temperature constraints are not usually available, most inversion approaches include an approximation depending on sensible heat flux, which can be (and previously had to be) inferred from the surface energy budget (i.e., by subtracting the ground heat flux and latent heat flux from net radiation). Not only does the lack of surface energy balance closure in EC measurements (Foken et al., 2010; Wilson & Baldocchi, 2000) suggest errors in inferring sensible heat flux from energy balance, but including latent heat flux in an equation for latent heat flux introduces circularity (Wohlfahrt, Haslwanter, et al., 2009). Modern sensible heat flux measurements avoid the need to estimate sensible heat flux, and thus, methods that incorporate the measured sensible heat flux should be used over methods that estimate the sensible heat flux. New canopy skin temperature measurements (e.g., Kim et al., 2016) may lead to even more accurate estimates of surface conductance.

Ecosystem-scale fluxes of other gases should be used to complement ecosystem-scale $g_s$ estimates from water vapor fluxes (e.g., Clifton et al., 2019). Carbon dioxide fluxes can be used to constrain $g_s$ through empirical or semiempirical modeling (see section 4.1.2) but require uncertain estimates of respiration (e.g., Wehr et al., 2016) to infer net photosynthesis. Carbonyl sulfide fluxes (e.g., Whelan et al., 2018) are used to validate an empirical $g_s$ model for Harvard Forest (Wehr et al., 2017; Wehr & Saleska, 2015) based on findings that they represent ecosystem-scale $g_s$ (Commane et al., 2015). Whether this approach transfers readily from Harvard Forest to other locations remains to be established.

Sap flow measurements on individual trees can also be useful for estimating the stomatal ozone flux (Fares et al., 2012; Goldstein, 2003; Matyssek et al., 2004; Nunn et al., 2010; Wieser et al., 2003, 2006) because sap flow isolates transpiration's contribution to the total water vapor flux. However, constraining ecosystem-scale $g_s$ with sap flow requires nontrivial scaling from individual trees to the ecosystem. At a mixed forest in Europe, the stomatal fraction of the ozone flux from sap measurements is 42% lower than inverting ecosystem-scale water vapor fluxes (Nunn et al., 2010). While differences may be due to evaporation from foliage and soil influencing the inversion of ecosystem-scale water vapor flux, uncertainties in sap flow measurements and scaling techniques (e.g., Poyatos et al., 2016) may also contribute to differences between approaches.

#### 4.1.2. Modeling Stomatal Conductance

The most popular prognostic $g_s$ models in dry deposition schemes are empirical and closely adhere to the Jarvis (1976) multiplicative approach (e.g., Emberson, et al., 2000; Wesely, 1989). In the Jarvis approach, a prescribed maximum $g_s$ is multiplied by several factors, and each factor is a function of a particular environmental condition. The conditions may be meteorological or biophysical (e.g., soil moisture and leaf age). The Jarvis type of model is informed by leaf level and sometimes ecosystem-scale observational $g_s$ constraints (e.g., Büker et al., 2007, 2012; Kelliher et al., 1995).

An increasingly common method for prognostic $g_s$ modeling is coupling $g_s$ with net photosynthesis ($A_{net}$) (hereafter, $A_{net}$-$g_s$ model), providing an estimate of carbon dioxide exchange across stomata driven by the carbon supply and demand for photosynthesis. In an $A_{net}$-$g_s$ model, $g_s$ is modeled according to a relationship with $A_{net}$ (Miner et al., 2017; S. C. Wong et al., 1979) that varies with some metric of humidity, as constrained by leaf-level data (Ball et al., 1987; Leuning, 1995; Medlyn et al., 2011). Recent work assigns a physical basis to this relationship by reconciling mechanistic and empirical approaches with optimization theory for maximizing carbon gain and minimizing water loss (Cowan & Farquhar, 1977; Y. S. Lin et al., 2015; Medlyn et al., 2011). However, whether stomata function optimally as assumed under this particular theory is uncertain (e.g., Buckley & Mott, 2013; C. Lin et al., 2018; Sperry et al., 2017; Wolf et al., 2016; S. Zhou et al., 2013).

In general, whether modeled through empirical or mechanistic prognostic approaches, $g_s$ is calculated for a single leaf and scaled to the ecosystem by multiplying leaf-level $g_s$ by leaf area index (LAI) or using canopy scaling factors or a multilayer canopy or resistance model. It is uncertain which scaling approach best estimates $g_s$.

While some dry deposition schemes employ $A_{net}$-$g_s$ models (Charusombat et al., 2010; Clifton, 2018; Hollaway et al., 2016; M. Lin et al., 2019; Ran et al., 2017; Val Martin et al., 2014), the Jarvis type of model remains ubiquitous (e.g., Emberson, et al., 2000; Hardacre et al., 2015). $A_{net}$-$g_s$ models are more closely based on physiological principles, but the simplicity, adaptability, and computation efficiency of the Jarvis approach make it attractive for many applications. However, the Jarvis approach requires tuning for the ecosystems and environmental conditions represented, and its success is limited by dearth of data for many ecosystems (e.g., tropical forests) and conditions. Nonetheless, $A_{net}$-$g_s$ models are semiempirical in that

they require one to a few parameters to be defined (Franks et al., 2018; Y. S. Lin et al., 2015; Medlyn et al., 2011; Miner et al., 2017). Both model types are typically tuned with leaf-level data due the historical lack of ecosystem-scale data. Recent efforts to tune models with ecosystem-scale measurements (e.g., J. Li, Duan, et al., 2018; Raoult et al., 2016), such as latent heat and carbon dioxide fluxes, can complement leaf-level approaches by allowing for insight into what happens at larger scales.

To evaluate the strengths and weaknesses of prognostic $g_s$ models in simulating stomatal ozone uptake, the community would benefit from better understanding of model sensitivities to parameters and variables as well as their physiological realism. For example, connections between $g_s$ and soil moisture and the ability of models to capture such connections (e.g., Anderegg et al., 2017; Bonan et al., 2014; Kennedy et al., 2019; Verhoef & Egea, 2014; S. Zhou et al., 2013) may be critical for capturing stomatal ozone uptake.

#### 4.1.3. Ozone Damage to Plants, as Relevant for Stomatal Uptake of Ozone

Ozone damage to plants may lead to myriad ecosystem responses. Here we focus on the direct influence of ozone on $g_s$ and thus stomatal ozone dry deposition.

Stomatal ozone uptake changes $g_s$ through both short-term and long-term responses. In the short term, stomatal ozone uptake decreases $g_s$ by changing guard cell turgor pressure and signaling pathways (Freer-Smith & Dobson, 1989; Hassan et al., 1994; Maier-Maercker & Koch, 1991; Manes et al., 2001; Mills et al., 2009; Torsethaugen et al., 1999).

In the long term, the mean $g_s$ response to stomatal ozone uptake across plant physiological studies is a decrease (Lombardozzi et al., 2013). However, both $g_s$ increases and decreases are observed. For example, stomatal ozone uptake can lead to reduced photosynthetic efficiency, which increases internal carbon dioxide and signals stomatal closure (Calatayud et al., 2007; Farage et al., 1991; Herbinger et al., 2007; Manes et al., 2001; Noormets et al., 2001; Paoletti & Grulke, 2005; Reich, 1987). On the other hand, stomatal ozone uptake can lead to $g_s$ increases in the long term through decreased sensitivity to abscisic acid (Mills et al., 2009), which alters stomatal cell ion exchange (Manes et al., 2001; Torsethaugen et al., 1999), and the collapse of epidermal cells surrounding guard cells (Hassan et al., 1994), which can lead to sluggish stomatal responses to external stimuli (Freer-Smith & Dobson, 1989; Maier-Maercker & Koch, 1991; Manes et al., 1998, 2001; McLaughlin et al., 2007; Paoletti, 2005; Paoletti & Grulke, 2010). Stomatal ozone uptake may also cause early and a more rapid onset of senescence (e.g., Ainsworth et al., 2012), which reduces $g_s$ through growing season length and physiologically active LAI.

Two types of model parameterization allow for stomatal ozone uptake to influence itself. In the first type, a response integrated across several physiological processes is used to parameterize impact of ozone on a single physiological process (Clark et al., 2011; Sitch et al., 2007; Yue & Unger, 2014). For example, the observed effect of stomatal ozone uptake on plant biomass or crop yield may be equated to the ozone impact on photosynthesis in models and parameterized accordingly, and thus, any impact on stomatal ozone uptake is due to ozone's parameterized impact on photosynthesis (e.g., Sitch et al., 2007).

The second type of model considers the ozone impact on the same physiological process considered in the observational evidence (Ewert & Porter, 2000; Deckmyn et al., 2007; Lombardozzi, Levis, et al., 2012; Lombardozzi, Sparks, et al., 2012; Lombardozzi et al., 2015; Martin et al., 2001; Tao et al., 2017). For example, Lombardozzi et al. (2013) investigate the effects of cumulative stomatal ozone uptake on $g_s$ versus photosynthesis with a meta-analysis of published chamber data. Finding differing observed effects on the two processes, consistent with other work (e.g., Koch et al., 1998; Paoletti & Grulke, 2010), Lombardozzi et al. (2013) parameterize the effect of the cumulative stomatal ozone uptake on each process separately.

Another difference across models parameterizing ozone damage with stomatal ozone uptake is whether damage is tied to the instantaneous or cumulative stomatal ozone uptake. There are a few models, most commonly for crops, considering both instantaneous and cumulative stomatal uptake (Emberson et al., 2018; Ewert & Porter, 2000; Tao et al., 2017). Plant damage is often assumed more closely related to cumulative, rather than instantaneous, stomatal ozone uptake (Ducker et al., 2018; Massman et al., 2000; Matyssek et al., 2004).

Stomatal ozone uptake does not account for plant abilities to cope with the oxidative stress that ozone causes (i.e., detoxify). Detoxification ability controls the plant sensitivity to ozone and thus determines the ozone plant injury (e.g., Matyssek et al., 2008; Musselman et al., 2006). Detoxification is often simulated by

assuming a constant threshold of stomatal ozone uptake below which damage does not occur due to detoxification. Detoxification is highly uncertain and may vary with environmental variables and come at a cost to the plant (U.S. EPA, 2006; Ainsworth et al., 2012; Ainsworth, 2017; Musselman et al., 2006; Matyssek et al., 2008).

Current knowledge of the effects of stomatal ozone uptake on $g_s$ at large scales (e.g., ecosystem or region) is largely based on scaling up leaf-level effects (Massman et al., 2000; Matyssek et al., 2008). Limited leaf-level data (e.g., most data are for temperate species) and lack of clear response across existing data sets (e.g., Lombardozzi et al., 2013) limit the fidelity of given empirical parameterization. In general, large-scale responses to stomatal ozone uptake are poorly understood and not widely evaluated given the paucity of observational constraints on ozone damage at larger scales. Understanding ecosystem abilities to detoxify is sorely needed to pinpoint stomatal ozone uptake's influence on itself.

#### 4.1.4. Main Takeaways

1. Water vapor EC fluxes are typically used to constrain ecosystem-scale $g_s$, but multiple independent observational approaches are needed and ideally agreement among them would be used to draw robust conclusions.
2. $A_{net}$-$g_s$ models represent current mechanistic understanding, but how much $A_{net}$-$g_s$ models improve $g_s$ estimates over widely used empirical approaches is uncertain.
3. Identification of the key parameters to which prognostic $g_s$ models are most sensitive and an understanding of the physiological realism of modeled sensitivities are needed.
4. Ecosystem-scale constraints on stomatal ozone uptake and the ecosystem's ability to detoxify are missing but key for understanding the influence of stomatal ozone uptake on itself.

### 4.2. Leaf Cuticles

#### 4.2.1. Controls on Ozone Dry Deposition to Leaf Cuticles: Field, Modeling, and Laboratory Evidence

The following synthesis suggests aqueous heterogeneous chemistry is the primary mechanism controlling ozone dry deposition to leaf cuticles. Direct constraints on cuticular ozone uptake are slim but insightful. For example, ozone and carbon dioxide leaf uptake measured with chambers at Hyytiälä provide strong evidence for a dependence of cuticular ozone uptake on relative humidity (Altimir et al., 2006). A laboratory study that induced stomatal closure in young trees by treating leaves with abscisic acid also shows increases in ozone uptake with relative humidity (S. Sun, Moravek, Trebs, et al., 2016) (Figure 6). Increases in cuticular uptake with humidity suggest aqueous ozone-destroying chemistry on the cuticle; liquid surface films form when humidity increases because there is absorption of water to the leaf surface, capillary condensation, or deliquescence of deposited particles (Burkhardt & Eiden, 1994; Burkhardt & Hunsche, 2013; Eiden et al., 1994).

Several field studies report increases in inferred nonstomatal uptake over vegetation with relative humidity, providing evidence that aqueous surface chemistry on leaves may be important at ecosystem scales (Altimir et al., 2006; Clifton et al., 2019; Lamaud et al., 2009; Q. Li, Gabay et al., 2018; Neirynck & Verstraeten, 2018; Rannik et al., 2012; L. Zhang et al., 2002). However, at some field sites, nonstomatal uptake increases with humidity at high humidity but decreases with humidity at low humidity (Coyle et al., 2009; Hogg et al., 2007). This diverging behavior may reflect a change in the mechanism controlling cuticular uptake with thermal decomposition dominating at lower humidity (Coyle et al., 2009; Grøntoft et al., 2004; Pöschl & Shiraiwa, 2015). In general, the degree to which ecosystem-scale nonstomatal uptake estimates represent cuticular uptake is uncertain because other processes, such as ozone uptake by soil and ambient chemistry, cannot always be discounted. Additionally, imperfect estimates of stomatal deposition and transport imply at least some error in residual nonstomatal deposition estimates.

A recent review of ozone dry deposition to building surfaces concludes the influence of relative humidity on ozone uptake is uncertain (Shen & Gao, 2018). It may be that only some ozone-destroying surface reactions are expedited in water films and water films only form easily on some surfaces. Increased cuticular uptake at higher humidity may also be associated with stomatal exudation of reactive compounds when leaves are wet (Potier et al., 2017). For example, water around stomata can act as a bridge into saturated stomatal pores (Burkhardt, 2010), and stomata may leach ascorbate compounds into the water on the cuticle. If ozone

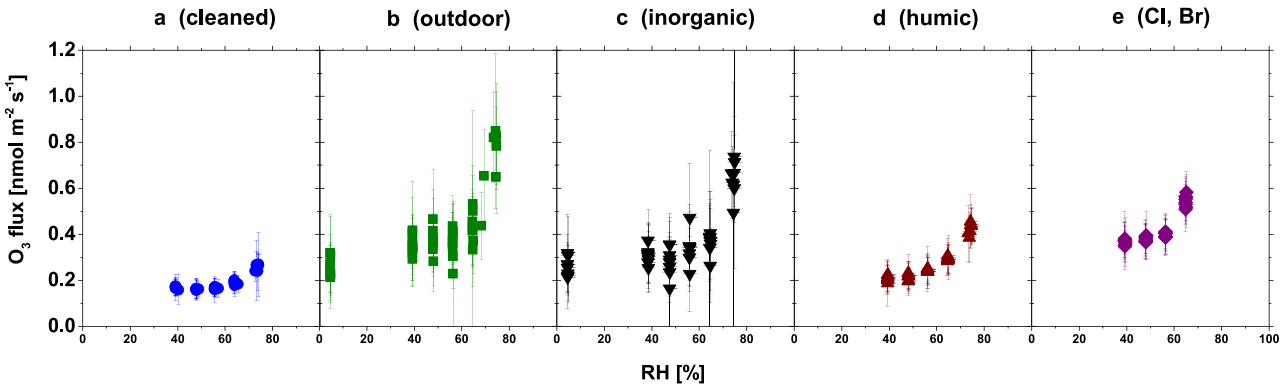


**Figure 6.** Differences in cuticular ozone flux to *Quercus ilex* leaves treated with various compounds (a–e) and abscisic acid to induce stomatal closure in the laboratory. (a) is for clean leaves, (b) is for leaves exposed to outdoor air, (c) is for leaves treated with inorganic compounds, (d) is for leaves treated with humic acid solution, and (e) is for leaves treated with chloride/bromide solution. Cuticular ozone fluxes are shown as a function of relative humidity (RH). Error bars represent the random error calculated according to S. Sun, Moravek, von der Heyden, et al. (2016). Figure is adapted from Figure 6 of S. Sun, Moravek, Trebs, et al. (2016) with permission. 

destruction on cuticles is limited by ascorbate flowing out of stomata when leaves are wet, then a fundamental question is how much leakage occurs.

In their laboratory study examining ozone uptake to aluminum, stainless steel, beeswax, and hydrocarbon wax, Cape et al. (2009) find an Arrhenius-like dependence of ozone uptake on temperature and suggest a role for thermal decomposition of ozone when ozone deposits to leaf cuticles. There is some field evidence for this hypothesis in dry conditions, as discussed above. However, increases in temperature only lead to small increases in ozone uptake to building surfaces (Shen & Gao, 2018). In general, thermal decomposition of ozone on a given surface depends on the surface area and activation energy, which varies across materials (e.g., Cape et al., 2009). Whether thermal decomposition plays a role in governing cuticular ozone uptake needs to be better understood.

While light-mediated ozone destruction on cuticles received attention in previous reviews on ozone dry deposition (e.g., Fowler et al., 2009; Ganzeveld et al., 2015; Tuovinen et al., 2009), evidence for the importance and occurrence of this pathway is minimal. In brief, Coe et al. (1995) find a diel cycle in nonstomatal deposition inferred from field measurements. The hypothesis that photochemistry on the leaf surface causes this diel cycle is given attention on the basis of Rondón (1993), an unpublished laboratory study. A more recent laboratory study finds similar cuticular ozone uptake for light and dark conditions (S. Sun, Moravek, Trebs, et al., 2016), suggesting cuticular uptake is unlikely to be related to photochemistry.

High $v_d$ after rain and dew observed in field studies is often attributed to increases in cuticular uptake (Altimir et al., 2006; Finkelstein et al., 2000; Fuentes et al., 1992; Grantz et al., 1995, 1997; Lamaud et al., 2002; Potier et al., 2015; Turnipseed et al., 2009). Increases in ozone dry deposition on wet leaves in the laboratory (Fuentes & Gillespie, 1992) and in a field chamber experiment after spraying the grass in the chamber with water (Pleijel et al., 1995) are also attributed to increases in cuticular uptake. While there are fairly consistent increases in $v_d$ over vegetation after rain and dew across field studies (Table 2), whether observed responses truly indicate changes in cuticular uptake remains an open question. For example, there may be changes in $g_s$ after rain (e.g., Clifton et al., 2019) or emissions of highly reactive species that influence the observed ozone flux (e.g., Altimir et al., 2006; Clifton et al., 2019; Turnipseed et al., 2009).

#### 4.2.2. Composition of the Leaf Cuticle

Composition of the cuticular surface likely determines ozone reactivity. Cuticular composition and thus reactivity may reflect deposited aerosols, the cuticular wax itself, and/or compounds exuded from the plant, but the relative importance of each source of reactivity is uncertain and may vary in space and time. Different wetting mechanisms may alter cuticular composition and thus ozone uptake. For example, rain may wash leaves of compounds (e.g., Xu et al., 2017; L. Zhang et al., 2019) with which ozone can react. Deliquescent salts on cuticles may also increase ozone solubility compared to pure water (e.g., Rischbieter et al., 2000). Below we discuss evidence for each source (deposited aerosols, cuticular wax, and exuded

Reviews of Geophysics

10.1029/2019RG000670

**Table 2**
*Summary of Field Studies Reporting Changes in Ozone Dry Deposition After Rain and Dew*

| Site name | Measurement period and type | Site description | Sign of response to rain | Sign of response to dew | Reference |
|---|---|---|---|---|---|
| Bondville (40.05°N, 88.37°W) | 2 months of ozone EC fluxes | Maize | Increase | Increase | L. Zhang et al. (2002) |
| Camp Borden (44°19′N, 79°56′W) | 5 days of ozone EC fluxes | Temperate deciduous forest | Increase[a] | Increase[a] | Fuentes et al. (1992) |
| | 2 months of ozone EC fluxes | | Decrease (day), no change (night) | Increase (episodic), no change (systematic) | Padro (1994) |
| CODE cotton (36°48′50″N, 120°40′38″W) | 1 month of ozone EC fluxes | Cotton | | No change[a] | Massman et al. (1994) |
| | | | | Decrease | Grantz et al. (1997) |
| CODE vineyard (36°51′36″N, 120°6′7″W) | 1 month of ozone EC fluxes | Vineyard | | No change[a] | Massman et al. (1994) |
| | | | | Increase | Grantz et al. (1995) |
| Flanders (51°18′N, 4°31′E) | 10 years of ozone fluxes from flux gradient technique | Temperate deciduous forest | Increase | Increase | Neirynck and Verstraeten (2018) |
| Grignon (48.84422°N, 1.95191°E) | 5 months of ozone EC fluxes from 3 years each | Wheat | Increase | Increase | Potier et al. (2015) |
| Harvard Forest (42.53°N, 72.18°W) | 4 months of ozone EC fluxes from 11 years each | Temperate deciduous forest | Increase[b] | | Clifton et al. (2019) |
| Hyytiälä (61.85°N, 24.28°E) | 6 months of ozone EC fluxes from 2 years each | Boreal forest | Increase | | Altimir et al. (2006) |
| Kane Experimental Forest (41.595°N, 78.766°W) | 4 months of ozone EC fluxes | Temperate deciduous forest | Increase[b] | | Clifton et al. (2019) |
| | 7 months of ozone EC fluxes | | Decrease (day), increase (night) | Increase (day), no change (night) | Finkelstein et al. (2000) |
| | | | Increase | Increase | L. Zhang et al. (2002) |
| Les Landes (44°12′N, 0°42′W) | 2 months of ozone EC fluxes from 2 years | Temperate coniferous forest | | Increase | Lamaud et al. (2002) |
| Nashville (36.65°N, 87.03°W) | 5 months of ozone EC fluxes | Soybean | Decrease | | L. Zhang et al. (2002) |
| Niwot Ridge (40.03°N, 105.55°W) | 3 to 7 months of ozone EC fluxes from 4 years each | Subalpine coniferous forest | increase | | Turnipseed et al. (2009) |
| Rush | 1 day of ozone EC fluxes | Senescent maize | | Decrease[a] | Wesely et al. (1978) |
| Sand Flats State Forest (43.565°N, 75.238°W) | 4 months of ozone EC fluxes | Temperate mixed forest | Increase[b] | | Clifton et al. (2019) |
| | 6 months of ozone EC fluxes | | Increase (day), no change (night; high LAI), increase (night; low LAI) | Increase (day), no change (night; high LAI), increase (night; low LAI) | Finkelstein et al. (2000) |
| | | | Increase | Increase | L. Zhang et al. (2002) |
| Sand Mountain (34.29°N, 85.97°W) | 2 months of ozone EC fluxes | Pasture | Decrease (day), increase (night) | Increase | L. Zhang et al. (2002) |
| Sangamon, Illinois | 2 days of ozone EC fluxes | Healthy maize | | Decrease[a] | Wesely et al. (1978) |

[a]Findings may be particularly uncertain due to low signal-to-noise ratio or authors do not calculate systematic differences (e.g., average over composites). [b]Study does not attribute changes, or all changes, to cuticular uptake.

compounds) contributing to ozone reactivity. We find that the dominant reactivity sources on cuticles needs to be established.

Depending on leaf size and shape, up to 50 μg $cm^{-2}$ of aerosols can accumulate on leaves (Burkhardt, 2010; Popek et al., 2013; Sæbø et al., 2012). In the laboratory study of S. Sun, Moravek, Trebs, et al. (2016), ozone uptake is highest for leaves either exposed to outdoor air or sprayed with a solution containing major inorganic components of typical continental aerosols relative to the other treatments (Figure 6), suggesting cuticular uptake through reaction with deposited aerosols may be important. However, evidence from kinetic studies on soot, mineral dust, and proxies for organic aerosols shows rapid declines in ozone uptake after high initial uptake (Chapleski et al., 2016; Disselkamp et al., 2000; Hanisch & Crowley, 2003; Karagulian & Rossi, 2006; McCabe & Abbatt, 2009), implying persistent ozone uptake requires sustained aerosol deposition to cuticles. The exception is uptake by organic photosensitizers (e.g., humic acid) in light (D'Anna et al., 2009; Jammoul et al., 2008).

Cuticular waxes mostly contain compounds derived from long-chain fatty acids unreactive with ozone but can contain unsaturated compounds (Buschhaus & Jetter, 2012; Jetter et al., 2006; Yeats & Rose, 2013) reactive with ozone. Clean cuticles have low but nonnegligible ozone uptake at relative humidity higher than 40% (Figure 6), but there is negligible cuticular uptake on the same species for lower humidity (S. Sun, Moravek, Trebs, et al., 2016) as well as on different species at 65% relative humidity (Omasa et al., 2000). While Fares et al. (2007) suggest negligible cuticular uptake by two tree species in their laboratory study, stomatal uptake does not fully explain ozone uptake for one of the species. Whether some species' waxes provide substantial ozone sinks, and whether this changes with environmental conditions like humidity, is unclear.

Compounds exuded by the plant, whether the compounds are sorbed BVOCs or organic compounds leached out of stomata, may contribute to ozone reactivity on the cuticle. Laboratory evidence and mechanistic modeling suggest that ascorbate leaching out of stomata on wet leaves may be an important contributor to ozone reactivity for some plant species and phenological states (Potier et al., 2015, 2017). Laboratory studies show conflicting evidence as to whether sorbed BVOCs may be an effective cuticular ozone sink. For example, high cuticular uptake due to reaction with sorbed α-pinene on waxes is not supported by Cape et al. (2009), but exuded terpenoids efficiently react on the cuticle with ozone in Jud et al. (2016).

#### 4.2.3. Modeling Ozone Dry Deposition to Leaf Cuticles

Models for ozone dry deposition to cuticles are largely empirical and stem from sparsely available laboratory and field measurements. Many models include only LAI and a tuning factor (e.g., Massman, 2004). Several models distinguish deposition between wet and dry cuticles, but there are differences across models in the direction of the simulated response. For example, Wesely (1989) prescribes a lower cuticular deposition when leaves are wet, but L. Zhang et al. (2002) prescribe higher cuticular deposition when leaves are wet. Some models include a dependence on relative humidity (Altimir et al., 2004; Clifton, 2018; Lamaud et al., 2009; Stella, Personne, et al., 2011; L. Zhang et al., 2002), which may represent the effect of thin water films on leaves.

We use mechanistic modeling to explore strengths and weaknesses of the simple approaches outlined above. The mechanistic equation for resistance to deposition through heterogeneous reaction of ozone on dry cuticles ($r_{cut,dry}$) (s $m^{-1}$) in a big-leaf approach follows

$$r_{cut,dry} = \frac{1}{\frac{1}{4} K_d \sqrt{\frac{8RT_{leaf}}{\pi M_{O_3}}} f_{dry} LAI}. \quad (14)$$

$K_d$ is the cuticular deposition coefficient (unitless), which is a measure of the probability that ozone reacts upon contact with the cuticle; $R$ is the universal gas constant (8.314 J $mol^{-1}$ $K^{-1}$); $T_{leaf}$ is leaf temperature (K); $M_{O_3}$ is the ozone molecular mass (0.048 kg $mol^{-1}$); $f_{dry}$ is the dry fraction of the leaf (unitless); and $LAI$ is leaf area index ($m^2$ $m^{-2}$). The model expressed by equation (14) simulates collision and reaction of a gas with a surface analogously to heterogeneous chemistry in the atmosphere (e.g., Jacob, 2000). While $K_d$ is challenging to infer at the ecosystem scale, the model expressed by equation (14) is structurally simple and relatable to existing approaches.

For the resistance to deposition to wet cuticles ($r_{\mathrm{cut,wet}}$; s m$^{-1}$) from either thin water films or droplets from rain or dew, Potier et al. (2015) present a physically based model based on the diffusion-reaction equation. We derive a form of this model in Appendix B and review its physical underpinnings. The following model represents ozone dissolution in the water on a cuticle and reaction with compounds in the water in a big-leaf approach:

$$r_{\mathrm{cut,wet}} = \frac{1}{k_H^{CC}\Gamma_{aq}D_{O_{3,aq}}\tanh\left(\Gamma_{aq}\delta_d\right)\left(1-f_{\mathrm{dry}}\right)LAI}. \quad (15)$$

$k_H^{cc}$ is the dimensionless Henry's law constant for ozone; $\Gamma_{aq} = \sqrt{\frac{\kappa^{aq}}{D_{O_{3,aq}}}}$; $\kappa^{aq}$ is the first-order reaction rate of ozone in the water mixture on the leaf (s$^{-1}$); $D_{O_{3,aq}}$ is the ozone diffusivity in water (m$^2$ s$^{-1}$); and $\delta_d$ is the thickness of the wetness on the cuticle (m).

Representation of reactivity on a cuticle is likely critical to model cuticular ozone dry deposition accurately. The fastest gain in understanding will likely happen when knowledge from studies on plant physiology and aerosol dry deposition is leveraged for information about cuticular composition (e.g., cuticular wax, deposited aerosols, and compounds exuded from stomata) and changes in time and space.

As is, this model's utility in representing ozone uptake by wet cuticles at large scales hinges on whether input variables can be estimated adequately (e.g., $\delta_d$ and $\kappa^{aq}$). We recommend exploring the model parameter space (e.g., $r_{\mathrm{cut,wet}}$ sensitivity to different inputs).

For both dry and wet cuticular deposition modeling, whether one- or two-sided LAI should be used depends on the source of wetness and reactivity as well as whether the plant has stomata on a single side of the leaf or both sides (i.e., if the model considers stomatally exuded compounds to be an important source of reactivity).

Ozone destruction on cuticles may decrease stomatal ozone uptake (Jud et al., 2016; Kanagendran et al., 2018), and thus, there may be interactions between stomatal and cuticular deposition. While the theoretical modeling of Jud et al. (2016) indeed shows cuticular ozone uptake reduces stomatal ozone uptake, the theoretical modeling of Altimir et al. (2008) shows stomatal ozone uptake is only reduced by unrealistically high cuticular ozone uptake. Because interactions between stomatal and cuticular uptake challenge assumptions underlying current modeling frameworks representing pathways as independent (e.g., Altimir et al., 2008; Jud et al., 2016), a better understanding of such interactions is warranted.

#### 4.2.4. Main Takeaways

1. Most field and laboratory studies support aqueous heterogeneous chemistry dominating cuticular ozone uptake, but there may be a role for thermal decomposition of ozone on cuticles, especially at low humidity.
2. The observed dependence of cuticular uptake on relative humidity likely represents surface water films promoting aqueous chemistry.
3. Representation of reactivity on a cuticle is likely critical to model cuticular ozone dry deposition accurately.
4. We derive models for mechanistic representation of ozone dry deposition to cuticles. We recommend further exploration of these mechanistic cuticular deposition models and their ability to represent uptake at large scales.

### 4.3. Soil

#### 4.3.1. Controls on Ozone Dry Deposition to Soil: Field, Modeling, and Laboratory Evidence

While a dominant pathway for ozone dry deposition to soil is considered to be reaction with unsaturated carbon bonds in soil organic material (e.g., Sorimachi & Sakamoto, 2007), mean daytime $v_d$ of ~0.1 cm s$^{-1}$ from a short-term field campaign in the Sahara Desert suggests ozone reaction with soil organic material is not the only soil deposition pathway (Güsten et al., 1996). It is possible thermal decomposition of ozone occurs on soil surfaces or gas-phase loss of ozone in soil pore spaces occurs through reaction with NO or BVOCs.

Evidence from eight field studies (Table 3), including one field chamber study (Fumagalli et al., 2016), and four laboratory-based studies (Aldaz, 1969; Sorimachi & Sakamoto, 2007; Toet et al., 2009; Turner et al.,

Reviews of Geophysics

10.1029/2019RG000670

**Table 3**
*Summary of Field Studies Examining the Response of Soil Ozone Dry Deposition to Soil Moisture (or a Related Quantity)*

| Site name | Measurement period and type | Site description | Sign of change for ozone dry deposition | Details | Reference |
|---|---|---|---|---|---|
| Braunschweig (53°18′N, 10°26′E) | 1 month of ozone EC fluxes | Cut and fertilized grassland | Decrease | Inferred from increases in ozone deposition following decrease in soil moisture | Mészáros, Horváth, et al. (2009) |
| Castelporziano (41.42°N, 12.21°E) | 2 months of subcanopy ozone EC fluxes | Urban forest | Decrease | Inferred from correlation between measured and modeled ozone flux below the canopy for mean diel cycle (model includes effect of soil water content on ozone dry deposition to soil) | Fares et al. (2014) |
| Central Plains Experimental Range (40°28′23″N, 104°45′15″W) | 2 years of ozone EC fluxes | Grassland | Decrease | Inferred based on comparison between two different years (one with wetter soil and one with drier soil) | Massman (1993), Stocker et al. (1993), and Massman (2004) |
| Grignon (48.84422°N, 1.95191°E) | 3 months of ozone EC fluxes | Bare agricultural soil | Decrease | Inferred from correlation between soil water content and $r_{soil}$[a] | Stella, Loubet, et al. (2011) |
| | 1 month of ozone EC fluxes | Bare agricultural soil | Increase | Increased ozone uptake by soil after rainfall (attributed increases to tillage and slurry application) | Vuolo et al. (2017) |
| Flanders (51°18′N, 4°31′E) | 10 years of ozone fluxes from flux gradient technique | Temperate mixed forest | Decrease | Inferred from correlation between $v_d$ and ground water table depth | Neirynck and Verstraeten (2018) |
| Harvard Forest (42.53°N, 72.18°W) | 9 years of ozone EC fluxes | Temperate deciduous forest | Decrease | Inferred from anticorrelation between summertime mean $v_d$ and cumulative rain over summer and modeling | Clifton et al. (2019) |
| Ispra (45.8126°N, 8.6336°E) | 1 year of ozone chamber flux measurements | Temperate deciduous forest | Decrease | Inferred from correlation between soil water content and $r_{soil}$ | Fumagalli et al. (2016) |
| Sinderhoeve (51.58°N, 5.42°E) | 10 days of ozone EC fluxes | Cornfield | Decrease | Inferred based on decreases in nonstomatal deposition with soil moisture | Van Pul and Jacobs (1994) |
| Walker Branch Watershed (35°57′30″N, 84°17′15″W) | 2 weeks in spring and 2 weeks in fall 1988 of ozone EC fluxes above soil | Mixed forest | No change | Data not shown; only concluded | Meyers and Baldocchi (1993) |
| Huntington Forest (43°59′N, 74°14′W) | 10 days in July 1990 of ozone EC fluxes above soil | Temperate deciduous forest | No change | Data not shown; only concluded | Meyers and Baldocchi (1993) |

[a] $r_{soil}$ is the resistance to ozone dry deposition to soil.

1973) suggests soil moisture inhibits ozone uptake by limiting diffusion through soil pore spaces. Decreases in soil ozone uptake with increasing soil moisture suggest moisture reduces surface area available for reaction with ozone, overriding any effect of moisture promoting heterogeneous chemistry (e.g., as observed on leaf cuticles). Indeed, employing the isotopic method discussed in section 2.2.3 to constrain ozone uptake by soil versus soil pore water, Toet et al. (2009) show ozone deposition to soil pore water is a substantial fraction of soil ozone uptake at 60% soil moisture but much lower than ozone uptake by soil at 30% soil moisture where it is only a small fraction of the total (<10%).

Short-term observed ozone EC fluxes above bare agricultural soils and a semiarid plain in Europe show an exponential decrease in soil ozone uptake with near-surface relative humidity (Stella et al., 2019) stronger than the relationship with soil water content for at least one of the sites (Stella, Loubet, et al., 2011). Stella, Loubet, et al. (2011) hypothesize surface relative humidity better indicates the water molecules on the ground preventing ozone from entering soil, relative to soil water content at a shallow depth. Stella et al. (2019) suggest variation in the relationships between soil ozone uptake and near-surface relative humidity among the six sites examined is caused by soil clay content because clay is a structural indicator of available surface area (e.g., Hillel, 1980) and clay modifies the amount of water in soil. In particular, regression analysis suggests the magnitude of soil uptake increases with soil clay content, but soil uptake decreases more quickly with surface relative humidity in soils with more clay content (Stella et al., 2019). Whether these findings hold more generally needs to be established.

#### 4.3.2. Modeling Ozone Dry Deposition to Soil

Ozone dry deposition to soil is often constant in large-scale models, sometimes varying by LULC type and season (e.g., Wesely, 1989). Most studies creating models for soil ozone dry deposition use short-term data. Massman (2004) compiles resistances to ozone dry deposition to soil ($r_{soil}$) inferred from observations, suggesting 100 s $m^{-1}$ for dry soil and 500 s $m^{-1}$ for wet soil. Later site-specific work defines similar empirical models (Bassin et al., 2004; Clifton et al., 2019; Fares et al., 2012, 2014; Mészáros, Horváth, et al., 2009), but studies more directly isolating $r_{soil}$ support stronger dependencies on soil moisture (Fumagalli et al., 2016) or surface relative humidity (Stella, Loubet, et al., 2011; Stella et al., 2019). Whether simple models accurately capture $r_{soil}$ magnitude and variability on a variety of scales is uncertain. Uncertainty may stem in part from a lack of observational constraints on $r_{soil}$ spatiotemporal variability.

To better understand processes governing soil ozone uptake and provide a roadmap for more robust empirical modeling, we present a more mechanistic model of $r_{soil}$ (derivation in Appendix B). The model represents ozone reaction with surfaces in soil and gases in soil pore spaces:

$$r_{soil} = \left[ \left( A K_d \frac{1}{4} \sqrt{\frac{8RT_{soil}}{\pi M_{O_3}}} + \sum_i K_{X_i,O_3} X_{i,soil} \right) \left( (\eta - \theta) \tau D_{O_3} \right) \right]^{-\frac{1}{2}}. \quad (16)$$

$A$ is surface area on which ozone dry deposition occurs per unit volume of the porous media ($m^2\ m^{-3}$); $K_d$ is a measure of the probability that an ozone molecule reacts once it comes into contact with the surface (unitless); $R$ is the universal gas constant (8.314 J $mol^{-1}\ K^{-1}$); $T_{soil}$ is soil temperature (K); $M_{O_3}$ is the ozone molecular mass (0.048 kg $mol^{-1}$); $K_{X,O_3}$ is the rate coefficient (ppmv $s^{-1}$) for chemical ozone destruction in soil pore spaces by gas species $X_{soil}$ (ppmv); $\eta$ is the volumetric air-filled soil pore space when completely dry ($m^3\ m^{-3}$); $\theta$ is volumetric soil moisture ($m^3\ m^{-3}$); $\tau$ is the soil tortuosity factor ($0 < \tau < 1$; unitless; a measure of how many paths ozone can take in soil); and $D_{O_3}$ is ozone diffusivity in air ($m^2\ s^{-1}$).

The utility of this model in representing soil ozone uptake hinges on whether (i) all relevant processes are represented accurately and (ii) model input variables can be estimated adequately. In terms of (i), the model assumes neither obstruction to transport into soil nor any thermal decomposition or aqueous ozone reaction in soil. Based on mechanistic modeling, we suggest the contribution of thermal decomposition may be important (see Appendix B). The results of Toet et al. (2009) also imply aqueous ozone reaction in soil at low soil moisture may dominate.

In terms of (ii), most of the inputs likely require a fair amount of parameterization and thus are uncertain. We should be able to leverage understanding of some input variables and parameters from the fields of soil

physics and chemistry. We recommend sensitivity analyses with the model expressed in equation (16) to identify the parameters and variables driving modeled variations under different conditions.

We also recommend more measurements of soil ozone uptake to constrain the observed driver(s) of soil ozone uptake under a given environmental condition and further parameterize and evaluate the model expressed in equation (16). Our synthesis indicates capturing ozone's ability to diffuse into and through soil pore spaces is key. Models should thus consider soil moisture as a limiting factor. Useful constraints on soil ozone uptake include ozone EC fluxes at heights in the lower canopy and over bare soil and chambers on the ground (e.g., Finco et al., 2018; Launiainen et al., 2013; Stella et al., 2019).

#### 4.3.3. Main Takeaways

1. Observations suggest soil moisture decreases ozone uptake by soil, hindering ozone's ability to diffuse into soil and through soil pore spaces.
2. The dominant pathway for soil ozone uptake is likely reaction with organic matter, but the contributions of thermal decomposition, aqueous chemistry, and reaction with gaseous compounds in soil cannot currently be discounted.
3. We derive a model for mechanistic representation of ozone dry deposition to soil. We recommend reconciling mechanistic and empirical modeling approaches and additional observational constraints on soil ozone uptake both in terms of longer data sets and representation of more ecosystems.

### 4.4. Turbulence

Atmospheric turbulence is generated by either shear or buoyancy forces, and complex surface elements (e.g., vegetation) drive stronger and more variable turbulence enhancing contact between air parcels and surfaces. Turbulence moves air and transports ozone-rich air parcels toward the surface and thus is fundamental to ozone's ability to deposit. Correlations between friction velocity and $v_d$ or ozone flux (El-Madany et al., 2017; Fares et al., 2014; Lamaud et al., 2002; Neirynck et al., 2012; Van Pul & Jacobs, 1994) indeed suggest turbulent transport is an important, and sometimes limiting, driver of ozone dry deposition.

Over vegetation, turbulent eddies of size similar to the canopy drive most of the exchange between the canopy and atmosphere, as well as among canopy layers (e.g., Gao et al., 1989; Patton & Finnigan, 2013). Fluid flow interacting with a canopy is hydrodynamically unstable, which produces eddies observed as combinations of sweeps of air from above the canopy penetrating into the canopy and bursts of air ejecting canopy air into the atmospheric surface layer above (e.g., Finnigan et al., 2009; Raupach et al., 1996). These bursts and sweeps facilitate uptake of trace gases and also lead to segregation of air masses in the canopy (e.g., Dupont & Patton, 2012; Patton et al., 2016; Steiner et al., 2011; Thomas & Foken, 2007).

Transfer of trace gases from the surface layer to the surface is typically modeled with MOST, an empirical formation based on dimensional analysis that accounts for atmospheric stability influences on near-surface turbulence and holds in the inertial sublayer. Different empirical formulations of MOST may contribute to differences among air quality models in simulated $v_d$ under stable conditions (Toyota et al., 2016).

There are substantial limitations to modeling approaches utilizing MOST to simulate canopy-atmosphere exchange. The underlying assumptions of MOST fail in the roughness sublayer above a plant canopy that can extend up to two to three canopy heights (e.g., Cellier & Brunet, 1992; Harman & Finnigan, 2007; Thom, 1975). Recent observations at the Amazon Tall Tower Observatory suggest the roughness sublayer above the forest merges directly into the mixed layer and does not even form the inertial sublayer where MOST is valid (Dias-Júnior et al., 2019). Another issue is many forest canopies reside in hilly or mountainous terrain, but MOST assumes horizontal homogeneity.

Multilayer canopy models are typically limited in simulating vertical exchange among canopy layers, but simulated turbulence in these models influences the canopy distribution of ozone and thus dry deposition and ambient chemistry. Most multilayer canopy models employ K-theory (Ashworth et al., 2015; Bryan et al., 2012; Ganzeveld et al., 2002; Stroud et al., 2005; Wolfe & Thornton, 2011; P. T. Zhou et al., 2017), which does not realistically simulate turbulence in a complex canopy environment. Some multilayer canopy models (Bryan et al., 2012; Stroud et al., 2005; Wolfe & Thornton, 2011) include near-field approximations (Makar et al., 1999), which leverage the Lagrangian perspective of dispersion in a canopy outlined by Raupach (1989). However, near-field parameterizations are designed for neutral stability conditions, and

their utility hinges on whether observed wind profiles and turbulence statistics can be prescribed (Harman & Finnigan, 2008).

The multilayer canopy model described by Bonan et al. (2018) with the Harman and Finnigan (2007, 2008) analytic roughness sublayer mixing scheme shows potential for prognostic simulation of canopy vertical exchange. While the Harman and Finnigan (2007, 2008) scheme relies on K-theory, its introduction of a length scale associated with the turbulent eddies produced by wind shear at the canopy top incorporates the influence of countergradient transport. Bonan et al. (2018) find that the Harman and Finnigan (2007, 2008) scheme improves simulation of friction velocity and ambient temperature at several forest and grassland sites. With a multilayer canopy large eddy simulation (LES) model explicitly resolving turbulence above and in a forest canopy, Patton et al. (2016) show atmospheric stability exerts a control on vertical exchange at the top of the canopy through the structure of the atmospheric boundary layer, suggesting roughness sublayer parameterizations consider the effect.

The representation of in-canopy turbulence is also limited in big-leaf dry deposition schemes. For example, in the Wesely (1989) scheme, there are two resistances to in-canopy turbulence, one for lower-canopy deposition and the other for soil uptake. Wesely (1989) defines a simple model based on solar radiation and slope of the terrain for the former and prescribes constants that vary with LULC type and season for the latter.

Later big-leaf schemes (e.g., Clifton, 2018; Emberson, et al., 2000; Erisman et al., 1994; Paulot et al., 2018; Pleim & Ran, 2011; L. Zhang et al., 2002, 2003) do not include deposition to the lower canopy and adopt or modify a model employing LAI, friction velocity, and canopy height based on 6 days of afternoon ozone fluxes over a corn field (Van Pul & Jacobs, 1994) for turbulent transport to the ground. As mentioned, several studies indeed find friction velocity as a driver of variation in ozone dry deposition (El-Madany et al., 2017; Fares et al., 2014; Lamaud et al., 2002; Neirynck et al., 2012). However, a site-specific model like Van Pul and Jacobs (1994) may not capture variability in the resistance to canopy turbulence across different landscapes and boundary-layer conditions. For example, daytime transport timescales near the ground over a grassland constrained with radon and thoron isotopes are 50% too low with the Van Pul and Jacobs (1994) model (Plake & Trebs, 2013). In general, multilayer canopy LES models offer an opportunity to explore how turbulent transport influences ozone dry deposition and refine parameterizations.

While most observational constraints on canopy turbulence are from sonic anemometers above the canopy, some recent studies employ sonic anemometers at multiple vertical or horizontal locations (e.g., Finco et al., 2018; Fuentes et al., 2016; Patton et al., 2011) to advance understanding of canopy turbulence and its impact on vertical exchange of trace gases. For example, Finco et al. (2018) use multiple sonic anemometers and fast ozone analyzers in the vertical at Bosco Fontana to pinpoint the distribution of ozone sinks in the canopy. Using profile measurements of ozone concentrations and turbulence statistics at a tropical forest, Freire et al. (2017) suggest the ozone concentration profile is primarily a function of turbulent mixing, although the authors only consider a single depositional sink for the entire canopy. Isotopic measurements of thoron and radon also offer constraints on turbulent transport near the ground in a plant canopy (Plake & Trebs, 2013), which may be useful in interpreting ozone flux measurements (e.g., separating ozone dry deposition to soil from canopy sinks).

#### 4.4.1. Main Takeaways

1. Turbulence is inherently fundamental to ozone's ability to deposit.
2. Constraints on turbulent transport are useful for interpreting observed ozone fluxes and establishing the relative importance of a given deposition pathway.
3. Current models for turbulent transport used to estimate or interpret measurements of ozone fluxes may not capture the magnitude or variability of transport accurately.
4. Explicitly resolving above- and in-canopy turbulence in models such as LES should be used to improve current turbulent transport parameterizations.

### 4.5. Fast Ambient Chemistry

While ambient chemistry is not technically ozone dry deposition, fast ambient chemistry influences observed ozone fluxes. We emphasize fast here because the timescale over which ambient chemistry operates is central to its influence on ozone fluxes. The rule of thumb is chemical reactions below the measurement height (hereafter, “in canopy”) must occur on timescales equivalent to or faster than the canopy residence time determined by turbulent transport to influence the ozone flux.

Timescales for turbulent transport ($\tau_{trans}$) and chemical reactions ($\tau_{chem}$) can be compared via the Damköhler number ($D_a$; Damköhler, 1940; Lenschow, 1982; Lenschow & Delany, 1987; Vilá-Guerau de Arellano, 2003; Vilá-Guerau de Arellano & Duynkerke, 1992):

$$D_a = \frac{\tau_{trans}}{\tau_{chem}}. \quad (17)$$

If $D_a$ is greater than 1, then chemistry can be a major influence on observed ozone fluxes; if $D_a$ is between 0.1 and 1, then the influence of chemistry should be moderate, while if $D_a$ is less than 0.1, then turbulent transport dominates, and the influence of chemistry should be negligible. If $D_a = 1$, then segregation (i.e., the spatial separation of reactants in the canopy by organization in turbulence) becomes a factor depending on the source (and likely sink) distributions of the reactants (e.g., Patton et al., 2001). However, $D_a$ does not always present an accurate picture of chemistry's influence on ozone fluxes; multilayer canopy modeling shows chemistry slower than turbulence (e.g., $D_a = 0.03$) still alters the ozone flux (Wolfe et al., 2011). Nonetheless, $D_a$ helps to establish which reactive gases are involved in chemistry relevant to interpreting ozone fluxes.

In considering fast ozone loss through reaction with NO, it is important to consider NO-$NO_2$-$O_3$ chemistry, which occurs on the timescale of turbulence (Duyzer et al., 1983; Van Aalst, 1982) and consists of the following reactions:

$$\begin{aligned} &\text{R1} \quad O_3 + NO \rightarrow NO_2 + O_2, \\ &\text{R2} \quad NO_2 + h\nu \rightarrow NO + O(^3P), \\ &\text{R3} \quad O_2 + O(^3P) \rightarrow O_3. \end{aligned}$$

Reaction with NO leads to a permanent ozone sink when $NO_2$ is oxidized to higher nitrogen oxides (Min et al., 2012, 2014; Turnipseed et al., 2006; Wolfe et al., 2009) or taken up by stomata (Delaria et al., 2018; Bakwin et al., 1990; Plake, Stella, et al., 2015; Rummel et al., 2002) and serves as a temporary reservoir if $NO_2$ is photolyzed and ozone is reformed. In a shaded forest canopy, photolysis of $NO_2$ (i.e., R2) is expected to be low. In general, the effects of R1 on ozone fluxes are usually small (Kramm et al., 1995; Plake, Sörgel, et al., 2015; Rannik et al., 2009; Stella et al., 2012; Vuolo et al., 2017) because there is typically much more ozone than $NO_x$ (=NO + $NO_2$). However, some studies suggest R1 accounts for a nonnegligible influence on observed ozone fluxes (Dorsey et al., 2004; Finco et al., 2018; Lamaud et al., 2009; Neirynck & Verstraeten, 2018; Rummel et al., 2007), especially at night when there is relatively high $NO_x$.

The contribution of NO-$NO_2$-$O_3$ chemistry to observed ozone fluxes can be estimated with ozone, NO, and $NO_2$ fluxes at two heights (Finco et al., 2018; Fitzjarrald & Lenschow, 1983; Lenschow & Delany, 1987; Vilá-Guerau de Arellano et al., 1993). An empirical technique only requiring flux measurements at one height (Duyzer et al., 1995) has also been used (e.g., Plake, Sörgel, et al., 2015; Stella et al., 2012; Vuolo et al., 2017). This empirical technique assumes flux divergences of NO, $NO_2$, and ozone are logarithmic with height, but the theoretical basis for this assumption is lacking. Both techniques may be limited with respect to key assumptions: first-order closure and negligible influence from other in-canopy chemical reactions. More explicitly resolving interactions between in-canopy turbulence and ambient chemistry (e.g., through LES modeling) will allow for stronger constraints on the influence of fast chemistry on ozone fluxes.

Some sesquiterpenes, such as $\beta$-caryophyllene and $\alpha$-humulene, and monoterpenes, such as $\alpha$-terpinene, react very quickly with ozone (Calogirou et al., 1999; Shu & Atkinson, 1994; Yee et al., 2018) and constitute a permanent ozone sink. Reactions of these compounds with ozone may account for a nonnegligible fraction of the observed ozone flux (Bouvier-Brown et al., 2009; Fares, McKay, et al., 2010; Fares et al., 2012; Goldstein et al., 2004; Holzinger et al., 2005; Helmig et al., 2006; Kurpius & Goldstein, 2003; Jardine et al., 2011; Wolfe et al., 2011). However, the ability to constrain the relative contribution of chemistry is limited by a lack of comprehensive isomer-resolved BVOC measurements and uncertainty in rates for reaction with ozone (Bouvier-Brown et al., 2009; Goldstein et al., 2004; Shu & Atkinson, 1994; Yee et al., 2018). Sesquiterpenes are difficult to measure due to their low volatility, which leads to underestimates from the

loss on sampling lines and instrument surfaces, and to their low concentrations, which require sensitive detection and/or lower time resolution methods.

Supporting evidence for the influence of highly reactive BVOCs on observed ozone fluxes is largely based on observations and modeling at Blodgett Forest in the Sierra Nevada Mountains of California. Evidence includes (i) a dependence of observed ozone fluxes on air temperature consistent with monoterpene emissions from vegetation (Kurpius & Goldstein, 2003; Fares, McKay, et al., 2010), (ii) similar enhancements in ozone fluxes and monoterpene concentrations following forest thinning (Goldstein et al., 2004), (iii) direct measurements of oxidation products (Holzinger et al., 2005), and (iv) multilayer canopy modeling (Wolfe et al., 2011). Constraints on highly reactive chemistry at other sites, in combination with large-scale modeling, are needed to understand the large-scale impact of ambient ozone loss through reaction with highly reactive BVOCs on observed ozone fluxes.

Substantial soil emissions of highly reactive sesquiterpenes are observed at an Amazonian forest (Bourtsoukidis et al., 2018). While measurements at other locations are needed to understand whether this phenomenon occurs elsewhere, neglecting a soil source of highly reactive BVOCs in interpreting ozone fluxes may lead to an overemphasis of the role of other processes.

In-canopy ambient chemistry impacts not only ozone but also other molecules. Reactions between ozone and highly reactive BVOCs may account for observed emission of oxidized organic species from the canopy (Alwe et al., 2019; Choi et al., 2010; Holzinger et al., 2005; Schobesberger et al., 2016) and subsequent secondary organic aerosol formation (Bouvier-Brown et al., 2009; Buzorius et al., 1998; Farmer et al., 2011; Goldstein et al., 2009; Wolfe et al., 2011), production of the hydroxyl radical (Faloona et al., 2001; Kurpius & Goldstein, 2003), and emission of reactive nitrogen oxides (Farmer & Cohen, 2008; Wolfe et al., 2009). Fluxes of oxidized organic and inorganic compounds may provide observational constraints on the location and mechanism of chemical influences on observed ozone fluxes.

#### 4.5.1. Main Takeaways

1. Fast ambient chemistry confounds ozone dry deposition estimates from ozone flux observations.
2. Observed colocated fluxes of ozone and highly reactive compounds and models resolving their in-canopy distributions and fluxes are needed to estimate the influence of fast chemistry on ozone fluxes.
3. Analytical challenges and uncertain reaction rates limit knowledge on the contribution of highly reactive BVOCs to observed ozone fluxes.

### 4.6. Snow-Covered Surfaces

Ozone deposition velocities over snow are typically low relative to the other terrestrial surfaces considered in this review but are highly uncertain. The range of observed $v_d$ over snow from both field and laboratory studies is −3.6 to 1.8 cm $s^{-1}$ with most of the data from 0 to 0.1 cm $s^{-1}$ (Figure 7).

The slowest observed $v_d$ are over polar snowpack (both glacial and sea ice), suggesting ozone uptake to snow-covered landscapes is not primarily controlled by snow presence. While ozone destruction by snow grains may be slow, the transport of air through snowpack (a porous medium with high surface area) to the bottom (Helmig, Bocquet, et al., 2007) occurs on timescales of minutes to hours, allowing ozone destruction through reaction with surfaces within or underneath the snowpack. Snow-covered forests exhibit the fastest $v_d$ relative to other snow-covered surfaces, followed by snow-covered grassland and soils (Figure 7).

Hypothesized or identified pathways for ozone dry deposition over snow-covered surfaces include reaction with organic or humic trace impurities, black carbon (Albert et al., 2002), and halogens (Peterson & Honrath, 2001). Based on snowpack chemical and transport modeling, reaction with bromine (Thomas et al., 2011) and formic acid in the aqueous phase (Murray et al., 2015) may be ozone deposition pathways for snow on glacial ice. In environments where vegetation protrudes from the snow, ozone uptake by biological materials may be the determining ozone sink.

For seasonally deep snowpack at midlatitudes, snowpack insulates the ground, promoting relatively warm and moist soil conditions that foster soil microbial processes resulting in a steady production and emission of NO. For example, interstitial air is enriched in NO by a factor of up to ~100 compared to the air above the surface at Niwot Ridge (Helmig, Seok, et al., 2009). Snowpack reaction between ozone and NO under low light conditions when $NO_2$ photolysis does not occur may be a primary route for ozone loss in this type of

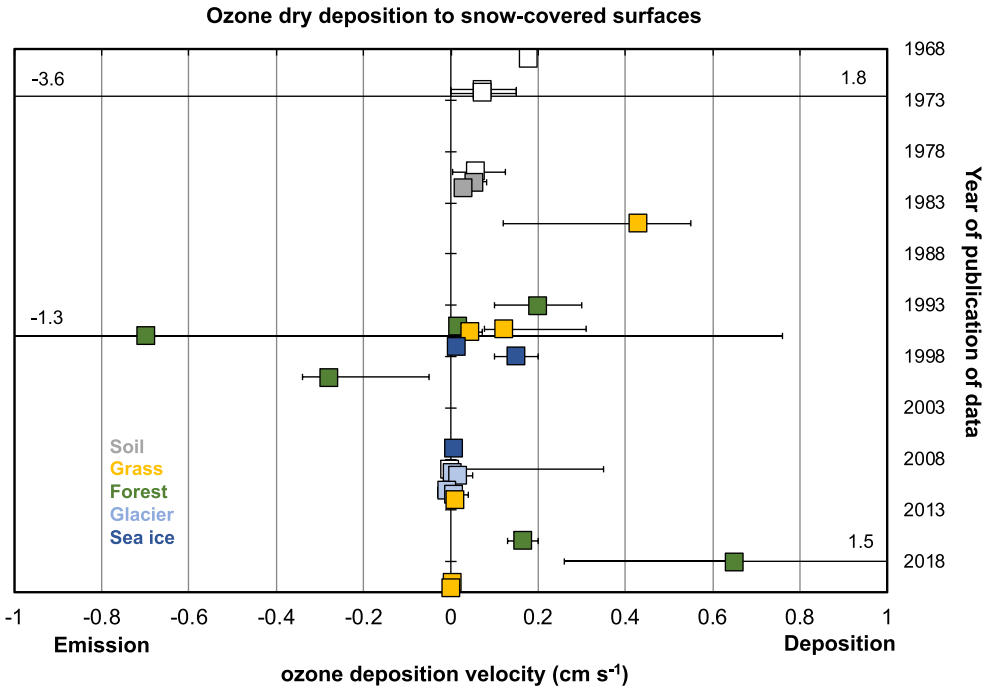


**Figure 7.** Range of ozone deposition velocities observed or inferred from observations over snow-covered surfaces. The vertical order of symbols reflects the year of the publication featuring the data (we impose small *y* axis shifts for multiple years with publications). Colors indicate land use/land cover type underneath the snow. Symbols without color indicate unspecified underlying land use/land cover type or laboratory measurements. Error bars are the range of reported values, except for the forest point with 0.017 cm $s^{-1}$ for which the error bars are one standard deviation. Numbers represent the value of the error bar cutoff by the *x* axis range. Figure is adapted from Helmig, Ganzeveld, et al. (2007). Data included are laboratory studies (Aldaz, 1969; Galbally & Roy, 1980) and field studies from Mawson, Antarctica (Galbally & Allison, 1972), Mt. Buller, Australia (Galbally & Allison, 1972), Illinois (Wesely et al., 1981), Lancaster, England (Colbeck & Harrison, 1985), Camp Borden (Padro, 1993; Padro et al., 1992; Z. Wu et al., 2016), GLEES Brooklyn Lake (Zeller, 2000; Zeller & Hehn, 1995, 1996), Central Plains Experimental Range (Stocker et al., 1995), Ice Camp Narwahl (Gong et al., 1997), Alert, Canada (Hopper et al., 1998), Arctic (Helmig, Bocquet, et al., 2007), Bruneck in the Southern Alps (Cieslik, 2009), Summit Greenland (Bocquet et al., 2011; Helmig, Cohen, et al., 2009), Flanders (Neirynck & Verstraeten, 2018), and Horsepool in the Uintah Basin (unpublished).

environment. Currently, there are no observations of ozone dry deposition over snow-covered permafrost soils. Such observations may help establish $v_d$ over snow-covered soils without the contribution of ozone reaction with NO.

Ozone deposition velocity over snow-covered surfaces also exhibits a diel cycle, with maximum values in the afternoon (Helmig, Cohen, et al., 2009; Neirynck & Verstraeten, 2018). The processes driving the diel cycle are uncertain.

Most models apply a constant resistance for ozone dry deposition to snow regardless of environmental conditions and the substrate underneath the snowpack. As evident from $v_d$ variability for snow-covered surfaces (Figure 7), a single resistance does not describe ozone dry deposition over myriad snow-covered environments accurately. A more comprehensive parameterization likely requires accounting for dependencies on snow conditions, chemical snow properties, and substrate underneath snowpack. Variability in observed $v_d$ for a given LULC also emphasizes the need for observational constraints.

A range of approaches has been used to study ozone fluxes over snow, including observing ozone decay in chambers filled with snow (Aldaz, 1969; Galbally & Roy, 1980), the flux gradient technique (Bocquet et al., 2011; Colbeck & Harrison, 1985; Helmig, Cohen, et al., 2009; Neirynck & Verstraeten, 2018; Z. Wu et al., 2016), EC (Stocker et al., 1995; Zeller & Hehn, 1996; Zeller & Nikolov, 2000), and near-surface vertical profiles measured with an automated elevator system (Van Dam et al., 2010).

Low snowpack ozone fluxes challenge instrument resolution and thus uncertainty needs to be considered. Snow cover promotes thermal inversions in the surface layer that weaken turbulence and limit the applicability of micrometeorological techniques for flux measurements. Methods for measuring ozone in air withdrawn from snowpack are highly sensitive and promising for constraining the controls on and strength of ozone snowpack sinks (Bocquet et al., 2007; Helmig, Bocquet, et al., 2007; Seok et al., 2015; Van Dam et al., 2015).

Several studies report negative $v_d$ over snow-covered surfaces, suggesting emission from the surface (Galbally & Allison, 1972; Zeller & Hehn, 1996; Zeller & Nikolov, 2000). Relatively large negative $v_d$ in earlier work has not been reproduced recently (Figure 7), bringing up the question of whether older findings are influenced by earlier experimental approaches with higher uncertainty. We recommend emphasizing newer relative to older measurements due to the improvement of EC instrumentation and refinement of data-analysis protocols.

Recent high-resolution ozone flux measurements show consistently negative (but relatively small) nighttime $v_d$ at Summit in Greenland with increasingly negative values toward summer (Helmig, Cohen, et al., 2009). Snowpack is not a location of ozone production: Ozone in snowpack interstitial air is generally depleted compared to above the surface (Albert et al., 2002; Bocquet et al., 2007; Helmig, Bocquet, et al., 2007; Peterson & Honrath, 2001; Seok et al., 2015), and ozone is always destroyed in snow chamber experiments (Aldaz, 1969; Bottenheim et al., 2002). However, ozone production in the poorly mixed layer right above snow may occur following the accumulation of ozone precursor emissions from the snowpack and enhanced irradiance from snow (e.g., Crawford et al., 2001; Cristofanelli et al., 2018; Helmig et al., 2008; Legrand et al., 2009, 2016).

#### 4.6.1. Main Takeaways

1. There is strong variability in observed $v_d$ over snow-covered surfaces.
2. Accurate modeling of ozone dry deposition to snow-covered surfaces requires better understanding of dependencies on underlying substrate, snow conditions, and meteorology.
3. We recommend emphasizing relatively newer measurements due to the improvement of EC instrumentation and refinement of data-analysis protocols.

## 5. Simulating Ozone Dry Deposition in Regional and Global Models

Most ozone dry deposition schemes used in regional and global models employ big-leaf resistance networks (section 3) and rely on lookup tables for component resistances and changes with season and LULC type (e.g., Simpson et al., 2001; Wesely, 1989; L. Zhang et al., 2002). While environmental conditions (e.g., temperature or surface wetness) sometimes modify lookup values, there is rarely mechanistic representation of processes in dry deposition schemes. Incomplete process representation limits the fidelity of these schemes in simulating ozone dry deposition impacts on air pollution, ecosystems, and climate.

Wesely (1989) is the basis of many large-scale models' dry deposition schemes. The Wesely (1989) scheme was designed to represent regional and seasonal average conditions. However, observations from very short time periods at only a few field sites informed Wesely (1989) as well as later schemes (e.g., L. Zhang et al., 2002), calling into question whether climatological $v_d$ is represented accurately in these schemes. There is also hardly an emphasis on $v_d$ variations on timescales other than seasonal or diel (e.g., daily and interannual) in past scheme development, limiting our understanding of variations in ozone pollution.

Despite the similar structure of commonly used dry deposition schemes, $v_d$ varies strongly across models (Bela et al., 2015; Herwehe et al., 2011; Hardacre et al., 2015; Park et al., 2014; Z. Wu et al., 2011). For example, monthly $v_d$ varies by $\pm$20% across models in the Task Force on Hemispheric Transport of Air Pollution (HTAP) ensemble (Figure 8). Because most HTAP models identify as employing Wesely (1989), substantial intermodel variation emphasizes the need to critically assess the implementation of a given scheme as well as input uncertainty (e.g., LULC distribution). Strong $v_d$ variability across models leads to uncertainty in the tropospheric ozone budget (Wild, 2007) as well as model estimates of ozone pollution (e.g., Hogrefe et al., 2018; Walker, 2014) and plant damage.

Substantial $v_d$ differences also occur among different ozone dry deposition schemes (Schwede et al., 2011; A. Y. H. Wong et al., 2019; Z. Wu et al., 2018). For example, there are twofold to threefold $v_d$ differences among five schemes all driven by the same forcing data at Borden Forest in Canada (Figure 9). There are also

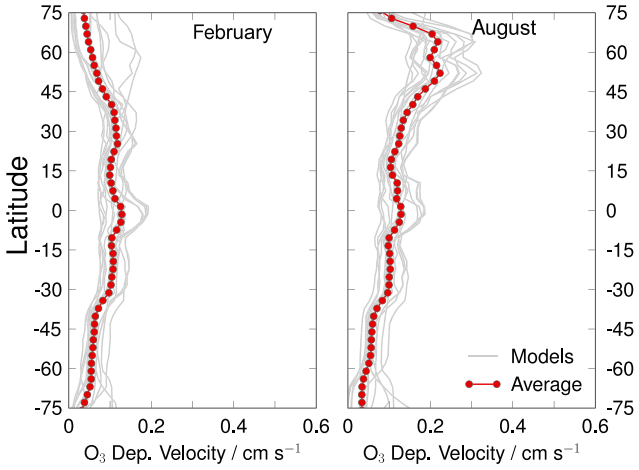


**Figure 8.** Variation in ozone deposition velocity across an ensemble of global models, most of which identify as using the Wesely (1989) scheme. Latitudinal averages per three degrees latitude band are shown. Gray lines indicate individual models participating in the Task Force on Hemispheric Transport of Air Pollution (HTAP) model intercomparison. Red circles show the multimodel average. Figure is from Hardacre et al. (2015).

large differences in summer interannual variability and 30-year trends in $v_d$ across four schemes implemented in one global atmospheric chemistry model (A. Y. H. Wong et al., 2019). Studies comparing schemes in depth (Schwede et al., 2011; Z. Wu et al., 2018) illustrate a variety of processes and parameters contributing to intermodel differences.

Improved understanding of parameter and process uncertainty in individual dry deposition schemes (Charusombat et al., 2010; Cooter & Schwede, 2000; Mészáros, Zsély, et al., 2009; Silva & Heald, 2018; Simpson et al., 2003; Tuovinen et al., 2001; Tuzet et al., 2011) is needed and will inform $v_d$ differences and similarities across models. We recommend archival of model diagnostics oriented toward processes and LULC types (see Figure 10) in multimodel comparison efforts because such diagnostics allow pinpointing the causes of intermodel similarities and differences.

Model ozone dry deposition evaluation typically consists of comparing simulated and observed seasonal $v_d$ averages or diel cycles with observations at sites with ozone fluxes (Centoni, 2017; Clifton, 2018; Hardacre et al., 2015; Silva & Heald, 2018; Val Martin et al., 2014; Z. Wu et al., 2018). Some observed climatological features are captured by current schemes. For example, the modified Wesely (1989) scheme in GEOS-Chem captures diel cycles and seasonality at various sites relatively well but does not capture the $v_d$ spatial distribution (Silva & Heald, 2018). However, in general, skill varies by model and site, and there is poor understanding of the processes leading to similarities and differences between models and observations (Centoni, 2017; Hardacre et al., 2015; Silva & Heald, 2018; Val Martin et al., 2014; Z. Wu et al., 2011).

Ozone flux data sets used for model evaluation typically span a couple of months at maximum. However, $v_d$ varies by a factor of 2 across 11 years of observations at Harvard Forest, which is not captured by the modified Wesely (1989) scheme in GEOS-Chem (Clifton et al., 2017). Strong unreproducible $v_d$ interannual variability suggests model evaluation with a single year of observations is inadequate. We recommend

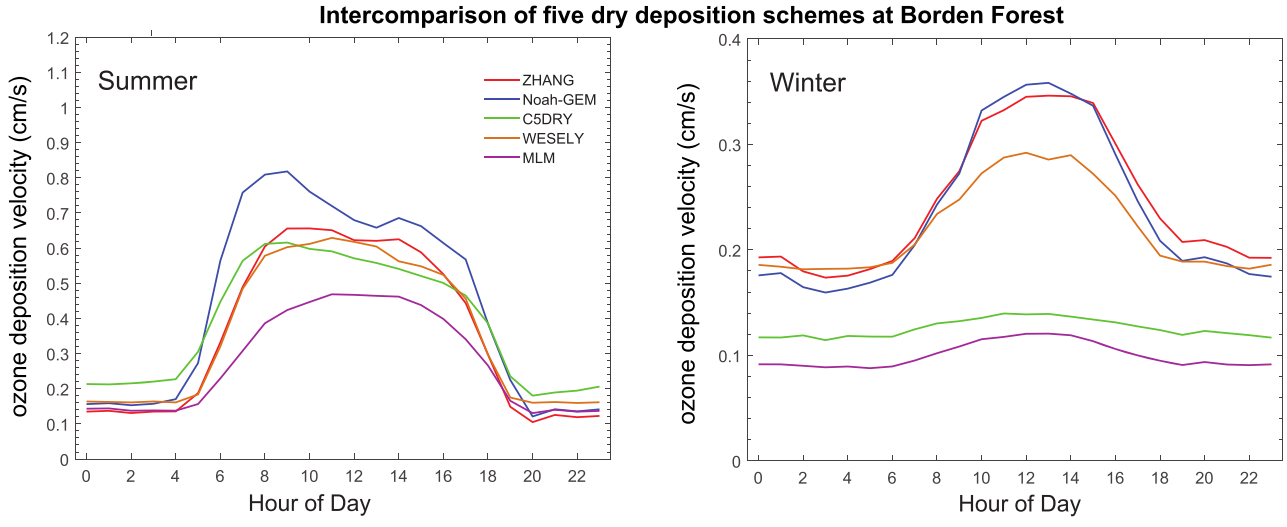


**Figure 9.** Variation in simulated ozone deposition velocity across single-point models all driven by the same forcing data from Borden Forest in Ontario, Canada. Figure is adapted from Figure 1 of Z. Wu et al. (2018) with permission. 

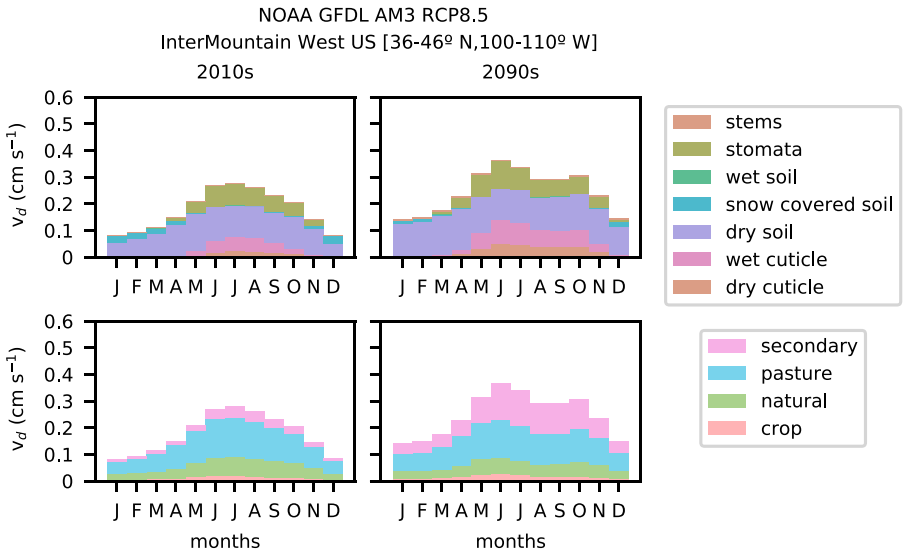


**Figure 10.** Model diagnostics for process understanding of simulated ozone deposition velocity ($v_d$) as illustrated by regional monthly daily mean $v_d$ for the InterMountain West United States at the beginning and end of the 21st century under RCP8.5 (a climate and emissions scenario designed for the Coupled Model Intercomparison Project 5, or CMIP5), as simulated by the NOAA GFDL atmospheric model version 3 (AM3) with dry deposition calculated in the land component of the model (Clifton, 2018; Paulot et al., 2018). Colors indicate contributions from deposition pathways (top panel) and land use/land cover types (bottom panel). The order of the labels on the legend reflects the order in which the corresponding $v_d$ contribution is included on the figure.

emphasizing multiyear averages from long-term ozone flux data sets over short-term data sets for climatological $v_d$ evaluation.

Ozone flux data sets are limited to homogeneous terrain (e.g., Wesely & Hicks, 2000), so models are unconstrained for complex terrain. Given that the theories underpinning current parameterizations assume horizontal heterogeneity, models likely perform poorly over complex landscapes.

Future work should evaluate model performance not only in terms of climatological seasonal and diel cycles of $v_d$ but also spatiotemporal variability and relationships with meteorological and biophysical parameters. For example, observations suggesting a weak dependence on LAI (Clifton et al., 2017, 2019; Mahrt et al., 1995; Wolfe et al., 2015) may imply the strong LAI sensitivity in many models (Charusombat et al., 2010; Schwede et al., 2011; Silva & Heald, 2018) is exaggerated. However, whether observations generally suggest a weak dependence on vegetation density is unknown; some work suggests a strong dependence (e.g., MacPherson et al., 1995). The most insightful model evaluation relies on process-oriented relationships yet to be identified from a meta-analysis of observations.

Only a few studies probe the roles of deposition processes driving model biases (e.g., Tuovinen et al., 2004; Z. Wu et al., 2018). Most studies largely assume stomatal uptake drives variations in $v_d$. We emphasize the contribution of nonstomatal deposition (Figure 4) should be considered in model evaluation. We recommend developing and archiving model diagnostics oriented toward processes (Figure 10). Isolating simulated $v_d$ for a specific LULC type from the grid-box average (Figure 10), which combines multiple LULC types, is also helpful for more direct comparison with observations (e.g., Paulot et al., 2018; Silva & Heald, 2018). For evaluation with such diagnostics to be most instructional, a firm grasp on the relative roles of individual ozone deposition pathways and the mechanisms responsible for differences across LULC types as gleaned from observations is needed.

In general, differences between site and model environmental variables (e.g., meteorology or soil moisture) and observational uncertainty confound model evaluation (Cooter & Schwede, 2000; Schwede et al., 2001; Silva & Heald, 2018; Tuovinen et al., 2001; Z. Wu et al., 2018). To reduce the impact of differences between site and model variables on model evaluation and thus separate input uncertainty from process and parameter uncertainty (e.g., Z. Wu et al., 2018), we recommend driving standalone schemes with observed

**Table 4**
*Recommendations for Ecosystem-Scale Field Measurement Setups Including Ozone Eddy Covariance Flux and Ozone Concentration Profiles, Organized by the Scientific Question Determining the Highest-Priority Measurements*

| Scientific question | Other measurements (long term) | Other measurements (short term) |
|---|---|---|
| What is the contribution of stomatal uptake to ozone dry deposition?* | Water vapor flux, carbon dioxide flux, friction velocity | Other independent tracers of stomatal conductance (e.g., carbonyl sulfide flux) and canopy skin temperature |
| What is the contribution of leaf cuticular uptake to ozone dry deposition? | Humidity, leaf/canopy wetness, leaf area index, dew point temperature, precipitation, same as * to obtain residual ecosystem-scale nonstomatal conductance | Chamber fluxes for ozone around branches including tracers of stomatal conductance to isolate cuticular uptake and composition of cuticles |
| What is the contribution of soil uptake to ozone dry deposition? | Soil moisture and temperature, same as * to obtain residual ecosystem-scale nonstomatal conductance | Lower canopy ozone fluxes, fluxes of NO, $NO_2$, and highly reactive BVOC emission from soil, chambers measuring ozone uptake by soil, and soil properties (e.g., organic content, clay content, porosity, and hydraulic conductivity) |
| What is the contribution of chemistry in the canopy air space to ozone dry deposition? | NO and $NO_2$ fluxes, highly reactive BVOC fluxes, same as * to obtain residual ecosystem-scale nonstomatal conductance | Fluxes of oxidation products |
| How do snow-covered surfaces influence ozone dry deposition? | Horizontal and vertical extent of snow cover, snow age | Snow impurities and NO content of snowpack |

variables representative of the flux-tower footprint. Given more observational constraints on the processes controlling observed $v_d$, driving models with flux-tower data will allow identification of realistic and robust schemes. Otherwise, as is the case for modeling at regional-to-global scales, agreement with observations may stem from incorrect contributions from the various deposition pathways.

## 6. Remaining Gaps and Recommendations for Future Work

Ozone dry deposition intersects multiple fields, including atmospheric chemistry, plant physiology/ecology, and boundary-layer meteorology, all with distinct research questions on the subject (e.g., Hosker & Lindberg, 1982). While ecologists aim to quantify stomatal ozone uptake and understand the ensuing damage to plants, atmospheric chemists aim to quantify ozone deposition velocity over different surfaces and understand the impact of ozone dry deposition on tropospheric chemistry and composition. Identifying current measurement techniques, modeling, and available data as well as assessing and advancing knowledge on ozone dry deposition requires bridging across distinct research communities.

Current understanding of ozone dry deposition is largely based on only a few ozone flux data sets, many of which only span short time intervals. It is generally uncertain which aspects of observed ozone dry deposition are specific to a given site versus represent the broader region or LULC type or are climatological versus episodic. Our top recommendation is establishing key field sites with long-term ozone EC fluxes. The highest priority complementary measurements depend on the specific question ranked as most important (Table 4). If robust evaluation of variability across sites is a desired outcome of future field studies, then a coordinated approach across sites is needed to ensure consistency across measurements.

We also recommend that older data sets be revisited in order to build on the deeper mechanistic understanding revealed by our synthesis here. Our efforts to document ozone flux records since 1985 identifies over 100 sites with measurements. A central archive of ozone fluxes along with complementary data would facilitate broad synthetic meta-analyses and hasten progress toward robust scientific advances. Quantifying uncertainty in data, particularly with respect to random and systematic errors associated with measurement technique, is essential when synthesizing information across data sets. We suggest holistic examinations of older data sets will lead to new knowledge of the processes and conditions driving ozone dry deposition on different temporal and spatial scales.

Because there are only a handful of sites with long-term ozone flux records and many no longer measure ozone fluxes, we emphasize that continued support of current and past sites and establishment of new long-term sites are fundamental to advance knowledge. Because ozone dry deposition is closely related to

carbon and water exchange and associated conditions (e.g., ambient humidity and soil organic content), science will progress most rapidly when ozone fluxes are added to sites already well characterized in terms of carbon and water cycling and boundary-layer meteorology.

For both future short-term campaigns and long-term monitoring, we recommend measuring ozone flux through ozone EC. That the fast ozone analyzers required for ozone EC either require frequent maintenance or are expensive and require toxic or flammable compressed gases is a potential roadblock. We emphasize the importance of developing new analytical methods for fast ozone measurement. An effort to coordinate across research groups measuring ozone fluxes is sorely needed and should promote best practices learned from the carbon dioxide flux community in calculating fluxes, filtering data sets, and sharing data. Such an effort should also include validation and intercomparison of different fast ozone analyzers.

While our review offers an unprecedented synthesis of process-based knowledge of ozone deposition pathways, the relative importance of individual depositional pathways remains uncertain. In particular, we emphasize large uncertainty in the partitioning of ozone dry deposition occurring through pathways other than through plant stomata. Our synthesis of observationally based estimates of the stomatal fraction of ozone dry deposition across peer-reviewed literature shows on average the stomatal fraction over physiologically active vegetation is 45%, underscoring the importance of nonstomatal deposition.

Process-oriented investigation of spatiotemporal variations and trends in ozone fluxes is necessary to quantify the relative importance of various deposition pathways and will inform the degree of complexity needed to model deposition of ozone at large scales. If coordinated with short-term field intensives, laboratory studies, and mechanistic modeling, measurements from a few long-term sites as described in Table 4 would bridge the molecular to ecosystem scales needed to establish the relative importance of various deposition pathways and the extent to which they vary in space and time.

Advancing understanding of dry deposition of ozone is also relevant for dry deposition of other reactive trace gases that alter atmospheric chemistry, climate, and ecosystems because similar physical and chemical processes govern their uptake. Process knowledge of dry deposition for ozone can be translated to any trace gas that reacts with surfaces (e.g., nitrogen dioxide or oxygenated volatile organic compounds). Additionally, models frequently parameterize dry deposition of other reactive trace gases by using ozone and sulfur dioxide as end members. Specifically, a gas's oxidizing ability is scaled to ozone dry deposition, while a gas's solubility is scaled to sulfur dioxide dry deposition given ozone is an oxidant but insoluble and sulfur dioxide is not an oxidant but soluble. Building on the mechanistic framework for ozone dry deposition outlined in this review should inform the strengths and limitations of such a parameterization.

The optimal parameterization for ozone dry deposition remains elusive, but the process understanding synthesized in this review lays the groundwork for one. Representation of most deposition processes in current models should be regarded as insufficient. While current parameterizations capture some of the main observed features of ozone dry deposition, the underlying brazen empiricism of these schemes hinders a full mechanistic understanding of the influence of ozone dry deposition on air pollution, ecosystems, and climate.

## Appendix A: Ecosystem-Scale Ozone Flux Data Sets

Appendix A contains the table of ecosystem-scale ozone flux data sets from 1985 onward.

## Appendix B: Mechanistic Modeling

### B1. Mechanistic Modeling of Ozone Dry Deposition to Leaf Cuticles

Here we derive and review the Potier et al. (2015) physically based model for ozone dry deposition to wet leaves. We begin with the steady-state diffusion/reaction equation for aqueous ozone ($O_{3,aq}$) (mol m$^{-3}$):

$$-D_{O_{3,aq}}\left(\frac{d^2O_{3,aq}}{dz^2}\right) = L_{O_{3,aq}}. \tag{B1}$$

$D_{O_{3,aq}}$ (m$^2$ s$^{-1}$) is ozone diffusivity in water; $z$ is distance from the leaf surface ($z = 0$ at the leaf surface); and $L_{O_{3,aq}}$ is the aqueous ozone chemical sink. With a first-order rate constant $\kappa^{aq}$ (s$^{-1}$) such that $L_{O_{3,aq}} = -\kappa^{aq} O_{3,aq}$, we have

$$\frac{d^2O_{3,aq}}{dz^2} = \left(\frac{\kappa^{aq}}{D_{O_{3,aq}}} O_{3,aq}\right) \equiv \Gamma_{aq}^2 O_{3,aq}. \tag{B2}$$

We now derive the resistance for aqueous ozone uptake ($r_{\text{cut},aq}$) (s m$^{-1}$) by water droplets and films on a leaf surface. The boundary condition at the upper surface of the water (i.e., the air-water interface) is $O_{3,aq}(\delta_d)$ where $\delta_d$ is the thickness of the film or droplet. The boundary condition at the lower surface of the water (i.e., the leaf-water interface) is

$$D_{O_{3,aq}} \frac{\partial O_{3,aq}}{\partial z} = \frac{O_{3,aq}(0)}{r_{\text{cut}}}. \tag{B3}$$

$r_{\text{cut}}$ (m s$^{-1}$) is the resistance to aqueous ozone uptake by cuticle underneath the water. Defining $\gamma = \left(r_{\text{cut}}\Gamma_{aq}D_{O_{3,aq}}\right)^{-1}$, the solution to equation (B2) is

$$O_{3,aq}(z) = O_{3,aq}(\delta_d)\left(\frac{(1-\gamma)e^{-\Gamma_{aq}z} + (1+\gamma)e^{\Gamma_{aq}z}}{(1-\gamma)e^{-\Gamma_{aq}\delta_d} + (1+\gamma)e^{\Gamma_{aq}\delta_d}}\right), \tag{B4}$$

$$\frac{dO_{3,aq}}{dz} = O_{3,aq}(\delta_d)\,\Gamma_{aq}\left(\frac{-(1-\gamma)e^{-\Gamma_{aq}z} + (1+\gamma)e^{\Gamma_{aq}z}}{(1-\gamma)e^{-\Gamma_{aq}\delta_d} + (1+\gamma)e^{\Gamma_{aq}\delta_d}}\right). \tag{B5}$$

Then, we have

$$D_{O_{3,aq}} \left.\frac{dO_{3,aq}}{dz}\right|_{z=\delta_d} = \frac{O_{3,aq}(\delta_d)}{r_{\text{cut},aq}}, \tag{B6}$$

which yields

$$r_{\text{cut},aq} = \frac{1}{\Gamma_{aq}D_{O_{3,aq}}}\left(\frac{(1-\gamma)e^{-\Gamma_{aq}\delta_d} + (1+\gamma)e^{\Gamma_{aq}\delta_d}}{-(1-\gamma)e^{-\Gamma_{aq}\delta_d} + (1+\gamma)e^{\Gamma_{aq}\delta_d}}\right). \tag{B7}$$

However, the definition of the resistance to ozone uptake on wet cuticles is usually defined relative to the gas phase, not the aqueous phase. We therefore replace equation (B6) with

$$D_{O_{3,aq}} \left.\frac{dO_{3,aq}}{dz}\right|_{z=\delta_d} = \frac{O_3(\delta_d)}{r_{\text{cut,wet}}}. \tag{B8}$$

$O_3(\delta_d)$ (mol m$^{-3}$) is gaseous ozone concentration at the surface of the water; $r_{\text{cut,wet}}$ (s m$^{-1}$) is the resistance to gaseous ozone uptake by wet cuticles. Fully specifying $r_{\text{cut,wet}}$ requires a relationship between $O_3$ and $O_{3,aq}$, and the simplest approach is assuming $O_3$ and $O_{3,aq}$ are in equilibrium with Henry's law:

$$O_3(\delta_d) = \frac{O_{3,aq}(\delta_d)}{k_H^{cc}}. \tag{B9}$$

$k_H^{cc}$ is the dimensionless Henry's law constant (e.g., Sander, 1999, 2015). Then, we have

$$r_{\text{cut,wet}} = \frac{r_{aq}}{k_H^{cc}} = \frac{1}{k_H^{cc}\Gamma_{aq}D_{O_{3,aq}}}\left(\frac{(1-\gamma)e^{-\Gamma_{aq}\delta_d} + (1+\gamma)e^{\Gamma_{aq}\delta_d}}{-(1-\gamma)e^{-\Gamma_{aq}\delta_d} + (1+\gamma)e^{\Gamma_{aq}\delta_d}}\right). \tag{B10}$$

This $r_{\text{cut,wet}}$ expression is the same as Potier et al. (2015) equation (A5) except for our using the dimensionless form of Henry's law constant.

Given that ozone diffusion through water is slow and the underlying cuticle may not be very reactive with ozone, we may be able to assume the lower boundary condition is zero. This gives us a simpler expression for $r_{\text{cut,wet}}$:

Reviews of Geophysics

10.1029/2019RG000670

**Table A1**
*Ecosystem-Scale Ozone Flux Data Sets From 1985 Onward*

| Site name | Region | Latitude | Longitude | Length of observational data set | Measurement Type | Land use/land cover | Previous literature |
|---|---|---|---|---|---|---|---|
| Alice Holt | England | 51.17°N | 0.87°W | July–August 2005 | EC | Oak forest | |
| Amazon Tall Tower Observatory | Brazil | 2.1459°S | 59.00°W | December 2015 and March 2016 to present | EC | Tropical forest | |
| Auchencorth Moss | Scotland | 55°47′30″N | 3°14′20″W | 1995–1998 | Gradient | Moorland | Fowler et al. (2001) and Tuovinen et al. (2004) |
| Beaufort | Southeast United States | 34.88°N | 76.62°W | 10 June to 1 August 1993 | EC | Crop | Finkelstein et al. (2000) and Meyers et al. (1998) |
| Beijing | China | 39.98°N | 116.39°E | August–November 2016 and May–June 2017 | EC | Urban | |
| Bergamo | Italy | 45°36′51″N | 9°40′22″E | May–June 2001 | EC | Wheat field | Gerosa et al. (2003) |
| Bily Kriz | Czech Republic | 49°33′N | 18°32′E | July–August 2008 and 2012–2017 (gradient), summer 2017 (EC) | EC and gradient | Norway spruce forest, established in 1981 by planting 4-year-old seedlings in rows | Juráň et al. (2019) and Zapletal et al. (2011) |
| Blodgett Forest | California | 38.9°N | 120.63°W | June–September 1997, May–November 1998, June 1999 to June 2000, and January 2001 to December 2006 | EC | Ponderosa pine plantation | Bauer et al. (2000), Fares, McKay, et al. (2010), Goldstein (2003), Goldstein et al. (2004), Kurpius et al. (2002), Kurpius and Goldstein (2003), and Wolfe et al. (2011) |
| Bondville | Midwest United States | 40.05°N | 88.37°W | 18 August to 1 October 1994 | EC | Corn | Finkelstein et al. (2000), Finkelstein (2001), Meyers et al., (1998), Y. Wu, et al. (2003), and L. Zhang, et al. (2002) |
| Bosco Fontana | Italy | 45°12′02″N | 10°44′44″E | 12 June to 11 July 2012 | EC | Mixed oak-hornbeam forest | Finco et al. (2018) |
| Braunschweig | Germany | 53°18′N | 10°26′E | 20 May to 15 June 2000 | EC | Intensively managed grassland | Bassin et al. (2004) and Mészáros, Horváth, et al. (2009) |
| Bruneck | Italy | 46°49′N | 11°55′E | December 1999 | EC | Snow-covered mountain valley | Cieslik (2009) |
| Bugacpuszta | Hungary | 46.69°N | 19.60°E | August 2012 to January 2014 | EC | Seminatural semiarid sandy grassland | Horváth et al. (2017) |
| Bukit Atur | Malaysia | 4°58′49.10″N | 117°51′19.12″E | 7 April to 24 July 2008 | EC and gradient | Tropical forest | Fowler et al. (2011) |
| Burriana | Spain | 39°55′N | 0°03′W or 0.04′W | 16–29 July 1995, 28 April to 3 May 1996, and 2–16 June 1997 | EC | Orange grove | Cieslik (2004) |
| Cala Violina | Italy | 42°55′N | 10°30′E | June–December 2005 and July–September 2006 | EC | Mixed oak forest in complex terrain | Cieslik (2009) and Gerosa et al. (2007) |
| Camp Borden | Canada | 44°19′N | 79°56′W | July–August 1988 (EC), March–April 1990 (EC), and May 2008 | EC and gradient | Temperate mixed forest | Fuentes et al. (1992), Padro (1993, 1994), Padro et al. (1991), |

Reviews of Geophysics

10.1029/2019RG000670

**Table A1** *(continued)*

| Site name | Region | Latitude | Longitude | Length of observational data set | Measurement Type | Land use/land cover | Previous literature |
|---|---|---|---|---|---|---|---|
| | | | | to April 2013 (gradient) | | | and Z. Wu et al. (2016, 2018) |
| Castelporziano | Italy | 41.42°N | 12.21°E | June 1993 and May 1994 | EC | Mediterranean pseudo steppe | Cieslik (2004) and Cieslik and Labatut (1997) |
| Castelporziano | Italy | 41.42°N | 12.21°E | August–September 2003, June–November 2004, June–October 2003, and 2011–2015 | EC | Holm oak forest | Gerosa et al. (2005, 2007), Gerosa, Finco, Mereu, Marzuoli, et al. (2009), Fares et al. (2013, 2014), Hoshika et al. (2017), Rydsaa et al. (2016), Savi and Fares (2014), and Vitale et al. (2005) |
| Castile and Leon | Spain | 42°1′N | 4°32′W | 5, 6, and 8 May 1994 and 6 days in July 1995 | Gradient | Semiarid steppe on a plateau covered in barley | De Miguel and Bilbao (1999) and Sánchez et al. (1997) |
| Central Plains Experimental Range | Western United States | 40°28′23″N | 104°45′15″W | 5 March to 2 August 1988, 24 January to 21 February 1989, and 7 June to 10 July 1989 | EC | Bare patches of soil and dead or senescent vegetation or snow | Massman (1993) and Stocker et al. (1993, 1995) |
| Chinese Research Academy of Environmental Sciences | Beijing | | | September and November 2000, 10 days each | Gradient | Grassland | Sorimachi et al. (2003) |
| CODE cotton | California | 36°48′50″N | 120°40′38″W | 8 July to 6 August 1991 | EC | Cotton | Grantz et al. (1997), Massman et al. (1994), Padro et al. (1994), and Padro (1996) |
| CODE grassland | California | 37°02′N | 119°48′30″W | 30 days during summer 1991 | EC | Grassland | Massman et al. (1994), Padro, Massman, Shaw, et al. (1994), and Padro (1996) |
| CODE vineyard | California | 36°51′36″N | 120°6′7″W | 11 July to 1 August 1991 and 8 July to 6 August 1991 | EC | Grape | Grantz et al. (1995), Massman et al. (1994), Padro, Massman, Den Hartog, et al. (1994), and Padro (1996) |
| Colt Park | England | 54.19°N | 2.34°W | August to October 2005 | EC | Seminatural grassland | |
| Comun Nuovo | Italy | 45°37′N | 9°40′E | May–June 2001, July–September 2001, and May–June 2002 | EC | Wheat, soybean, or barley | Bassin et al. (2004), Cieslik (2009), Gerosa et al. (2003), Tuovinen et al. (2004), and Rydsaa et al. (2016) |
| Cuatro Vientos | Spain | 40°40′N | 3°56′W | 2–13 May 1997 | EC | Low vegetation | Cieslik (2004) |
| Dakhla Oasis | Egypt | | | 23 March to 9 April 1993 | EC | Saharan desert | Güsten et al. (1996) |
| Diepoholz | Germany | 52°39′8″N | 8°39′12″E | | EC | Peatland | El-Madany et al. (2017) |

Reviews of Geophysics

10.1029/2019RG000670

**Table A1** *(continued)*

| Site name | Region | Latitude | Longitude | Length of observational data set | Measurement Type | Land use/land cover | Previous literature |
|---|---|---|---|---|---|---|---|
| | | | | 30 June to 4 August 2014 | | | |
| Duke Forest | Southeast United States | | | Spring 2017 to 2019 | EC | Bottomland mixed hardwood forest along urban to rural gradient | |
| Duke Forest Blackwood Division | Southeast United States | 35.97°N | 79.13°W | 15 April to 15 May 1996 | EC | Loblolly pine plantation | Finkelstein et al. (2000) and Meyers et al. (1998) |
| Easter Bush | Scotland | | | August 2007 | EC | Grasslands with predominately perennial rye-grass with grazing in adjacent fields | Muller et al. (2009, 2010) |
| Flanders | Belgium | 51°18′N | 4°31′E | 2000–2015 | Gradient | Mixed forest in a suburban area | Neirynck et al. (2012) and Neirynck and Verstraeten (2018) |
| Gilchriston Farm | Scotland | 55.9°N | 2.8°W | 1 month in summer 2006 | EC | Potato canopy | Coyle et al. (2009) |
| GLEES Brooklyn Lake | Western United States | 41°22′N | 106°14.5′W | 14–27 April, 6–19 May, June, and 2–9 July 1992, 15–26 January 1993, and 30 July to 8 August 1996 | EC | Subalpine coniferous forest | Zeller (2000), Zeller and Hehn (1995, 1996), and Zeller and Nikolov (2000) |
| GLEES Brooklyn Lake | Western United States | 41°22′N | 106°14.5′W | 24 April to 3 May 1994, and 7–21 June and 2–10 August 1994 | EC | Open meadow | Zeller and Hehn (1995) |
| Grignon | France | 48.84°N | 1.95°E | 19 June to 7 October 2002, 26 July to 1 October 2002, 2004–2009, and 7 August 2012 to 13 March 2013 | EC | Crop (sometimes bare soil, maize, and winter wheat) | Lamaud et al. (2009), Loubet et al. (2013), Stella, Loubet, et al. (2011), Stella, Personne, et al. (2011), Stella et al. (2012, 2013, 2019), Tuzet et al. (2011), and Vuolo et al. (2017) |
| Halvergate Trace Gas Exchange Experiment | England | | | 15 September 1989 | Gradient | Drained marshland pasture | Hargreaves et al. (1992) and Kramm et al. (1991) |
| Hartheim | Germany | 47°56′N | 7°37′E | 17–20 May 1992 | Gradient | Scots pine plantation | Joss and Graber (1996) |
| Harvard Forest | Northeast United States | 42.53°N | 72.18°W | 1990–2000 | EC and gradient | Temperate deciduous forest | Clifton et al. (2017, 2019), Munger et al. (1996), and Z. Y. Wu et al. (2015) |
| Hesse | France | 48°0′27″N | 7°03′52″E | September 2010 to March 2011 | EC | European beech | Le Morvan-Quéméner et al. (2018) |
| Hohenpeissenberg | Germany | 47°48′N | 11°02′E | 29 August to 20 September 2005 | EC | Meadow and pre-alpine landscape | Stella et al. (2013) |
| Horsepool | | | | | EC | | |

Reviews of Geophysics

10.1029/2019RG000670

**Table A1** *(continued)*

| Site name | Region | Latitude | Longitude | Length of observational data set | Measurement Type | Land use/land cover | Previous literature |
|---|---|---|---|---|---|---|---|
| | Western United States | | | 25 January to 2 April 2013 | | Dry, sandy soil and low-lying sage brush | |
| Hortobágy | Hungary | | | 19–30 June 1993, 5 May to 21 June 1994, and 13–30 September 1994 | Gradient | Grassland | Horváth et al. (1997) |
| Hurdal | Norway | | | 1 July 2000 to 31 March 2003 | Gradient | Norway spruce forest | Hole et al. (2004) |
| Hyytiälä | Finland | 61.85°N | 24.28°E | 2001–2013 | EC | Coniferous forest | Altimir et al. (2006), Launiainen et al. (2013), Rannik et al. (2009, 2012), and P. T. Zhou et al. (2017) |
| Ispra forest | Italy | 45.8126°N | 8.6336°E | 2013–2015 | EC | Deciduous forest | |
| Ispra grassland | Italy | 44°48′N | 8°38′E | September 1997 | EC | Grassland | Cieslik (2009) |
| Kaamanen | Finland | 69°08′N | 27°17′E | September 1995 | EC | Open fark fen (ridges and open water pools) | Tuovinen et al. (1998, 2004) |
| Kane Experimental Forest | Northeast United States | 41.60°N | 78.77°W | 29 April to 23 October 1997 | EC | Deciduous forest | Finkelstein et al. (2000), Finkelstein (2001), Meyers et al. (1998), L. Zhang et al. (2001, 2002) |
| Keenly Fell | England | 54°53′49.0″N | 2°19′26.6″W | June 2007 to December 2011 | EC | Seminatural grassland | |
| Klippeneck | Germany | 48°10′N | 8°45′E | 10–22 September 1992 | | Grassland | Cieslik (2004) |
| Konza Praire Research Natural Area | Central United States | | | 26 May to 6 June 1987, 25 June to 11 July, 6–21 August 1987, and 5–16 October 1987 | EC | Predominately big bluestem grass; recent fire | Gao et al. (1992) |
| Kranzberger Forst | Germany | 48°25′N | 11°39′E | 2–29 July 2007 | EC | Mixed forest | Nunn et al. (2010) |
| La Barben | France | 43°35′N | 5°15′E | 29 June to 13 July 2001 | EC | Mediterranean shrubland, mostly *Quercus coccifera* | Michou et al. (2005) |
| La Cape Sud | France | 44°24′N | 0°38′W | 26 July 2007 to 4 March 2008 | EC | Crop | Stella, Personne, et al. (2011) and Stella et al. (2019) |
| La Crau | France | 43°34′N | 4°49′E | 20 April to 31 May 2001 | EC | Semiarid part of the La Crau plain and totally flat, uniform, almost bare soil with mainly pebbles | Michou et al. (2005) and Stella et al. (2019) |
| Lake Kinisheo | Canada | | | Late June to July 1990 | | Lichen bogs and small conifer shrubs | Fuentes et al. (1994) |
| Lake Kuivajärvi | Finland | 61°50′N | 24°17′E | | EC | Boreal lake | Fung (2018) |

Reviews of Geophysics

10.1029/2019RG000670

**Table A1** *(continued)*

| Site name | Region | Latitude | Longitude | Length of observational data set | Measurement Type | Land use/land cover | Previous literature |
|---|---|---|---|---|---|---|---|
| | | | | August to September 2012 | | | |
| Lamasquére | France | 43°49′N | 1°23′W | 2008–2010 | EC | Crop | Stella, Personne, et al. (2011) and Stella et al. (2019) |
| Le Bray | France | 44°34′33.24″N | 0°46′33.72″W | May to August 2007 and May to August 2008 | EC | Stand of maritime pines planted in 1970 | Le Morvan-Quéméner et al. (2018) |
| Le Dézert | France | 44°05′N | 0°43′W | 16–18 April 1997 | EC | Coniferous forest | Cieslik (2004) |
| Les Landes | France | 44°12′N | 0°42′W | June 1994, 21 June to 3 July 1997, 21–24 February 1997, June 1996, and October 1996 | EC and gradient | Mixed forest | Lamaud et al. (2002) and Sánchez et al. (1997) |
| Lincove | California | 36.36°N | 119.09°W | October 2009 to November 2010 | EC | Orange orchard | Fares et al. (2012) |
| Lochristi | Belgium | 51°06′44″N | 3°51′02″E | 2010–2016 | EC | Short-rotation coppice poplar plantation | Zenone et al. (2016) and Zona et al. (2014) |
| London | England | 51.52°N | 0.14°W | October 2011 to August 2013 | EC | Urban | |
| Lusignan | France | 46°24′N | 0°07′E | 17 March to 5 May 2011 | EC | Crop | Stella et al. (2019) |
| Lusignan | France | 46°26′08″N | 0°07′25″E | August to September 2010 | EC | Meadow | Le Morvan-Quéméner et al. (2018) |
| Manaus | Brazil | 3°S | 60°W | At most a couple of days in July–August 1985 | Gradient | Tropical forest | Kirchhoff et al. (1988) |
| Mea Moh | Thailand | 18.28°N | 99.72°E | January–April 2002 and January–August 2004 | Gradient | Teak forest | Matsuda et al. (2005, 2006) |
| Mekrijärvi | Finland | 62°52′N | 30°55′E | July 1995 | EC | Low Scots pine forest on border of southern and middle boreal zones | Tuovinen et al. (2001, 2004) |
| Meyrargues | France | 43°39′N | 5°32′E | 12–28 June 2001 | EC | Maize | Michou et al. (2005) |
| Monmeyan | France | 43°39′N | 6°05′E | 10–26 June 2001 | EC | Mediterranean forest (95% *Quercus Pubescens*) | Michou et al. (2005) |
| Nashville/ Keysburg | Southeast United States | 36.65°N | 87.03°W | 22 June to 11 October 1995 | EC | Soybean | Finkelstein et al. (2000), Finkelstein (2001), Meyers et al. (1998), Pleim et al. (2001), Y. Wu et al. (2003), and L. Zhang et al. (2002) |
| Neustift | Austria | 47°07′N | 11°19′E | 11 July to 20 October 2008 | EC and gradient | Temperate mountain meadow | Wohlfahrt, Hörtnagl, et al. (2009) |
| Niwot Ridge | Western United States | 40.03°N | 105.55°W | 6 June to 31 August 2002, 1 April to 19 November 2003, 21 May to 30 June 2004, | EC | Coniferous subalpine forest | Turnipseed et al. (2009) |

Reviews of Geophysics

10.1029/2019RG000670

**Table A1** *(continued)*

| Site name | Region | Latitude | Longitude | Length of observational data set | Measurement Type | Land use/land cover | Previous literature |
|---|---|---|---|---|---|---|---|
| | | | | and 20 May to 31 August 2005 | | | |
| Norwood Park | England | | | 25–28 July 1994 | EC | Fruit orchard | Walton, Gallagher, Choularton, et al. (1997) and Walton et al. (1997) |
| Nyírjes | Hungary | | | 5–30 September 1991, 20 March to 16 April 1992, 28 January to 17 February 1993, 8 July to 29 August 1993, and 15 July to 6 August 1994 | Gradient | Norway spruce forest | Horváth et al. (1997) |
| Oshiba Highland | Japan | 32°52′N | 137°58′E | April–September 2001 | Gradient | Red pine forest | S. Zhang et al. (2005) |
| Palatinate | Germany | 49.16°N | 8.28°E | April–September 1992 | EC | Barley or flat harvested field | Güsten et al. (1997) |
| Petsikko | Finland | 69°52′N | 27°14′E | Beginning of June to August 18 1996 | EC | Subarctic mountain birch | Tuovinen et al. (2001) |
| Plymouth | Southeast United States | 35.70°N | 76.80°W | 15 July to 15 August 1996 | EC | Soybean | Finkelstein et al. (2000), Meyers et al. (1998), and Y. Wu et al. (2003) |
| Polder Piloto de Sarazola | Portugal | 40°42′N | 8°37′W | November 1994 to October 1995 | Gradient | Meadow | Pio and Feliciano (1996), Pio et al. (2000), and Tuovinen et al. (2004) |
| Ramat Hanadiv Nature Park | Israel | 32°33′19.87″N | 34°56′50.23″E | 31 July to 30 September 2015, 1 February to 31 March 2016, 1 June to 7 July 2016, 2 August to 17 September 2016, 5 January to 22 May 2017, and 12 June to 2 July 2017 | EC | Shrub 3.6 km away from eastern Mediterranean seashore | Q. Li, Gabay, et al. (2018) |
| Reserve Adolfo Ducke | Amazonia | 2°57′S | 59°57′W | 22 April to 8 May 1987 | EC | Tropical forest | Fan et al. (1990) |
| Rhine Valley | Germany | | | September 1992 | Gradient | Short sparse wheat | Horváth et al. (1998) |
| Rhineland-Palatinate | Germany | 49.9685°N | 8.1481°E | July–October 2011 | EC | Natural nutrient-poor steppe-like grassland and occasionally subject to management in past | Ermel et al. (2013) and Plake, Stella, et al. (2015) |
| Rivox | Scotland | 55°19′57″N | 3°31′43″W | May 1992 | EC | Sitka spruce plantation | Coe et al. (1995) |
| Rondonia | Amazonia | 10°04′55″S | 61°55′48″W | 4–22 May 1999 and 21 September to 20 October 1999 | EC | Wet and dry season, la Niña year | Rummel et al. (2007) |
| Rondonia | Amazonia | 10°45′44″S | 62°21′27″W | 30 April to 17 May 1999 and 24 September to 27 October 1999 | EC | Pasture and transition seasons “wet-dry” | Kirkman et al. (2002) and Rummel et al. (2007) |

10.1029/2019RG000670

**Table A1** *(continued)*

| Site name | Region | Latitude | Longitude | Length of observational data set | Measurement Type | Land use/land cover | Previous literature |
|---|---|---|---|---|---|---|---|
| | | | | | | and "dry-wet," la Niña year | |
| S. Pietro Capofiume | Italy | 44°39′N | 11°37′E | 2–11 June 1993 | EC | Beet | Cavicchioli et al. (1997) and Cieslik (2004, 2009) |
| Sabah | Malaysia | 5°14′58.69″N | 118°27′15.76″E | 4–11 June 2008 | EC | Crop | Fowler et al. (2011) |
| San Rossore | Italy | 43°43′55″N | 10°17′27″E | 20 January to 10 February 2013, 22 April to 12 May 2013, 8–27 July 2013, and 9–29 September 2013 | EC | Coniferous forest (*Pinus pinea*) | Hoshika et al. (2017) |
| Sand Flats State Forest | Northeast United States | 43.57°N | 75.24°W | 12 May to 20 October 1998 | EC | Mixed forest | Finkelstein et al. (2000), Finkelstein (2001), Meyers et al. (1998), and L. Zhang et al. (2002, 2001) |
| Sand Mountain | Southeast United States | 34.29°N | 85.97°W | 15 April to 13 June 1995 | EC | Grassland | Finkelstein et al. (2000), Finkelstein (2001), Meyers et al. (1998), Y. Wu et al. (2003), and L. Zhang et al. (2002) |
| Schachtenau | Germany | | | June to September 1987 and 18–28 September 1989 | EC | Coniferous forest | Enders (1992) and Enders et al. (1992) |
| Schefferville | Canada | 54°50′N | 66°40′W | July to August 1990 | EC | Spruce woodland | Munger et al. (1996) |
| Scherzheim | Germany | | | 11–22 September 1992 | EC | Harvested and harrowed wheat field with regrown wheat | Pilegaard et al. (1998) |
| Sinderhoeve | Netherlands | 51.58°N | 5.42°E | 30 June 1988, 6, 19, 25, and 28 July 1988, 12 and 28 August 1988, 12 and 22 September 1988, and 4 October 1988 | EC | Maize | Van Pul and Jacobs (1994) |
| Speulderbos | Netherlands | | | 9 months in 1993 | EC | Douglas fir plantation | Dorsey et al. (2004) and Duyzer et al. (1995) |
| Summit | Greenland | 72.34°N | 38.29°W | 19–30 July 2003, 22 March to 14 August 2004, and 17 March to 28 April 2005 | Gradient | Polar snowpack on glacial ice | Helmig, Bocquet, et al. (2007) and Helmig, Cohen, et al. (2009) |
| Toolik Lake | Alaska | 68.6°N | 149.6°N | May–August 2011 | EC | Tundra | Van Dam et al. (2016) |
| Turro | Italy | 44°59′N | 9°42′E | March–April 2014 | EC | Crop | Stella et al. (2019) |
| Ulborg | Denmark | 56°17′N | 8°25′E | 7 days in April 1995, 10 days in June 1994, 7 days in August 1997, 5 days in September 1995, and May–June 1995, 2003 | EC and gradient | Mixed forest (mostly Norway spruce) | Mikkelsen et al. (2000, 2004), Pilegaard et al. (1995), Ro-Poulsen et al. (1998), and Tuovinen et al. (2004) |

10.1029/2019RG000670

**Table A1** *(continued)*

| Site name | Region | Latitude | Longitude | Length of observational data set | Measurement Type | Land use/land cover | Previous literature |
|---|---|---|---|---|---|---|---|
| | | | | (EC) and 1994–2000 (gradient) | | | |
| UMBS Prophet | Midwest United States | 45.5°N | 84.7°W | 27 June to 28 September 2002, 7 August to 15 October 2003, 15 June to 15 September 2004, and 15 June to 3 September 2005 | EC | Mixed forest (bigtooth aspen, white pine, red oak, red maple, and paper birch) | Hogg et al. (2007) and Hogg (2007) |
| Viols-en-Laval | France | 43°41′N | 3°47′E | 16–24 July 1998 | EC | Mediterranean shrub | Cieslik (2004) |
| Virginia Forest Research Facility | Southeast United States | 37.92°N | 78.27°W | July 2019 to present | EC | Mixed forest | |
| Voghera | Italy | 45°01′N | 9°00′E | May–July 2003 | EC | Onion | Cieslik (2009) and Gerosa et al. (2007) |
| Yucheng Comprehensive Experimental Station of the Chinese Academy of Sciences | China | 36°50′N | 116°34′E | 9 August to 28 September 2011 and 2 March to 6 June 2012 | EC | Corn and wheat | Zhu et al. (2014) and Zhu (2019) |
| Yukon Delta National Wildlfie Refuge | Alaska | 61°05.41′N | 162°00.92′W | 14 July to 12 August 1988 | EC | Tundra | Jacob et al. (1992) |
| Zegveld | Netherlands | | | 6 September 1994 | Gradient | Dutch pasture | Galmarini et al. (1997) |

$$r_{\text{cut,wet}} = \frac{1}{k_H^{CC}\Gamma_{aq}D_{O_{3,aq}}\tanh\left(\Gamma_{aq}\delta_d\right)}. \tag{B11}$$

### B.2. Mechanistic Modeling of Ozone Dry Deposition to Soil

Here we derive a mechanistic model for the resistance to ozone uptake by soil ($r_{\text{soil}}$), generalizing the approach of Tuzet et al. (2011) who analytically solve the steady-state equation of mass conservation for ozone within soil pore spaces ($O_{3,\text{soil}}$) to obtain $r_{\text{soil}}$. We begin with the steady-state diffusion-only mass conservation equation for $O_{3,\text{soil}}$:

$$\frac{\mathrm{d}}{\mathrm{d}z}\left(F_{O_{3,\text{soil}}}\right) = Dep_{O_{3,\text{soil}}} + L_{O_{3,\text{soil}}}. \tag{B11}$$

$z$ refers to depth below the soil surface; $Dep_{O_{3,\text{soil}}}$ (ppbv $s^{-1}$) is the soil ozone depositional sink; and $L_{O_{3,\text{soil}}}$ (ppbv $s^{-1}$) is the chemical sink within soil pore space. $F_{O_{3,\text{soil}}}$ (ppbv m $s^{-1}$) is the ozone vertical diffusive flux within soil (e.g., Hillel, 1980) and follows

$$F_{O_{3,\text{soil}}} = -(\eta-\theta)\tau D_{O_3}\frac{\mathrm{d}O_{3,\text{soil}}}{\mathrm{d}z}. \tag{B12}$$

$\eta$ is volumetric air-filled soil pore space when completely dry ($m^3$ $m^{-3}$); $\theta$ is volumetric soil moisture ($m^3$ $m^{-3}$); $\tau$ is the soil tortuosity factor ($0 < \tau < 1$; unitless) (a measure of the how many paths ozone can take in soil); and $D_{O_3}$ is ozone diffusivity in air ($m^2$ $s^{-1}$).

To insure equation (B11) is amenable to analytical solution, we approximate

$$\frac{\mathrm{d}}{\mathrm{d}z}\left(F_{O_{3,\text{soil}}}\right) = -(\eta-\theta)\tau D_{O_3}\frac{d^2O_{3,\text{soil}}}{\mathrm{d}z^2}. \tag{B13}$$

However, soils vary vertically in terms of $\eta$, $\tau$, $\theta$, and temperature ($T_{\text{soil}}$), which may influence variables such as $D_{O_3}$.

The next steps are to construct $L_{O_{3,\text{soil}}}$ and $Dep_{O_{3,\text{soil}}}$. We parameterize $L_{O_{3,\text{soil}}}$ as $-\sum_i K_{X_i,O_3}O_{3,\text{soil}}X_{i,\text{soil}}$ where $K_{X,O_3}$ (ppmv $s^{-1}$) is the rate coefficient for ozone chemical destruction in soil pore spaces by some gas species $X_{\text{soil}}$.

For porous media, the basic approach for a sink term ($S^*$) associated with dry deposition is to assume $S^* = AF^*$ where $A$ ($m^2$ $m^{-3}$) is the surface area on which dry deposition occurs per unit volume of the porous media and $F^*$ (ppmv m $s^{-1}$) is the net flux to that surface. Following this approach and Morrison and Nazaroff (2002) for ozone dry deposition to carpet, we parameterize $F^*$ analogously to heterogeneous chemistry in the atmosphere (e.g., Jacob, 2000):

$$F^* = \frac{1}{4}K_d v O_{3,\text{soil}}. \tag{B14}$$

$K_d$ is the surface deposition coefficient (unitless), which provides a measure of the probability that an ozone molecule reacts once it comes into contact with the surface; $v = \sqrt{\frac{8RT_{\text{soil}}}{\pi M_{O_3}}}$; $R$ is the universal gas constant (8.314 J $mol^{-1}$ $K^{-1}$); and $M_{O_3}$ is ozone molecular mass (0.048 kg $mol^{-1}$).

We now have

$$(\eta-\theta)\tau D_{O_3}\frac{d^2O_{3,\text{soil}}}{\mathrm{d}z^2} = AK_d\frac{1}{4}\sqrt{\frac{8RT_{\text{soil}}}{\pi M_{O_3}}}O_{3,\text{soil}} + \sum_i K_{X_i,O_3}O_{3,\text{soil}}X_{i,\text{soil}}. \tag{B15}$$

The solution to equation (B15) is

$$O_{3,\mathrm{soil}}(z) = ae^{-\sqrt{\Gamma}z} + be^{\sqrt{\Gamma}z}, \tag{B16}$$

$$F_{O_3,\mathrm{soil}}(z) = -(\eta-\theta)\tau D_{O_3}\sqrt{\Gamma}\left(-ae^{-\sqrt{\Gamma}z} + be^{\sqrt{\Gamma}z}\right), \tag{B17}$$

where

$$\Gamma = \frac{\left(AK_d\frac{1}{4}\sqrt{\frac{8RT_{\mathrm{soil}}}{\pi M_{O_3}}} + \sum_i K_{X_i,O_3}X_{i,\mathrm{soil}}\right)}{(\eta-\theta)\tau D_{O_3}}. \tag{B18}$$

$a$ and $b$ are constants determined by the boundary conditions. The upper boundary condition (at $z = 0$) is $F_{O_3,\mathrm{soil}}(0) = \frac{O_{3,\mathrm{soil}}(0)}{r_{\mathrm{soil}}}$, assuming ozone flux is continuous across the soil surface (this assumption is not valid when diffusion into soil is blocked).

A general lower boundary condition follows from noting $O_{3,\mathrm{soil}}(z)$ should remain bounded for all soil depths (i.e., $\lim_{z\to-\infty} O_{3,\mathrm{soil}}(z) = 0$). Because $z \le 0$, a bounded lower boundary condition can be assured unconditionally by requiring $a \equiv 0$.

Combining $a \equiv 0$ with $O_{3,\mathrm{soil}}(0)$ and $F_{O_3,\mathrm{soil}}(0)$ yields the following expression for $r_{\mathrm{soil}}$:

$$r_{\mathrm{soil}} = \frac{1}{(\eta-\theta)\tau D_{O_3}\sqrt{\Gamma}} \equiv \left[\left(AK_d\frac{1}{4}\sqrt{\frac{8RT_{\mathrm{soil}}}{\pi M_{O_3}}} + \sum_i K_{X_i,O_3}X_{i,\mathrm{soil}}\right)\left((\eta-\theta)\tau D_{O_3}\right)\right]^{-\frac{1}{2}}. \tag{B19}$$

### B.3. Incorporating Thermal Decomposition Into Mechanistic Modeling of Ozone Dry Deposition to Soil

We construct a similar mechanistic model for ozone dry deposition to soil as above but one that includes thermal decomposition of ozone on soil surfaces in order to explore the role of this process. We generalize the approach outlined by Seinfeld and Pandis (2006) for thermal decomposition, assuming as they do that thermal decomposition follows first-order chemical kinetics:

$$Dep^{\mathrm{therm}}_{O_3,\mathrm{soil}} = \frac{A}{4}\left(K_0^{\mathrm{therm}}e^{-\frac{E_a^{\mathrm{therm}}}{RT_{\mathrm{soil}}}}\right)\sqrt{\frac{8RT_{\mathrm{soil}}}{\pi M_{O_3}}}. \tag{B20}$$

$K_0^{\mathrm{therm}}$ is a proportionality parameter related to the probability of ozone colliding with a molecule on the soil surface (unitless); $E_a^{\mathrm{therm}}$ (J mol$^{-1}$) is the activation energy required for thermal decomposition to occur as a result of collision.

Following the same steps as before, the basic model for the ozone concentration profile within soil is

$$(\eta-\theta)\tau D_{O_3}\frac{d^2O_{3,\mathrm{soil}}}{dz^2} = AK_*\frac{1}{4}\sqrt{\frac{8RT_{\mathrm{soil}}}{\pi M_{O_3}}}O_{3,\mathrm{soil}} + \sum_i K_{X_i,O_3}O_{3,\mathrm{soil}}X_{i,\mathrm{soil}}, \tag{B21}$$

where $K_* = K_d + K_0^{\mathrm{therm}}e^{-\frac{E_a^{\mathrm{therm}}}{RT_{\mathrm{soil}}}}$.

Equation (B21) yields the following:

$$r_{\mathrm{soil}} \equiv \left(\left[\frac{A}{4}K_*\sqrt{\frac{8RT_{\mathrm{soil}}}{\pi M_{O_3}}} + \sum_i K_{X_i,O_3}X_{i,\mathrm{soil}}\right](\eta-\theta)\tau D_{O_3}\right)^{-\frac{1}{2}}. \tag{B22}$$

To estimate whether ozone dry deposition via thermal decomposition on soil surfaces may be important, we present $r_{\mathrm{soil}}$ assuming soil dry deposition only occurs through thermal decomposition:

$$r_{soil} = \left( \left[ \frac{A}{4} K_0^{therm} e^{-\frac{E_a^{therm}}{RT_{soil}}} \sqrt{\frac{8RT_{soil}}{\pi M_{O_3}}} \right] (\eta - \theta)\tau D_{O_3} \right)^{-1/2}. \quad \text{(B23)}$$

Previous studies infer $E_a^{therm}$ using regression analyses, assuming the resistance to uptake ($r_i$) is $r_i = ae^{\frac{b}{RT}}$ where $a$ and $b$ are empirical coefficients. For sandy-loam soil at Ispra forest in Italy, $b$ is 40,000 J mol$^{-1}$ (Fumagalli et al., 2016). For aluminum, stainless steel, beeswax, and paraffin wax (Cape et al., 2009), $b$ is 16,000 to 30,000 J mol$^{-1}$. To estimate $r_{soil}$ from equation (B23), we use $b = 25{,}000$ J mol$^{-1}$ which corresponds to $E_a^{therm} = 50{,}000$ J mol$^{-1}$ because equation (B23) is analogous to $r_i = ae^{\frac{b}{2RT}}$. If $E_a^{therm} = 50{,}000$ J mol$^{-1}$ and $T_{soil} = 15$ °C, then $r_{soil} = \frac{9.5\times10^5}{\sqrt{AK_0^{therm}(\eta-\theta)\tau}}$.

Depending on the magnitude of $A$, $K_0^{therm}$, and $(\eta - \theta)\tau$, thermal decomposition of ozone on surfaces could be an important contribution to ozone dry deposition. For example, $A$ ranges from $3 \times 10^7$ to $1 \times 10^9$ m$^2$ m$^{-3}$ for various clay minerals (Kabata-Pendias, 2004), assuming a bulk density of 1.3 g cm$^{-3}$ (Warrick & Nielsen, 1980). If we assume the unity upper bounds of $K_0^{therm}$ and $(\eta - \theta)\tau$, then this range in $A$ leads an upper bound of $r_{soil}$ from thermal decomposition as 30 to 170 s m$^{-1}$, connoting efficient ozone removal.

## Appendix C: Workshop Participants

Appendix C contains the table of participants at a workshop on ozone dry deposition at Lamont Doherty Earth Observatory of Columbia University in October 2017.

**Table C1**
*Participants at a Workshop on Ozone Dry Deposition at Lamont-Doherty Earth Observatory of Columbia University in October 2017*

| In-person participants | Affiliation |
|---|---|
| Alex Guenther | University of California Irvine |
| Allison Steiner | University of Michigan |
| Anthony Y. H. Wong | Boston University |
| Arlene Fiore | Lamont-Doherty Earth Observatory/Columbia University |
| Ashok Luhar | Commonwealth Scientific and Industrial Research Organisation Climate Science Centre, Australia |
| Barry Lefer | NASA |
| W. J. Massman | United States Forest Service |
| J. W. Munger | Harvard University |
| Catherine Hardacre | United Kingdom Met Office |
| Christopher Holmes | Florida State University |
| Colette Heald | Massachusetts Institute of Technology |
| Colleen Baublitz | Lamont-Doherty Earth Observatory/Columbia University |
| Delphine Farmer | Colorado State University |
| Dennis Baldocchi | University of California Berkeley |
| Detlev Helmig | Institute for Arctic and Alpine Research/University of Colorado Boulder |
| Donna Schwede | United States Environmental Protection Agency |
| Dylan Jones | University of Toronto |
| Dylan Millet | University of Minnesota |
| Elena McDonald-Buller | University of Texas at Austin |
| Erin Delaria | University of California Berkeley |
| Garry Hayman | United Kingdom Centre for Ecology and Hydrology, Wallingford, United Kingdom |
| Giacomo Gerosa | Università Cattolica del Sacro Cuore, Brescia, Italy |
| Glenn Wolfe | NASA Goddard Space Flight Center and University of Maryland Baltimore Campus |
| Jason Ducker | Florida State University |
| Jennifer Murphy | University of Toronto |
| Jingqiu Mao | University of Alaska Fairbanks |
| Joanna Joiner | NASA Goddard Space Flight Center |
| Katie Travis | Massachusetts Institute of Technology |
| Kenneth Mooney | NOAA Climate Program Office |
| Kevin Griffin | Columbia University |
| Larry Horowitz | NOAA Geophysical Fluid Dynamics Laboratory |

**Table C1** *(continued)*

| In-person participants | Affiliation |
|---|---|
| Leiming Zhang | Environment and Climate Change Canada |
| Lisa Emberson | Stockholm Environment Institute, University of York |
| Maria Val Martin | University of Sheffield |
| Matthias Sörgel | Max Planck Institute for Chemistry |
| Meiyun Lin | Princeton University and NOAA Geophysical Fluid Dynamics Laboratory |
| Mhairi Coyle | United Kingdom Centre for Ecology and Hydrology Edinburgh |
| Monika Kopacz | NOAA/ University Corporation for Atmospheric Reseach |
| Olivia Clifton | Lamont-Doherty Earth Observatory/Columbia University |
| Peter Zoogman | Minerva Schools at KGI |
| Phil Stevens | Indiana University |
| Sally Pusede | University of Virginia |
| Sam Silva | Massachusetts Institute of Technology |
| Sarah Kavassalis | University of Toronto |
| Stefano Galmarini | European Commission/ Joint Research Centre |
| Xiaomeng Jin | Lamont-Doherty Earth Observatory/Columbia University |
| Zhiyong Wu | United States Environmental Protection Agency |
| **Remote participants** | **Affiliation** |
| Amos Tai | Chinese University of Hong Kong |
| Amanda Cole | Environment and Climate Change Canada |
| Andrew Langford | NOAA Earth System Research Laboratory Chemical Sciences Division |
| Christian Hogrefe | United States Environmental Protection Agency |
| Eiko Nemitz | United Kingdom Centre for Ecology and Hydrology Edinburgh |
| Frank Dentener | European Commission |
| Jeff Geddes | Boston University |
| Gabriele Pfister | National Center for Atmospheric Research |
| Jonathan Pleim | United States Environmental Protection Agency |
| Kenneth Mooney | NOAA Climate Program Office |
| Liji David | Departments of Chemistry and Atmospheric Science, Colorado State University |
| Louisa Emmons | National Center for Atmospheric Research |
| Nadine Unger | University of Exeter |
| William Porter | University of California Riverside |

**Acknowledgments**
This material is based upon work supported by the National Center for Atmospheric Research, which is a major facility sponsored by the National Science Foundation under Cooperative Agreement 1852977. O. E. C. also acknowledges support from an NSF Graduate Research Fellowship (DGE 16-44869). A. M. F. acknowledges funding from NOAA's Climate Program Office's Atmospheric Chemistry, Carbon Cycle, and Climate program Grant NA14OAR4310133. O. E. C. acknowledges conversations with participants from a workshop on ozone dry deposition at Lamont-Doherty Earth Observatory in October 2017. The full list of participants in this workshop is given in Appendix C. The workshop was supported by the Lamont Climate Center, NASA, and NOAA. O. E. C. is also grateful for conversations with Róisín Commane, Adriana Bailey, and Andrew Weinheimer and thanks Don Lenschow, Jonathan Pleim, and Robert Pinder for comments on the manuscript. Disclaimer: The views expressed in this article are those of the authors and do not necessarily represent the views or policies of the U. S. Environmental Protection Agency. Data sets generated for Figures 2, 3, 4, 7, and 10 are available online (https://doi.org/10.5065/w2zc-bt87). Other figures containing scientific data are reprinted from the peer-reviewed literature: S. Sun, Morvakev, Trebs, et al. (2016) for Figure 6, Hardacre et al. (2015) for Figure 8, and Z. Wu et al. (2018) for Figure 9. O. E. C. thanks three anonymous reviewers for their constructive comments on this manuscript.

## References

Ainsworth, E. A. (2017). Understanding and improving global crop response to ozone pollution. *The Plant Journal*, *90*, 886–897.

Ainsworth, E. A., Yendrek, C. R., Sitch, S., Collins, W. J., & Emberson, L. D. (2012). The effects of tropospheric ozone on net primary productivity and implications for climate change. *Annual Review of Plant Biology*, *63*(1), 637–661. https://doi.org/10.1146/Annurev-Arplant-042110-103829

Albert, M. R., Grannas, A. M., Bottenheim, J., Shepson, P. B., & Perron, F. E. (2002). Processes and properties of snow-air transfer in the high Arctic with application to interstitial ozone at Alert, Canada. *Atmospheric Environment*, *36*(15-16), 2779–2787. https://doi.org/10.1016/S1352-2310(02)00118-8

Aldaz, L. (1969). Flux measurements of atmospheric ozone over land water. *Journal of Geophysical Research*, *74*(28), 6943–6946. https://doi.org/10.1029/JC074i028p06943

Almand-Hunter, B. B., Walker, J. T., Masson, N. P., Hafford, L., & Hannigan, M. P. (2015). Development and validation of inexpensive, automated, dynamic flux chambers. *Atmospheric Measurement Techniques*, *8*(1), 267–280. https://doi.org/10.5194/amt-8-267-2015

Altimir, N., Kolari, P., Tuovinen, J.-P., Vesala, T., Bäck, J., Suni, T., et al. (2006). Foliage surface ozone deposition: A role for surface moisture? *Biogeosciences*, *2*(6), 1739–1793. https://doi.org/10.5194/bgd-2-1739-2005

Altimir, N., Tuovinen, J.-P., Vesala, T., Kulmala, M., & Hari, P. (2004). Measurements of ozone removal by Scots pine shoots: Calibration of a stomatal uptake model including the non-stomatal component. *Atmospheric Environment*, *38*(15), 2387–2398.

Altimir, N., Vesala, T., Aalto, T., Bäck, J., & Hari, P. (2008). Stomatal-scale modelling of the competition between ozone sinks at the air-leaf interface. *Tellus Series B: Chemical and Physical Meteorology*. https://doi.org/10.1111/j.1600-0889.2008.00344.x

Altimir, N., Vesala, T., Keronen, P., Kulmala, M., & Hari, P. (2002). Methodology for direct field measurements of ozone flux to foliage with shoot chambers. *Atmospheric Environment*, *36*(1), 19–29.

Alwe, H. D., Millet, D. B., Chen, X., Raff, J. D., Payne, Z. C., & Fledderman, K. (2019). Oxidation of volatile organic compounds as the major source of formic acid in a mixed forest canopy. *Geophysical Research Letters*, *46*(5), 2940–2948. https://doi.org/10.1029/2018GL081526

Anav, A., Proietti, C., Menut, L., Carnicelli, S., De Marco, A., & Paoletti, E. (2018). Sensitivity of stomatal conductance to soil moisture: Implications for tropospheric ozone. *Atmospheric Chemistry and Physics*, *18*(8), 5747–5763. https://doi.org/10.5194/acp-18-5747-2018

Anderegg, W. R. L., Wolf, A., Arango-Velez, A., Choat, B., Chmura, D. J., Jansen, S., et al. (2017). Plant water potential improves prediction of empirical stomatal models. *PLoS ONE*, *12*(10), e0185481. https://doi.org/10.1371/journal.pone.0185481

Arnold, S. R., Lombardozzi, D., Lamarque, J.-F., Richardson, T., Emmons, L. K., Tilmes, S., et al. (2018). Simulated global climate response to tropospheric ozone-induced changes in plant transpiration. *Geophysical Research Letters*, *45*(23), 13,070–13,079. https://doi.org/10.1029/2018GL079938

Arya, S. P. (2001). *Introduction to micrometeorology* (2nd ed.). San Diego, CA: Academic Press.

Ashworth, K., Chung, S. H., Griffin, R. J., Chen, J., Forkel, R., Bryan, A. M., & Steiner, A. L. (2015). FORest Canopy Atmosphere Transfer (FORCAsT) 1.0: A 1-D model of biosphere-atmosphere chemical exchange. *Geoscientific Model Development*, *8*, 3765–3784. https://doi.org/10.5194/gmd-8-3765-2015

Aubinet, M., Vesala, T., & Papale, D. (Eds.) (2012). *Eddy covariance: A practical guide to measurement and data analysis*. Netherlands: Springer Science & Business Media.

Bakwin, P. S., Wofsy, S. C., Fan, S. M., Keller, M., Trumbore, S. E., & Costa, J. M. D. (1990). Emission of nitric oxide (NO) from tropical forest soils and exchange of NO between the forest canopy and atmospheric boundary layers. *Journal of Geophysical Research*, *95*(D10), 16,755–16,764. https://doi.org/10.1029/JD095iD10p16755

Baldocchi, D., & Meyers, T. (1998). On using eco-physiological, micrometeorological and biogeochemical theory to evaluate carbon dioxide, water vapor and trace gas fluxes over vegetation: A perspective. *Agricultural and Forest Meteorology*, *90*, 1–25.

Baldocchi, D. D., Hicks, B. B., & Camara, P. (1987). A canopy stomatal resistance model for gaseous deposition to vegetated surfaces. *Atmospheric Environment*, *2*(1), 91–101.

Baldocchi, D. D., Luxmoore, R. J., & Hatfield, J. L. (1991). Discerning the forest from the trees: An essay on scaling canopy stomatal conductance. *Agricultural and Forest Meteorology*, *54*, 197–226.

Ball, J. T., Woodrow, I. E., & Berry, J. A. (1987). A model predicting stomatal conductance and its contribution to the control of photosynthesis under different environmental conditions. In J. Biggens (Ed.), *Progress in photosynthesis research* (pp. 221–224). The Hague: Martinus Nijhoff.

Bariteau, L., Helmig, D., Fairall, C. W., Hare, J. E., Hueber, J., & Lang, E. K. (2010). Determination of oceanic ozone deposition by ship-borne eddy covariance flux measurements. *Atmospheric Measurement Techniques*, *3*(2), 441–455.

Bassin, S., Calanca, P., Weidinger, T., Gerosa, G., & Fuhrer, J. (2004). Modeling seasonal ozone fluxes to grassland and wheat: Model improvement, testing, and application. *Atmospheric Environment*, *38*, 2349–2359. https://doi.org/10.1016/j.atmosenv.2003.11.004

Bauer, M. R., Hultman, N. E., Panek, J. A., & Goldstein, A. H. (2000). Ozone deposition to a ponderosa pine plantation in the Sierra Nevada Mountains (CA): A comparison of two different climatic years. *Journal of Geophysical Research*, *105*(D17), 22,123–22,136. https://doi.org/10.1029/2000JD900168

Beddows, A. V., Kitwiroon, N., Williams, M. L., & Beevers, S. D. (2017). Emulation and sensitivity analysis of the community multiscale air quality model for a UK Ozone pollution episode. *Environmental Science & Technology*, *51*(11), 6229–6236.

Bela, M. M., Longo, K. M., Freitas, S. R., Moreira, D. S., Beck, V., Wofsy, S. C., et al. (2015). Ozone production and transport over the Amazon Basin during the dry-to-wet and wet-to-dry transition seasons. *Atmospheric Chemistry and Physics*, *15*(2), 757–782. https://doi.org/10.5194/acp-15-757-2015

Bocquet, F., Helmig, D., & Oltmans, S. J. (2007). Ozone in interstitial air of the mid-latitude, seasonal snowpack at Niwot Ridge, Colorado. *Arctic Antarctic and Alpine Research*, *39*, 375–387.

Bocquet, F., Helmig, D., Van Dam, B. A., & Fairall, C. W. (2011). Evaluation of the flux gradient technique for measurement of ozone surface fluxes over snowpack at Summit, Greenland. *Atmospheric Measurement Techniques*, *4*, 2305–2321. https://doi.org/10.5194/amt-4-2305-2011

Bonan, G. B., Patton, E. G., Harman, I. N., Oleson, K. W., Finnigan, J. J., Lu, Y. Q., & Burakowski, E. A. (2018). Modeling canopy-induced turbulence in the Earth system: A unified parameterization of turbulent exchange within plant canopies and the roughness sublayer (CLM-ml v0). *Geoscientific Model Development*, *11*, 1467–1496. https://doi.org/10.5194/gmd-11-1467-2018

Bonan, G. B., Williams, M., Fisher, R. A., & Oleson, K. W. (2014). Modeling stomatal conductance in the earth system: Linking leaf water-use efficiency and water transport along the soil–plant–atmosphere continuum. *Geoscientific Model Development*, *7*(5), 2193–2222.

Bottenheim, J. W., Fuentes, J. D., Tarasick, D. W., & Anlauf, K. G. (2002). Ozone in the Arctic lower troposphere during winter and spring 2000 (ALERT2000). *Atmospheric Environment*, *36*, 2535–2544. https://doi.org/10.1016/s1352-2310(02)00121-8

Bourtsoukidis, E., Behrendt, T., Yañez-Serrano, A. M., Hellén, H., Diamantopoulos, E., Catão, E., et al. (2018). Strong sesquiterpene emissions from Amazonian soils. *Nature Communications*, *9*(1), 2226. https://doi.org/10.1038/s41467-018-04658-y

Bouvier-Brown, N. C., Goldstein, A. H., Gilman, J. B., Kuster, W. C., & de Gouw, J. A. (2009). In-situ ambient quantification of monoterpenes, sesquiterpenes, and related oxygenated compounds during BEARPEX: Implications for gas- and particle-phase chemistry. *Atmospheric Chemistry and Physics*, *9*, 5505–5518.

Breuninger, C., Oswald, R., Kesselmeier, J., & Meixner, F. X. (2012). The dynamic chamber method: Trace gas exchange fluxes (NO, $NO_2$, $O_3$) between plants and the atmosphere in the laboratory and in the field. *Atmospheric Measurement Techniques*, *5*(5), 955–989.

Brutsaert, W. (1979). Heat and mass transfer to and from surfaces with dense vegetation or similar permeable roughness. *Boundary-Layer Meteorology*, *16*, 365–388.

Bryan, A. M., Bertman, S. B., Carroll, M. A., Dusanter, S., Edwards, G. D., Forkel, R., et al. (2012). In-canopy gas-phase chemistry during CABINEX 2009: Sensitivity of a 1-D canopy model to vertical mixing and isoprene chemistry. *Atmospheric Chemistry and Physics*, *12*(18), 8829–8849. https://doi.org/10.5194/acp-12-8829-2012

Buckley, T. N., & Mott, K. A. (2013). Modelling stomatal conductance in response to environmental factors. *Plant, Cell & Environment*, *36*(9), 1691–1699.

Büker, P., Emberson, L. D., Ashmore, M. R., Cambridge, H. M., Jacobs, C. M. J., Massman, W. J., et al. (2007). Comparison of different stomatal conductance algorithms for ozone flux modelling. *Environmental Pollution*, *146*(3), 726–735. https://doi.org/10.1016/j.envpol.2006.04.007

Büker, P., Morrissey, T., Briolat, A., Falk, R., Simpson, D., Tuovinen, J.-P., et al. (2012). $DO_3SE$ modelling of soil moisture to determine ozone flux to forest trees. *Atmospheric Chemistry and Physics*, *12*(12), 5537–5562. https://doi.org/10.5194/acp-12-5537-2012

Burkhardt, J. (2010). Hygroscopic particles on leaves: Nutrients or desiccants? *Ecological Monographs*, *80*(3), 369–399. https://doi.org/10.1890/09-1988.1

Burkhardt, J., & Eiden, R. (1994). Thin water films on coniferous needles. *Atmospheric Environment*, *28*(12), 2001–2011. https://doi.org/10.1016/1352-2310(94)90469-3

Burkhardt, J., & Hunsche, M. (2013). "Breath figures" on leaf surfaces—Formation and effects of microscopic leaf wetness. *Frontiers in Plant Science*, *4*(422). https://doi.org/10.3389/fpls.2013.00422

Buschhaus, C., & Jetter, R. (2012). Composition and physiological function of the wax layers coating arabidopsis leaves: β-amyrin negatively affects the intracuticular water barrier. *Plant Physiology*, *160*(2), 1120–1129. https://doi.org/10.1104/pp.112.198473

Businger, J. A. (1986). Evaluation of the accuracy with which dry deposition can be measured with current micrometeorological techniques. *Journal of Climate and Applied Meteorology*, *25*(8), 1100–1124.

Businger, J. A., Wyngaard, J. C., Izumi, Y., & Bradley, E. F. (1971). Flux-profile relationships in the atmospheric surface layer. *Journal of the Atmospheric Sciences*, *28*(2), 181–189. https://doi.org/10.1175/1520-0469(1971)028<0181:FPRITA>2.0.CO;2

Buzorius, G., Rannik, Ü., Makela, J. M., Vesala, T., & Kulmala, M. (1998). Vertical aerosol particle fluxes measured by eddy covariance technique using condensational particle counter. *Journal of Aerosol Science*, *29*(1-2), 157–171. https://doi.org/10.1016/S0021-8502(97)00458-8

Calatayud, V., Cerveró, J., & Sanz, M. J. (2007). Foliar, physiological and growth responses of four maple species exposed to ozone. *Water, Air, and Soil Pollution*, *185*(1-4), 239–254. https://doi.org/10.1007/s11270-007-9446-5

Calogirou, A., Larsen, B. R., & Kotzias, D. (1999). Gas-phase terpene oxidation products: a review. *Atmospheric Environment*, *33*(9), 1423–1439. https://doi.org/10.1016/S1352-2310(98)00277-5

Campbell, P. C., Bash, J. O., & Spero, T. L. (2019). Updates to the Noah Land Surface Model in WRF-CMAQ to improve simulated meteorology, air quality, and deposition. *Journal of Advances in Modeling Earth Systems*, *11*(1), 231–256. https://doi.org/10.1029/2018MS001422

Cape, J. N., Hamilton, R., & Heal, M. R. (2009). Reactive uptake of ozone at simulated leaf surfaces: Implications for "non-stomatal" ozone flux. *Atmospheric Environment*, *43*(5), 1116–1123. https://doi.org/10.1016/j.atmosenv.2008.11.007

Cavicchioli, C., Manzi, G., Catenacci, G., Brusasca, G., & Borgarello, M. (1997). Dry deposition inferential meaesurement in a rural region of Northern Italy. In S. Slanina (Ed.), *Transport and chemical transformation of pollutants in the troposphere: Experimental and theoretical studies of biogenic emissions and of pollutant deposition* (pp. 457–466). Berlin: Springer.

Cellier, P., & Brunet, Y. (1992). Flux-gradient relationships above tall plant canopies. *Agricultural and Forest Meteorology*, *58*(1-2), 93–117. https://doi.org/10.1016/0168-1923(92)90113-I

Centoni, F. (2017). Global scale modelling of ozone deposition processes and interactions between surface ozone and climate change (Doctoral dissertation). Edinburgh, UK: The University of Edinburgh.

Cernusak, L. A., Ubierna, N., Jenkins, M. W., Garrity, S. R., Rahn, T., Powers, H. H., et al. (2018). Unsaturation of vapour pressure inside leaves of two conifer species. *Scientific Reports*, *8*(1), 7667. https://doi.org/10.1038/s41598-018-25838-2

Chang, K.-Y., Paw U, K. T., & Chen, S.-H. (2018). Canopy profile sensitivity on surface layer simulations evaluated by a multiple canopy layer higher order closure land surface model. *Agricultural and Forest Meteorology*, *252*, 192–207. https://doi.org/10.1016/j.agrformet.2018.01.027

Chapleski, R. C., Zhang, Y., Troya, D., & Morris, J. R. (2016). Heterogeneous chemistry and reaction dynamics of the atmospheric oxidants, $O_3$, $NO_3$, and OH, on organic surfaces. *Chemical Society Reviews*, *45*(13), 3731–3746. https://doi.org/10.1039/c5cs00375j

Charusombat, U., Niyogi, D., Kumar, A., & Wang, X. (2010). Evaluating a new deposition velocity module in the Noah land-surface model. *Boundary-Layer Meteorology*, *137*(2), 271–290. https://doi.org/10.1007/s10546-010-9531-y

Choi, W., Faloona, I. C., Bouvier-Brown, N. C., McKay, M., Goldstein, A. H., Mao, J., et al. (2010). Observations of elevated formaldehyde over a forest canopy suggest missing sources from rapid oxidation of boreal hydrocarbons. *Atmospheric Chemistry and Physics*, *10*(18), 8761–8781. https://doi.org/10.5194/acp-10-8761-2010

Choudhury, B. J., & Monteith, J. L. (1988). A four-layer model for the heat budget of homogeneous land surfaces. *Quarterly Journal of the Royal Meteorological Society*, *114*(480), 373–398.

Chu, H., Baldocchi, D. D., John, R., Wolf, S., & Reichstein, M. (2017). Fluxes all of the time? A primer on the temporal representativeness of FLUXNET. *Journal of Geophysical Research: Biogeosciences*, *122*, 289–307. https://doi.org/10.1002/2016JG003576

Cieslik, S. (2009). Ozone fluxes over various plant ecosystems in Italy: A review. *Environmental Pollution*, *157*(5), 1487–1496. https://doi.org/10.1016/j.envpol.2008.09.050

Cieslik, S., & Labatut, A. (1997). Ozone and heat fluxes over a Mediterranean pseudosteppe. *Atmospheric Environment*, *31*, 177–184. https://doi.org/10.1016/S1352-2310(97)00084-8

Cieslik, S. A. (2004). Ozone uptake by various surface types: A comparison between dose and exposure. *Atmospheric Environment*, *38*(15), 2409–2420. https://doi.org/10.1016/j.atmosenv.2003.10.063

Clark, D. B., Mercado, L. M., Sitch, S., Jones, C. D., Gedney, N., Best, M. J., et al. (2011). The Joint UK Land Environment Simulator (JULES), model description—Part 2: Carbon fluxes and vegetation dynamics. *Geoscientific Model Development*, *4*(3), 701–722. https://doi.org/10.5194/gmd-4-701-2011

Clifton, O. E. (2018). Constraints on ozone removal by land and implications for 21$^{st}$ Century ozone pollution (Doctoral dissertation). New York, New York: Columbia University in the City of New York. https://doi.org/10.7916/D8709J8T

Clifton, O. E., Fiore, A. M., Munger, J. W., Malyshev, S., Horowitz, L. W., Shevliakova, E., et al. (2017). Interannual variability in ozone removal by a temperate deciduous forest. *Geophysical Research Letters*, *44*, 542–552. https://doi.org/10.1002/2016GL070923

Clifton, O. E., Fiore, A. M., Munger, J. W., & Wehr, R. (2019). Spatiotemporal controls on observed daytime ozone deposition velocity over Northeastern U.S. forests during summer. *Journal of Geophysical Research: Atmospheres*, *124*, 5612–5628. https://doi.org/10.1029/2018JD029073

Coe, H., Gallagher, M. W., Choularton, T. W., & Dore, C. (1995). Canopy scale measurements of stomatal and cuticular $O_3$ uptake by Sitka spruce. *Atmospheric Environment*, *29*(12), 1413–1423. https://doi.org/10.1016/1352-2310(95)00034-V

Colbeck, I., & Harrison, R. M. (1985). Dry deposition of ozone—Some measurements of deposition velocity and of vertical profiles to 100-metres. *Atmospheric Environment*, *19*(11), 1807–1818. https://doi.org/10.1016/0004-6981(85)90007-1

Commane, R., Meredith, L. K., Baker, I. T., Berry, J. A., Munger, J. W., Montzka, S. A., et al. (2015). Seasonal fluxes of carbonyl sulfide in a midlatitude forest. *Proceedings of the National Academy of Sciences*, *112*(46), 14,162–14,167. https://doi.org/10.1073/pnas.1504131112

Cook, G. D., & Viskanta, R. (1968). Mutual diffusional interference between adjacent stomata of a leaf. *Plant Physiology*, *43*(7), 1017–1022. https://doi.org/10.1104/pp.43.7.1017

Cooter, E. J., & Schwede, D. B. (2000). Sensitivity of the National Oceanic and Atmospheric Administration multilayer model to instrument error and parameterization uncertainty. *Journal of Geophysical Research*, *105*(D5), 6695–6707. https://doi.org/10.1029/1999JD901080

Cowan, I. R., & Farquhar, G. D. (1977). Stomatal function in relation to leaf metabolism and environment. In D. H. Jennings (Ed.), *Integration of activity in the higher plant* (pp. 471–505). Cambridge, UK: Cambridge University Press.

Coyle, M. (2005). The gaseous exchange of ozone at terrestrial surfaces: Nonstomatal deposition to grassland (Doctoral dissertation). Edinburgh, UK: The University of Edinburgh.

Coyle, M., Nemitz, E., Storeton-West, R., Fowler, D., & Cape, J. N. (2009). Measurements of ozone deposition to a potato canopy. *Agricultural and Forest Meteorology*, *149*(3-4), 655–666. https://doi.org/10.1016/j.agrformet.2008.10.020

Crawford, J. H., Davis, D. D., Chen, G., Buhr, M., Oltmans, S., Weller, R., et al. (2001). Evidence for photochemical production of ozone at the South Pole surface. *Geophysical Research Letters*, *28*(19), 3641–3644. https://doi.org/10.1029/2001GL013055

Cristofanelli, P., Putero, D., Bonasoni, P., Busetto, M., Calzolari, F., Camporeale, G., et al. (2018). Analysis of multi-year near-surface ozone observations at the WMO/GAW "Concordia" station (75°06′S, 123°20′E, 3280 m a.s.l. - Antarctica). *Atmospheric Environment*, *177*, 54–63. https://doi.org/10.1016/j.atmosenv.2018.01.007

Cros, B., Delon, C., Affre, C., Marion, T., Druilhet, A., Perros, P. E., & Lopez, A. (2000). Sources and sinks of ozone in savanna and forest areas during EXPRESSO: Airborne turbulent flux measurements. *Journal of Geophysical Research*, *105*(D24), 29,347–29,358. https://doi.org/10.1029/2000JD900451

Damköhler, G. (1940). Der einfluss der turbulenz auf die flammengeschwindigkeit in gasgemischen. *Zeitschrift für Elektrochemie und Angewandte Physikalische Chemie*, *46*(11), 601–626.

D'Anna, B., Jammoul, A., George, C., Stemmler, K., Fahrni, S., Ammann, M., & Wisthaler, A. (2009). Light-induced ozone depletion by humic acid films and submicron aerosol particles. *Journal of Geophysical Research*, *114*, D12301. https://doi.org/10.1029/2008JD011237

Daudet, F. A., Le Roux, X., Sinoquet, H., & Adam, B. (1999). Wind speed and leaf boundary layer conductance variation within tree crown: Consequences on leaf-to-atmosphere coupling and tree functions. *Agricultural and Forest Meteorology*, *97*, 171–185.

De Miguel, A., & Bilbao, J. (1999). Ozone dry deposition and resistances onto green grassland in summer in central Spain. *Journal of Atmospheric Chemistry*, *34*(3), 321–338.

Deckmyn, G., De Beeck, M. O., Löw, M., Then, C., Verbeeck, H., Wipfler, P., & Ceulemans, R. (2007). Modelling ozone effects on adult beech trees through simulation of defence, damage, and repair costs: Implementation of the CASIROZ ozone model in the ANAFORE forest model. *Plant Biology*, *9*(02), 320–330.

Delaria, E. R., Vieira, M., Cremieux, J., & Cohen, R. C. (2018). Measurements of NO and $NO_2$ exchange between the atmosphere and *Quercus agrifolia*. *Atmospheric Chemistry and Physics*, *18*(19), 14,161–14,173.

Desjardins, R. L., MacPherson, J. I., Neumann, H., den Hartog, G., & Schuepp, P. H. (1995). Flux estimates of latent and sensible heat, carbon dioxide, and ozone using an aircraft-tower combination. *Atmospheric Environment*, *29*(21), 3147–3158.

Dias-Júnior, C. Q., Luís Dias, N., Santos, R. M. N., Sörgel, M., Araújo, S., Tsokankunku, A., et al. (2019). Is there a classical inertial sublayer over the Amazon forest? *Geophysical Research Letters*, *46*(10), 5614–5622. https://doi.org/10.1029/2019GL083237

Disselkamp, R. S., Carpenter, M. A., Cowin, J. P., Berkowitz, C. M., Chapman, E. G., Zaveri, R. A., & Laulainen, N. S. (2000). Ozone loss in soot aerosols. *Journal of Geophysical Research*, *105*(D8), 9767–9771. https://doi.org/10.1029/1999JD901189

Dorsey, J. R., Duyzer, J. H., Gallagher, M. W., Coe, H., Pilegaard, K., Westrate, J. H., et al. (2004). Oxidized nitrogen and ozone interaction with forests. I: Experimental observations and analysis of exchange with Douglas fir. *Quarterly Journal of the Royal Meteorological Society*, *130*(600), 1941–1955. https://doi.org/10.1256/qj.03.124

Droppo, J. G. (1985). Concurrent measurements of ozone dry deposition using eddy correlation and profile flux methods. *Journal of Geophysical Research*, *90*(D1), 2111–2118. https://doi.org/10.1029/JD090iD01p02111

Drummond, J. W., Topham, L. A., Mackay, G. I., & Schiff, H. I. (1991). Use of chemiluminescence techniques in portable, lightweight, highly sensitive instruments for measuring $NO_2$, $NO_x$, and $O_3$. In H. I. Schiff (Ed.), *Measurement of Atmospheric Gases* (Vol. 1433, pp. 224–232). International Society for Optics and Photonics. https://doi.org/10.1117/12.46166

Ducker, J. A., Holmes, C. D., Keenan, T. F., Fares, S., Goldstein, A. H., Mammarella, I., et al. (2018). Synthetic ozone deposition and stomatal uptake at flux tower sites. *Biogeosciences*, *15*(17), 5395–5413. https://doi.org/10.5194/bg-15-5395-2018

Dupont, S., & Patton, E. G. (2012). Momentum and scalar transport within a vegetation canopy following atmospheric stability and seasonal canopy changes: The CHATS experiment. *Atmospheric Chemistry and Physics*, *12*, 5913–5935.

Duyzer, J., Deinum, G., & Baak, J. (1995). The interpretation of measurements of surface exchange of nitrogen oxides: Correction for chemical reactions. *Philosophical Transactions of the Royal Society of London A*, *351*, 231–248.

Duyzer, J., & Westrate, H. (1995). The use of the gradient method to monitor trace gas fluxes over forest: Flux-profile functions for ozone and heat. In G. J. Heij & J. W. Erisman (Eds.), *Acid Rain Research: Do we have enough answers?* (pp. 21–30). Elsevier Science BV.

Duyzer, J. H., Dorsey, J. R., Gallagher, M. W., Pilegaard, K., & Walton, S. (2004). Oxidized nitrogen and ozone interaction with forests. II: Multi-layer process-oriented modelling results and a sensitivity study for Douglas fir. *Quarterly Journal of the Royal Meteorological Society*, *130*(600), 1957–1971. https://doi.org/10.1256/qj.03.125

Duyzer, J. H., Meyer, G. M., & van Aalst, R. M. (1983). Measurement of dry deposition velocities of NO, $NO_2$, and $O_3$ and the influence of chemical reactions. *Atmospheric Environment*, *17*(10), 2117–2120.

Eastman, J. A., & Stedman, D. H. (1977). A fast response sensor for ozone eddy-correlation flux measurements. *Atmospheric Environment*, *11*(12), 1209–1211.

Eiden, R., Burkhardt, J., & Burkhardt, O. (1994). Atmospheric aerosol particles and their role in the formation of dew on the surface of plant leaves. *Journal of Aerosol Science*, *25*(2), 367–376. https://doi.org/10.1016/0021-8502(94)90087-6

Eller, A. S., & Sparks, J. P. (2006). Predicting leaf-level fluxes of $O_3$ and $NO_2$: The relative roles of diffusion and biochemical processes. *Plant, Cell & Environment*, *29*(9), 1742–1750.

El-Madany, T., Niklasch, K., & Klemm, O. (2017). Stomatal and non-stomatal turbulent deposition flux of ozone to a managed peatland. *Atmosphere*, *8*(9), 175.

Emberson, L. D., Nitwiroon, N., Beevers, S., Büker, P., & Cinderby, S. (2013). Scorched Earth: how will changes in the strength of the vegetation sink to ozone deposition affect human health and ecosystems? *Atmospheric Chemistry and Physics*, *13*(14), 6741–6755. https://doi.org/10.5194/acp-13-6741-2013

Emberson, L. D., Pleijel, H., Ainsworth, E. A., Van den Berg, M., Ren, W., Osborne, S., et al. (2018). Ozone effects on crops and consideration in crop models. *European Journal of Agronomy*, *100*, 19–34. https://doi.org/10.1016/j.eja.2018.06.002

Emberson, L. D., Simpson, D., Tuovinen, J.-P., Ashmore, M. R., & Cambridge, H. M. (2000). Towards a model of ozone deposition and stomatal uptake over Europe (Research Note No. 42). Norwegian Meteorological Institute.

Enders, G. (1992). Deposition of ozone to a mature spruce forest: Measurements and comparison to models. *Environmental Pollution*, *75*, 61–67.

Enders, G., Dlugi, R., Steinbrecher, R., Clement, B., Daiber, R., Eijk, J. V., et al. (1992). Biosphere/atmosphere interactions: Integrated research in a European coniferous forest ecosystem. *Atmospheric Environment*, *26A*(1), 171–189.

Erisman, J. W., Van Pul, A., & Wyers, P. (1994). Parameterization of surface resistance for the quantification of atmospheric deposition of acidifying pollutants and ozone. *Atmospheric Environment*, *28*, 2595–2607.

Ermel, M., Oswald, R., Mayer, J.-C., Moravek, A., Song, G., Beck, M., et al. (2013). Preparation methods to optimize the performance of sensor discs for fast chemiluminescence ozone analyzers. *Environmental Science & Technology*, *47*(4), 1930–1936. https://doi.org/10.1021/es3040363

Ewert, F., & Porter, J. R. (2000). Ozone effects on wheat in relation to $CO_2$: Modelling short-term and long-term responses of leaf photosynthesis and leaf duration. *Global Change Biology*, *6*(7), 735–750.
Falk, S., & Søvde Haslerud, A. (2019). Update and evaluation of the ozone dry deposition in Olso CTM3 v1.0. *Geoscientific Model Development*, *12*(11), 4705–4728. https://doi.org/10.5194/gmd-12-4705-2019
Faloona, I., Tan, D., Brune, W., Hurst, J., Barket, D., Couch, T. L., et al. (2001). Nighttime observations of anomalously high levels of hydroxyl radicals above a deciduous forest canopy. *Journal of Geophysical Research*, *106*(D20), 24,315–24,333. https://doi.org/10.1029/2000JD900691
Fan, S. M., Wofsy, S. C., Bakwin, P. S., Jacob, D. J., & Fitzjarrald, D. R. (1990). Atmosphere-biosphere exchange of $CO_2$ and $O_3$ in the central Amazon forest. *Journal of Geophysical Research*, *95*(D10), 16,851–16,864. https://doi.org/10.1029/JD095iD10p16851
Farage, P. K., Long, S. P., Lechner, E. G., & Baker, N. R. (1991). The sequence of change within the photosynthetic apparatus of wheat following short-term exposure to ozone. *Plant Physiology*, *95*(2), 529–535.
Fares, S., Alivernini, S., Conte, A., & Maggi, F. (2019). Ozone and particle fluxes in a Mediterranean forest predicted by the AIRTREE model. *Science of the Total Environment*, *682*, 494–504.
Fares, S., Loreto, F., Kleist, E., & Wildt, J. (2007). Stomatal uptake and stomatal deposition of ozone in isoprene and monoterpene emitting plants. *Plant Biology*. https://doi.org/10.1055/s-2007-965257
Fares, S., Matteucci, G., Scarascia Mugnozza, G., Morani, A., Calfapietra, C., Salvatori, E., et al. (2013). Testing of models of stomatal ozone fluxes with field measurements in a mixed Mediterranean forest. *Atmospheric Environment*. https://doi.org/10.1016/j.atmosenv.2012.11.007
Fares, S., McKay, M., Holzinger, R., & Goldstein, A. H. (2010). Ozone fluxes in a Pinus ponderosa ecosystem are dominated by non-stomatal processes: Evidence from long-term continuous measurements. *Agricultural and Forest Meteorology*, *150*(3), 420–431.
Fares, S., Park, J.-H., Ormeno, E., Gentner, D. R., McKay, M., Loreto, F., et al. (2010). Ozone uptake by citrus trees exposed to a range of ozone concentrations. *Atmospheric Environment*, *44*(28), 3404–3412. https://doi.org/10.1016/j.atmosenv.2010.06.010
Fares, S., Savi, F., Muller, J., Matteucci, G., & Paoletti, E. (2014). Simultaneous measurements of above and below canopy ozone fluxes help partitioning ozone deposition between its various sinks in a Mediterranean Oak Forest. *Agricultural and Forest Meteorology*, *198*, 181–191.
Fares, S., Weber, R., Park, J.-H., Gentner, D., Karlik, J., & Goldstein, A. H. (2012). Ozone deposition to an orange orchard: partitioning between stomatal and non-stomatal sinks. *Environmental Pollution*, *169*, 258–266.
Farmer, D. K., & Cohen, R. C. (2008). Observations of $HNO_3$, SAN, SPN and $NO_2$ fluxes: Evidence for rapid $HO_x$ chemistry within a pine forest canopy. *Atmospheric Chemistry and Physics*, *8*(14), 3899–3917.
Farmer, D. K., Kimmel, J. R., Phillips, G., Docherty, K. S., Worsnop, D. R., Sueper, D., et al. (2011). Eddy covariance measurements with high-resolution time-of-flight aerosol mass spectrometry: A new approach to chemically resolved aerosol fluxes. *Atmospheric Measurement Techniques*, *4*(6), 1275–1289. https://doi.org/10.5194/amt-4-1275-2011
Finco, A., Coyle, M., Nemitz, E., Marzuoli, R., Chiesa, M., Loubet, B., et al. (2018). Characterization of ozone deposition to mixed oak-hornbeam forest–flux measurements at five levels above and inside the canopy and their interactions with nitric oxide. *Atmospheric Chemistry and Physics*, *18*(24), 17,945–17,961. https://doi.org/10.5194/acp-18-17945-2018
Finkelstein, P. L. (2001). Deposition velocities of $SO_2$ and $O_3$ over agricultural and forest ecosystems. *Water, Air, & Soil Pollution: Focus*, *1*(5-6), 49–57.
Finkelstein, P. L., Ellestad, T. G., Clarke, J. F., Meyers, T. P., Schwede, D. B., Hebert, E. O., & Neal, J. A. (2000). Ozone and sulfur dioxide dry deposition to forests: Observations and model evaluation. *Journal of Geophysical Research*, *105*(D12), 15,365–15,377. https://doi.org/10.1029/2000JD900185
Finkelstein, P. L., & Sims, P. F. (2001). Sampling error in eddy correlation flux measurements. *Journal of Geophysical Research*, *106*(D4), 3503–3509. https://doi.org/10.1029/2000JD900731
Finnigan, J. J., Shaw, R. H., & Patton, E. G. (2009). Turbulence structure above a vegetation canopy. *Journal of Fluid Mechanics*, *637*, 387–424.
Fiscus, E. L., Booker, F. L., & Burkey, K. O. (2005). Crop responses to ozone: Uptake, modes of action, carbon assimilation and partitioning. *Plant, Cell & Environment*, *28*(8), 997–1011. https://doi.org/10.1111/J.1365-3040.2005.01349.X
Fitzjarrald, D. R., & Lenschow, D. H. (1983). Mean concentration and flux profiles for chemically reactive species in the atmospheric surface-layer. *Atmospheric Environment*, *17*(12), 2505–2512.
Foken, T., Mauder, M., Liebethal, C., Wimmer, F., Beyrich, F., Leps, J. P., et al. (2010). Energy balance closure for the LITFASS-2003 experiment. *Theoretical and Applied Climatology*, *101*(1-2), 149–160. https://doi.org/10.1007/s00704-009-0216-8
Fowler, D., Flechard, C., Cape, J. N., Storeton-West, R. L., & Coyle, M. (2001). Measurements of ozone deposition to vegetation quantifying the flux, the stomatal and non-stomatal components. *Water, Air, and Soil Pollution*, *130*, 63–74. https://doi.org/10.1023/A:1012243317471
Fowler, D., Nemitz, E., Misztal, P., Di Marco, C., Skiba, U., Ryder, J., et al. (2011). Effects of land use on surface-atmosphere exchanges of trace gases and energy in Borneo: Comparing fluxes over oil palm plantations and a rainforest. *Philosophical Transactions of the Royal Society, B: Biological Sciences*, *366*(1582), 3196–3209. https://doi.org/10.1098/rstb.2011.0055
Fowler, D., Pilegaard, K., Sutton, M. A., Ambus, P., Raivonen, M., Duyzer, J., et al. (2009). Atmospheric composition change: Ecosystems-atmosphere interactions. *Atmospheric Environment*, *43*(33), 5193–5267. https://doi.org/10.1016/j.atmosenv.2009.07.068
Franks, P. J., Bonan, G. B., Berry, J. A., Lombardozzi, D. L., Holbrook, N. M., Herold, N., & Oleson, K. W. (2018). Comparing optimal and empirical stomatal conductance models for application in Earth system models. *Global Change Biology*, 1–16. https://doi.org/10.1111/gcb.14445
Franz, M., Simpson, D., Arneth, A., & Zaehle, S. (2017). Development and evaluation of an ozone deposition scheme for coupling to a terrestrial biosphere model. *Biogeosciences*, *14*, 45–71. https://doi.org/10.5194/bg-14-45-2017
Freer-Smith, P. H., & Dobson, M. C. (1989). Ozone flux to *Picea sitchensis (bong) carr* and *Picea abies (l) karst* during short episodes and the effects of these on transpiration and photosynthesis. *Environmental Pollution*, *59*(2), 161–176.
Freire, L. S., Gerken, T., Ruiz-Plancarte, J., Wei, D., Fuentes, J. D., Katul, G. G., et al. (2017). Turbulent mixing and removal of ozone within an Amazon rainforest canopy. *Journal of Geophysical Research: Atmospheres*, *122*, 2791–2811. https://doi.org/10.1002/2016JD026009
Fuentes, J. D., Chamecki, M., Nascimento dos Santos, R. M., Von Randow, C., Stoy, P. C., Katul, G., et al. (2016). Linking meteorology, turbulence, and air chemistry in the Amazon rain forest. *Bulletin of the American Meteorological Society*, *97*(12), 2329–2342. https://doi.org/10.1175/BAMS-D-15-00152.1
Fuentes, J. D., den Hartog, G., Neumann, H. H., & Gillespie, T. J. (1994). Measurements and modelling of ozone deposition to wet foliage. In *Air pollutants and the leaf cuticle* (pp. 239–253). Berlin, Germany: Springer.

Fuentes, J. D., & Gillespie, T. J. (1992). A gas exchange system to study the effects of leaf surface wetness on the deposition of ozone. *Atmospheric Environment*, *26A*(6), 1165–1173. https://doi.org/10.1016/0960-1686(92)90048-P

Fuentes, J. D., Gillespie, T. J., den Hartog, G., & Neumann, H. H. (1992). Ozone deposition onto a deciduous forest during dry and wet conditions. *Agricultural and Forest Meteorology*, *62*, 1–18.

Fumagalli, I., Gruening, C., Marzuoli, R., Cieslik, S., & Gerosa, G. (2016). Long-term measurements of $NO_x$ and $O_3$ soil fluxes in a temperate deciduous forest. *Agricultural and Forest Meteorology*, *228*, 205–216. https://dx.doi.org/10.1016/j.agrformet.2016.07.011

Fung, P. K. (2018). Ozone deposition over a boreal lake by the eddy covariance method (Masters dissertation). Helsinki, Finland: University of Helsinki.

Galbally, I., & Allison, I. (1972). Ozone fluxes over snow surfaces. *Journal of Geophysical Research*, *77*(21), 3946–3949. https://doi.org/10.1029/JC077i021p03946

Galbally, I. E. (1971). Ozone profiles and ozone fluxes in atmospheric surface layer. *Quarterly Journal of the Royal Meteorological Society*, *97*(411), 18–29. https://doi.org/10.1002/qj.49709741103

Galbally, I. E., & Roy, C. R. (1980). Destruction of Ozone at the Earth's surface. *Quarterly Journal of the Royal Meteorological Society*, *106*, 599–620.

Gallagher, M. W., Beswick, K. M., & Coe, H. (2001). Ozone deposition to coastal waters. *Quarterly Journal of the Royal Meteorological Society*, *127*, 539–558.

Galmarini, S., de Arellano, J. V. G., & Duyzer, J. (1997). Fluxes of chemically reactive species inferred from mean concentration measurements. *Atmospheric Environment*, *31*(15), 2371–2374.

Ganzeveld, L., Ammann, C., & Loubet, B. (2015). Modelling atmosphere-biosphere exchange of ozone and nitrogen oxides. In R.-S. Massad & B. Loubet (Eds.), *Review and integration of biosphere-atmosphere modelling of reactive trace gases and volatile aerosols* (pp. 85–105). Netherlands: Springer.

Ganzeveld, L., Helmig, D., Fairall, C. W., Hare, J., & Pozzer, A. (2009). Atmosphere-ocean ozone exchange: A global modeling study of biogeochemical, atmospheric and waterside turbulence dependencies. *Global Biogeochemical Cycles*, *23*, GB4021. https://doi.org/10.1029/2008GB003301

Ganzeveld, L. N., Lelieveld, J., Dentener, F. J., Krol, M. C., & Roelofs, G. J. (2002). Atmosphere-biosphere trace gas exchanges simulated with a single-column model. *Journal of Geophysical Research*, *107*(D16), 4297. https://doi.org/10.1029/2001JD000684

Gao, W., Shaw, R. H., & Paw U, K. T. (1989). Observation of organized structure in turbulent flow within and above a forest canopy. *Boundary-Layer Meteorology*, *47*, 349–377.

Gao, W., Wesely, M. L., Cook, D. R., & Hart, R. L. (1992). Air-surface exchange of $H_2O$, $CO_2$, and $O_3$ at a tallgrass prairie in relation to remotely sensed vegetation indices. *Journal of Geophysical Research*, *97*(D17), 18,663-18,671.https://doi.org/10.1029/91JD03175

Garland, J. A., & Penkett, S. A. (1976). Absorption of peroxy acetyl nitrate and ozone by natural surfaces. *Atmospheric Environment*, *10*, 1127–1131.

Georgii, H.-W. (Ed.) (1989). *Mechanisms and effects of pollutant-transfer into forests*. Dordrecht: Kluwer Academic Publishers. https://doi.org/10.1007/978-94-009-1023-2

Gerosa, G., Cieslik, S., & Ballarin-Denti, A. (2003). Micrometeorological determination of time-integrated stomatal ozone fluxes over wheat: A case study in Northern Italy. *Atmospheric Environment*, *37*(6), 777–788. https://doi.org/10.1016/S1352-2310(02)00927-5

Gerosa, G., Cieslik, S., & Derghi, F. (2007). Comparison of different algorithms for stomatal ozone flux determination from micrometeorological measurements. *Water, Air, and Soil Pollution*, *179*(1-4), 309–321. https://doi.org/10.1007/s11270-006-9234-7

Gerosa, G., Finco, A., Mereu, S., Marzuoli, R., & Ballarin-Denti, A. (2009). Interactions among vegetation and ozone, water and nitrogen fluxes in a coastal Mediterranean maquis ecosystem. *Biogeosciences*, *6*, 1783–1798.

Gerosa, G., Finco, A., Mereu, S., Vitale, M., Manes, F., & Ballarin Denti, A. (2009). Comparison of seasonal variations of ozone exposure and fluxes in a Mediterranean Holm oak forest between the exceptionally dry 2003 and the following year. *Environmental Pollution*, *157*(5), 1737–1744. https://doi.org/10.1016/j.envpol.2007.11.025

Gerosa, G. A., Vitale, M., Finco, A., Manes, F., Ballarin Denti, A., & Cieslik, S. (2005). Ozone uptake by an evergreen Mediterranean forest (*Quercus ilex*) in Italy. Part I: Micrometeorological flux measurements and flux partitioning. *Atmospheric Environment*, *39*(18), 3255–3266. https://doi.org/10.1016/j.atmosenv.2005.01.056

Godowitch, J. M. (1990). Vertical ozone fluxes and related deposition parameters over agricultural and forested landscapes. *Boundary-Layer Meteorology*, *50*, 375–404.

Goldstein, A. H. (2003). Ozone uptake by a ponderosa pine in the Sierra Nevada: A measurement perspective. *Developments in Environmental Science*, *2*, 83–109.

Goldstein, A. H., Koven, C. D., Heald, C. L., & Fung, I. Y. (2009). Biogenic carbon and anthropogenic pollutants combine to form a cooling haze over the southeastern United States. *Proceedings of the National Academy of Sciences*, *106*(22), 8835–8840.

Goldstein, A. H., McKay, M., Kurpius, M. R., Schade, G. W., Lee, A., Holzinger, R., & Rasmussen, R. A. (2004). Forest thinning experiment confirms ozone deposition to forest canopy is dominated by reaction with biogenic VOCs. *Geophysical Research Letters*, *31*, L22106. https://doi.org/10.1029/2004GL021259

Gong, S. L., Walmsley, J. L., Barrie, L. A., & Hopper, J. F. (1997). Mechanisms for surface ozone depletion and recovery during polar sunrise. *Atmospheric Environment*, *31*(7), 969–981.

Grantz, D. A., Zhang, X. J., Massman, W. J., Delany, A., & Pederson, J. R. (1997). Ozone deposition to a cotton (*Gossypium hirsutum L.)* field: Stomatal and surface wetness effects during the California Ozone Deposition Experiment. *Agricultural and Forest Meteorology*, *85*(1-2), 19–31.

Grantz, D. A., Zhang, X. J., Massman, W. J., den Hartog, G., Neumann, H. H., & Pederson, J. R. (1995). Effects of stomatal conductance and surface wetness on ozone deposition in field-grown grape. *Atmospheric Environment*, *29*(21), 3189–3198.

Grøntoft, T., Henriksen, J. F., & Seip, H. M. (2004). The humidity dependence of ozone deposition onto a variety of building surfaces. *Atmospheric Environment*, *38*(1), 59–68.

Güsten, H., & Heinrich, G. (1996). On-line measurements of ozone surface fluxes. 1. Methodology and instrumentation. *Atmospheric Environment*, *30*(6), 897–909.

Güsten, H., Heinrich, G., Mönnich, E., Sprung, D., & Weppner, J. (1997). On-line measurements of ozone surface fluxes: Instrumentation and methodology. In S. Slanina (Ed.), *Transport and chemical transformation of pollutants in the troposphere: Experimental and theoretical studies of biogenic emissions and of pollutant deposition* (pp. 201–215). Berlin: Springer.

Güsten, H., Heinrich, G., Mönnich, E., Sprung, D., Weppner, J., Ramadan, A. B., et al. (1996). On-line measurements of ozone surface fluxes: Part II. Surface-level ozone fluxes onto the Sahara desert. *Atmospheric Environment*, *30*(6), 911–918. https://doi.org/10.1016/1352-2310(95)00270-7

Güsten, H., Heinrich, G., Schmidt, R. W. H., & Schurath, U. (1992). A novel ozone sensor for direct eddy flux measurements. *Journal of Atmospheric Chemistry*, *14*(1-4), 73–84.

Gut, A., Van Dijk, S., Scheibe, M., Rummel, U., Welling, M., Ammann, C., et al. (2002). NO emission from an Amazonian rain forest soil: Continuous measurements of NO flux and soil concentration. *Journal of Geophysical Research*, *107*(D20), 8057. https://doi.org/10.1029/2001JD000521

Hanisch, F., & Crowley, J. N. (2003). Ozone decomposition on Saharan dust: An experimental investigation. *Atmospheric Chemistry and Physics*, *3*(1), 119–130. https://doi.org/10.5194/acp-3-119-2003

Hardacre, C., Wild, O., & Emberson, L. (2015). An evaluation of ozone dry deposition in global scale chemistry climate models. *Atmospheric Chemistry and Physics*, *15*(11), 6419–6436. https://doi.org/10.5194/acp-15-6419-2015

Hargreaves, K. J., Fowler, D., Storeton-West, R. L., & Duyzer, J. H. (1992). The exchange of nitric oxide, nitrogen dioxide and ozone between pasture and the atmosphere. *Environmental Pollution*, *75*(1), 53–59.

Harman, I. N., & Finnigan, J. J. (2007). A simple unified theory for flow in the canopy and roughness sublayer. *Boundary-Layer Meteorology*, *123*(2), 339–363.

Harman, I. N., & Finnigan, J. J. (2008). Scalar concentration profiles in the canopy and roughness sublayer. *Boundary-Layer Meteorology*, *129*(3), 323–351.

Hassan, I. A., Ashmore, M. R., & Bell, J. N. B. (1994). Effects of $O_3$ on the stomatal behavior of Egyptian varieties of radish (*Raphanus sativus L. cv. Baladey*) and turnip (*Brassica rapa L. cv. Sultani*). *New Phytologist*, *128*, 243–249.

Helmig, D., Bocquet, F., Cohen, L., & Oltmans, S. J. (2007). Ozone uptake to the polar snowpack at Summit, Greenland. *Atmospheric Environment*, *41*(24), 5061–5076. https://doi.org/10.1016/j.atmosenv.2006.06.064

Helmig, D., Cohen, L. D., Bocquet, F., Oltmans, S., Grachev, A., & Neff, W. (2009). Spring and summertime diurnal surface ozone fluxes over the polar snow at Summit, Greenland. *Geophysical Research Letters*, *36*, L08809. https://doi.org/10.1029/2008gl036549

Helmig, D., Ganzeveld, L., Butler, T., & Oltmans, S. J. (2007). The role of ozone atmosphere-snow gas exchange on polar, boundary-layer tropospheric ozone—A review and sensitivity analysis. *Atmospheric Chemistry and Physics*, *7*(1), 15–30. https://doi.org/10.5194/acp-7-15-2007

Helmig, D., Johnson, B., Oltmans, S. J., Neff, W., Eisele, F., & Davis, D. D. (2008). Elevated ozone in the boundary layer at South Pole. *Atmospheric Environment*, *42*(12), 2788–2803. https://doi.org/10.1016/j.atmosenv.2006.12.032

Helmig, D., Lang, E. K., Bariteau, L., Boylan, P., Fairall, C. W., Ganzeveld, L., et al. (2012). Atmosphere-ocean ozone fluxes during the TexAQS 2006, STRATUS 2006, GOMECC 2007, GasEx 2008, and AMMA 2008 cruises. *Journal of Geophysical Research*, *117*, D04305. https://doi.org/10.1029/2011JD015955

Helmig, D., Ortega, J., Guenther, A., Herrick, J. D., & Geron, C. (2006). Sesquiterpene emissions from loblolly pine and their potential contribution to biogenic aerosol formation in the Southeastern US. *Atmospheric Environment*, *40*(22), 4150–4157.

Helmig, D., Seok, B., Williams, M. W., Hueber, J., & Sanford, R. (2009). Fluxes and chemistry of nitrogen oxides in the Niwot Ridge, Colorado, snowpack. *Biogeochemistry*, *95*(1), 115–130. https://doi.org/10.1007/s10533-009-9312-1

Herbinger, K., Then, C., Haberer, K., Alexou, M., Low, M., Remele, K., et al. (2007). Gas exchange and antioxidative compounds in young beech trees under free-air ozone exposure and comparisons to adult trees. *Plant Biology*, *9*, 288–297.

Herwehe, J. A., Otte, T. L., Mathur, R., & Rao, S. T. (2011). Diagnostic analysis of ozone concentrations simulated by two regional-scale air quality models. *Atmospheric Environment*, *45*(33), 5957–5969.

Hicks, B. B., Kolb, C. E., & Lenschow, D. H. (1989). New opportunities for flux measurement. In D. H. Lenschow, & B. B. Hicks (Eds.), *Global tropospheric chemistry: Chemical fluxes in the global atmosphere* (pp. 83–85). Boulder, CO: National Center for Atmospheric Research.

Hicks, B. B., Wesely, M. L., & Durham, J. L. (1980). Critique of methods to measure dry deposition workshop summary. United States.

Hillel, D. (1980). *Fundamentals of soil physics*. New York, NY: Academic Press.

Hogg, A. (2007). Stomatal and non-stomatal fluxes of ozone, $NO_x$, and $NO_y$ to a northern mixed hardwood forest (Doctoral dissertation). Ann Arbor, MI: The University of Michigan.

Hogg, A., Uddling, J., Ellsworth, D., Carroll, M. A., Pressley, S., Lamb, B., & Vogel, C. (2007). Stomatal and non-stomatal fluxes of ozone to a northern mixed hardwood forest. *Tellus Series B*, *59*(3), 514–525.

Hogrefe, C., Liu, P., Pouliot, G., Mathur, R., Roselle, S., Flemming, J., et al. (2018). Impacts of different characterizations of large-scale background on simulated regional-scale ozone over the continental United States. *Atmospheric Chemistry and Physics*, *18*(5), 3839–3864. https://doi.org/10.5194/acp-18-3839-2018

Högström, U. (1988). Non-dimensional wind and temperature profiles in the atmospheric surface layer: A re-evaluation. *Boundary-Layer Meteorology*, *42*, 55–78.

Hole, L. R., Semb, A., & Tørseth, K. (2004). Ozone deposition to a temperate coniferous forest in Norway; gradient method measurements and comparison with the EMEP deposition module. *Atmospheric Environment*, *38*(15), 2217–2223.

Hollaway, M. J., Arnold, S. R., Collins, W. J., Folberth, G., & Rap, A. (2016). Sensitivity of midnineteenth century tropospheric ozone to atmospheric chemistry-vegetation interactions. *Journal of Geophysical Research-Atmospheres*, *122*(4), 2452–2473. https://doi.org/10.1002/2016JD025462

Holzinger, R., Lee, A., Paw U, K. T., & Goldstein, A. H. (2005). Observations of oxidation products above a forest imply biogenic emissions of very reactive compounds. *Atmospheric Chemistry and Physics*, *5*, 67–75.

Hopper, J. F., Barrie, L. A., Silis, A., Hart, W., Gallant, A. J., & Dryfhout, H. (1998). Ozone and meteorology during the 1994 Polar Sunrise Experiment. *Journal of Geophysical Research*, *103*(D1), 1481–1492. https://doi.org/10.1029/97JD02888

Horváth, L., Führer, E., & Lajtha, K. (2006). Nitric oxide and nitrous oxide emission from Hungarian forest soils; linked with atmospheric N-deposition. *Atmospheric Environment*, *40*, 7786–7795.

Horváth, L., Koncz, P., Móring, A., Nagy, Z., Pintér, K., & Weidinger, T. (2017). An attempt to partition stomatal and non-stomatal ozone deposition parts on a short grassland. *Boundary-Layer Meteorology*, *167*(2), 303–326.

Horváth, L., Nagy, Z., & Weidinger, T. (1998). Estimation of dry deposition velocities of nitric oxide, sulfur dioxide, and ozone by the gradient method above short vegetation during the TRACT campaign. *Atmospheric Environment*, *32*(7), 1317–1322.

Horváth, L., Weidinger, T., Nagy, Z., & Führer, E. (1997). Measurement of dry deposition velocity of ozone, sulfur dioxide and nitrogen oxides above pine forest and low vegetation in different seasons by the gradient method. In S. Slanina (Ed.), *Transport and chemical transformation of pollutants in the troposphere: Experimental and theoretical studies of biogenic emissions and of pollutant deposition* (pp. 304–310). Berlin: Springer.

Hoshika, Y., Fares, S., Savi, F., Gruening, C., Goded, I., De Marco, A., et al. (2017). Stomatal conductance models for ozone risk assessment at canopy level in two Mediterranean evergreen forests. *Agricultural and Forest Meteorology*, *234*, 212–221.
Hoshika, Y., Katata, G., Deushi, M., Watanabe, M., Koike, T., & Paoletti, E. (2015). Ozone-induced stomatal sluggishness changes carbon and water balance of temperate deciduous forests. *Scientific Reports*, *5*, 9871.
Hosker, R. P., & Lindberg, S. E. (1982). Review: Atmospheric deposition and plant assimilation of gases and particles. *Atmospheric Environment*, *16*(5), 889–910.
Huang, L., McDonald-Buller, E. C., McGaughey, G., Kimura, Y., & Allen, D. T. (2016). The impact of drought on ozone dry deposition over eastern Texas. *Atmospheric Environment*, *127*, 176–186. https://doi.org/10.1016/j.atmosenv.2015.12.022
Jacob, D. J. (2000). Heterogenous chemistry and tropospheric ozone. *Atmospheric Environment*, *34*, 2131–2159.
Jacob, D. J., Fan, S. M., Wofsy, S. C., Spiro, P. A., Bakwin, P. S., Ritter, J. A., et al. (1992). Deposition of ozone to tundra. *Journal of Geophysical Research*, *97*(D15), 16,473–16,479. https://doi.org/10.1029/91JD02696
Jammoul, A., Gligorovski, S., George, C., & D'Anna, B. (2008). Photosensitized heterogeneous chemistry of ozone on organic films. *Journal of Physical Chemistry A*. https://doi.org/10.1021/jp074348t
Jardine, K., Yañez Serrano, A., Arneth, A., Abrell, L., Jardine, A., van Haren, J., et al. (2011). Within-canopy sesquiterpene ozonolysis in Amazonia. *Journal of Geophysical Research*, *116*, D19301. https://doi.org/10.1029/2011JD016243
Jarvis, P. G. (1976). The interpretation of the variations in leaf water potential and stomatal conductance found in canopies in the field. *Philosophical Transactions of the Royal Society of London. Series B, Biological Sciences*, *273*, 593–610.
Jensen, N. O., & Hummelshøj, P. (1995). Derivation of canopy resistance for water vapour fluxes over a spruce forest, using a new technique for the viscous sublayer resistance. *Agricultural and Forest Meteorology*, *73*(3-4), 339–352.
Jensen, N. O., & Hummelshøj, P. (1997). Derivation of canopy resistance for water vapor fluxes over a spruce forest, using a new technique for the viscous sublayer resistance (correction to vol. 73, pp. 339, 1995). *Agricultural and Forest Meteorology*, *85*(3-4), 289.
Jetter, R., Kunst, L., & Samuels, A. L. (2006). Composition of plant cuticular waxes. In M. Riederer & C. Müller (Eds.), *Biology of the plant cuticle, annual plant reviews* (Vol. 23, pp. 145–181). Oxford: Blackwell.
Joss, U., & Graber, W. K. (1996). Profiles and simulated exchange of $H_2O$, $O_3$, $NO_2$ between the atmosphere and the HartX Scots pine plantation. *Theoretical and Applied Climatology*, *53*(1-3), 157–172.
Jud, W., Fischer, L., Canaval, E., Wohlfahrt, G., Tissier, A., & Hansel, A. (2016). Plant surface reactions: An ozone defence mechanism impacting atmospheric chemistry. *Atmospheric Chemistry and Physics*. https://doi.org/10.5194/acpd-15-19873-2015
Juráň, S., Šigut, L., Holub, P., Fares, S., Klem, K., Grace, J., & Urban, O. (2019). Ozone flux and ozone deposition in a mountain spruce forest are modulated by sky conditions. *Science of The Total Environment*. https://doi.org/10.1016/j.scitotenv.2019.03.491
Kabata-Pendias, A. (2004). Soil–plant transfer of trace elements—An environmental issue. *Geoderma*, *122*(2-4), 143–149.
Kanagendran, A., Pazouki, L., Li, S., Liu, B., Kännaste, A., & Niinemets, Ü. (2018). Ozone-triggered surface uptake and stress volatile emissions in *Nicotiana tabacum 'Wisconsin'*. *Journal of Experimental Botany*, *69*(3), 681–697. https://doi.org/10.1093/jxb/erx431
Kaplan, W. A., Wofsy, S. C., Keller, M., & Da Costa, J. M. (1988). Emission of NO and deposition of $O_3$ in a tropical forest system. *Journal of Geophysical Research*, *93*(D2), 1389–1395. https://doi.org/10.1029/JD093iD02p01389
Karagulian, F., & Rossi, M. J. (2006). The heterogeneous decomposition of ozone on atmospheric mineral dust surrogates at ambient temperature. *International Journal of Chemical Kinetics*. https://doi.org/10.1002/kin.20175
Kavassalis, S. C., & Murphy, J. G. (2017). Understanding ozone-meteorology correlations: A role for dry deposition. *Geophysical Research Letters*, *44*(6), 2922–2931. https://doi.org/10.1002/2016GL071791
Kelliher, F. M., Leuning, R., Raupach, M. R., & Schulze, E. D. (1995). Maximum conductances for evaporation from global vegetation types. *Agricultural and Forest Meteorology*, *73*(1-2), 1–16.
Kennedy, D., Swenson, S., Oleson, K. W., Lawrence, D. M., Fisher, R., Lola da Costa, A. C., & Gentine, P. (2019). Implementing plant hydraulics in the Community Land Model, version 5. *Journal of Advances in Modeling Earth Systems*, *11*(2), 485–513. https://doi.org/10.1029/2018MS001500
Keronen, P., Reissell, A., Rannik, Ü., Pohja, T., Siivola, E., Hiltunen, V., et al. (2003). Ozone flux measurements over a Scots pine forest using eddy covariance method: Performance evaluation and comparison with flux-profile method. *Boreal Environment Research*, *8*(4), 425–443.
Kim, Y., Still, C. J., Hanson, C. V., Kwon, H., Greer, B. T., & Law, B. E. (2016). Canopy skin temperature variations in relation to climate, soil temperature, and carbon flux at a ponderosa pine forest in central Oregon. *Agricultural and Forest Meteorology*, *226*, 161–173.
Kirchhoff, V. W. J. H., Browell, E. V., & Gregory, G. L. (1988). Ozone measurements in the troposphere of an Amazonian rain forest environment. *Journal of Geophysical Research*, *93*(D12), 15,850–15,860. https://doi.org/10.1029/JD093iD12p15850
Kirkman, G., Gut, A., Ammann, C., Gatti, L., Cordova, A., Moura, M., et al. (2002). Surface exchange of nitric oxide, nitrogen dioxide, and ozone at a cattle pasture in Rondônia, Brazil. *Journal of Geophysical Research*, *107*(D20), 8083. https://doi.org/10.1029/2001JD000523
Koch, J. R., Scherzer, A. J., Eshita, S. M., & Davis, K. R. (1998). Ozone sensitivity in hybrid poplar is correlated with a lack of defense-gene activation. *Plant Physiology*, *118*(4), 1243–1252.
Kramm, G., Dlugi, R., Dollard, G. J., Foken, T., Mölders, N., Müller, H., et al. (1995). On the dry deposition of ozone and reactive nitrogen species. *Atmospheric Environment*, *29*(21), 3209–3231. https://doi.org/10.1016/1352-2310(95)00218-N
Kramm, G., Müller, H., Fowler, D., Höfken, K. D., Meixner, F. X., & Schaller, E. (1991). A modified profile method for determining the vertical fluxes of NO, $NO_2$, ozone, and $HNO_3$ in the atmospheric surface layer. *Journal of Atmospheric Chemistry*, *13*(3), 265–288.
Kurpius, M. R., & Goldstein, A. H. (2003). Gas-phase chemistry dominates $O_3$ loss to a forest, implying a source of aerosols and hydroxyl radicals to the atmosphere. *Geophysical Research Letters*, *30*(7), 1371. https://doi.org/10.1029/2002GL016785
Kurpius, M. R., McKay, M., & Goldstein, A. H. (2002). Annual ozone deposition to a Sierra Nevada ponderosa pine plantation. *Atmospheric Environment*, *36*(28), 4503–4515.
Kvalevåg, M. M., & Myhre, G. (2013). The effect of carbon-nitrogen coupling on the reduced land carbon sink caused by tropospheric ozone. *Geophysical Research Letters*, *40*(12), 3227–3231. https://doi.org/10.1002/grl.50572
Laisk, A., Kull, O., & Moldau, H. (1989). Ozone concentration in leaf intercellular air spaces is close to zero. *Plant Physiology*, *90*(3), 1163–1167. https://doi.org/10.1104/pp.90.3.1163
Lamaud, E., Carrara, A., Brunet, Y., López, A., & Druilhet, A. (2002). Ozone fluxes above and within a pine forest canopy in dry and wet conditions. *Atmospheric Environment*, *36*, 77–88.
Lamaud, E., Loubet, B., Irvine, M., Stella, P., Personne, E., & Cellier, P. (2009). Partitioning of ozone deposition over a developed maize crop between stomatal and non-stomatal uptakes, using eddy-covariance flux measurements and modelling. *Agricultural and Forest Meteorology*, *149*(9), 1385–1396. https://doi.org/10.1016/j.agrformet.2009.03.017

Launiainen, S., Katul, G. G., Grönholm, T., & Vesala, T. (2013). Partitioning ozone fluxes between canopy and forest floor by measurements and a multi-layer model. *Agricultural and Forest Meteorology*, *173*, 85–99. https://doi.org/10.1016/j.agrformet.2012.12.009

Le Morvan-Quéméner, A., Coll, I., Kammer, J., Lamaud, E., Loubet, B., Personne, E., & Stella, P. (2018). Impact of parameterization choices on the restitution of ozone deposition over vegetation. *Atmospheric Environment*, *178*, 49–65.

Lee, X., Massman, W., & Law, B. (Eds.) (2004). *Handbook of micrometeorology: A guide for surface flux measurement and analysis* (Vol. 29). Dordrecht: Springer Science & Business Media.

Legrand, M., Preunkert, S., Jourdain, B., Gallee, H., Goutail, F., Weller, R., & Savarino, J. (2009). Year-round record of surface ozone at coastal (Dumont d'Urville) and inland (Concordia) sites in East Antarctica. *Journal of Geophysical Research*, *114*, D20306. https://doi.org/10.1029/2008JD011667

Legrand, M., Preunkert, S., Savarino, J., Frey, M. M., Kukui, A., Helmig, D., et al. (2016). Inter-annual variability of surface ozone at coastal (Dumont d'Urville, 2004–2014) and inland (Concordia, 2007–2014) sites in East Antarctica. *Atmospheric Chemistry and Physics*, *16*(12), 8053–8069. https://doi.org/10.5194/acp-16-8053-2016

Lenschow, D. H. (1982). Reactive trace species in the boundary layer from a micrometeorological perspective. *Journal of the Meteorological Society of Japan*, *60*(1), 472–480. https://doi.org/10.2151/jmsj1965.60.1_472

Lenschow, D. H., & Delany, A. C. (1987). An analytic formulation for NO and $NO_2$ flux profiles in the atmospheric surface layer. *Journal of Atmospheric Chemistry*, *5*(3), 301–309. https://doi.org/10.1007/BF00114108

Lenschow, D. H., Delany, A. C., Stankov, B. B., & Stedman, D. H. (1980). Airborne measurements of the vertical flux of ozone in the boundary layer. *Boundary-Layer Meteorology*, *19*(2), 249–265. https://doi.org/10.1007/BF00117223

Lenschow, D. H., & Hicks, B. B. (Eds.) (1989). *Global tropospheric chemistry: Chemical fluxes in the global atmosphere*. Boulder, CO: National Center for Atmospheric Research.

Lenschow, D. H., Pearson, R. Jr., & Stankov, B. B. (1981). Estimating the ozone budget in the boundary layer by use of aircraft measurements of ozone eddy flux and mean concentration. *Journal of Geophysical Research*, *86*(C8), 7291–7297. https://doi.org/10.1029/JC086iC08p07291

Lenschow, D. H., & Raupach, M. R. (1991). The attenuation of fluctuations in scalar concentrations through sampling tubes. *Journal of Geophysical Research*, *96*(D8), 15,259–15,268. https://doi.org/10.1029/91JD01437

Leuning, R. (1995). A critical appraisal of a combined stomatal-photosynthesis model for C3 plants. *Plant, Cell & Environment*, *18*(4), 339–355.

Leuning, R., Neumann, H. H., & Thurtell, G. W. (1979). Ozone uptake by corn (*Zea mays L.*): A general approach. *Agricultural Meteorology*, *20*(2), 115–135.

Leuning, R., Unsworth, M. H., Neuman, H. N., & King, K. M. (1979). Ozone fluxes to tobacco and soil under field conditions. *Atmospheric Environment*, *13*, 1155–1163.

Li, J., Duan, Q., Wang, Y. P., Gong, W., Gan, Y., & Wang, C. (2018). Parameter optimization for carbon and water fluxes in two global land surface models based on surrogate modelling. *International Journal of Climatology*, *38*, e1016–e1031. https://doi.org/10.1002/joc.5428

Li, J., Mahalov, A., & Hyde, P. (2016). Simulating the impacts of chronic ozone exposure on plant conductance and photosynthesis, and on the regional hydroclimate using WRF/Chem. *Environmental Research Letters*, *11*(11), 114017. https://doi.org/10.1088/1748-9326/11/11/114017

Li, J., Mahalov, A., & Hyde, P. (2018). Simulating the effects of chronic ozone exposure on hydrometeorology and crop productivity using a fully coupled crop, meteorology and air quality modeling system. *Agricultural and Forest Meteorology*, *260-261*, 287–299. https://doi.org/10.1016/j.agrformet.2018.06.013

Li, Q., Gabay, M., Rubin, Y., Fredj, E., & Tas, E. (2018). Measurement-based investigation of ozone deposition to vegetation under the effects of coastal and photochemical air pollution in the Eastern Mediterranean. *Science of the Total Environment*, *645*, 1579–1597. https://doi.org/10.1016/j.scitotenv.2018.07.037

Lin, C., Gentine, P., Huang, Y., Guan, K., Kimm, H., & Zhou, S. (2018). Diel ecosystem conductance response to vapor pressure deficit is suboptimal and independent of soil moisture. *Agricultural and Forest Meteorology*, *250-251*, 24–34. https://doi.org/10.1016/j.agrformet.2017.12.078

Lin, J.-T., Youn, D., Liang, X.-Z., & Wuebbles, D. J. (2008). Global model simulation of summertime U.S. ozone diurnal cycle and its sensitivity to PBL mixing, spatial resolution, and emissions. *Atmospheric Environment*, *42*, 8470–8483.

Lin, M., Horowitz, L. W., Payton, R., Fiore, A. M., & Tonnesen, G. (2017). US surface ozone trends and extremes from 1980 to 2014: Quantifying the roles of rising Asian emissions, domestic controls, wildfires, and climate. *Atmospheric Chemistry and Physics*, *17*(4), 2943–2970. https://doi.org/10.5194/acp-17-2943-2017

Lin, M., Malyshev, S., Shevliakova, E., Paulot, F., Horowitz, L. W., Fares, S., et al. (2019). Sensitivity of ozone dry deposition to ecosystem-atmosphere-interactions: A critical appraisal of observations and simulations. *Global Biogeochemical Cycles*, *33*(10), 1264–1288. https://doi.org/10.1029/2018GB006157

Lin, Y. S., Medlyn, B. E., Duursma, R. A., Prentice, I. C., Wang, H., Baig, S., et al. (2015). Optimal stomatal behaviour around the world. *Nature Climate Change*, *5*(5), 459–464. https://doi.org/10.1038/nclimate2550

Lombardozzi, D., Levis, S., Bonan, G., Hess, P. G., & Sparks, J. P. (2015). The influence of chronic ozone exposure on global carbon and water cycles. *Journal of Climate*, *28*(1), 292–305. https://doi.org/10.1175/Jcli-D-14-00223.1

Lombardozzi, D., Levis, S., Bonan, G., & Sparks, J. P. (2012). Predicting photosynthesis and transpiration responses to ozone: Decoupling modeled photosynthesis and stomatal conductance. *Biogeosciences*, *9*(8), 3113–3130. https://doi.org/10.5194/bg-9-3113-2012

Lombardozzi, D., Sparks, J. P., & Bonan, G. (2013). Integrating $O_3$ influences on terrestrial processes: Photosynthetic and stomatal response data available for regional and global modeling. *Biogeosciences*, *10*(11), 6815–6831. https://doi.org/10.5194/bg-10-6815-2013

Lombardozzi, D., Sparks, J. P., Bonan, G., & Levis, S. (2012). Ozone exposure causes a decoupling of conductance and photosynthesis: Implications for the Ball-Berry stomatal conductance model. *Oecologia*, *169*, 651–659.

Loreto, F., & Fares, S. (2007). Is ozone flux inside leaves only a damage indicator? Clues from volatile isoprenoid studies. *Plant Physiology*, *143*(3), 1096–1100.

Loubet, B., Cellier, P., Fléchard, C., Zurfluh, O., Irvine, M., Lamaud, E., et al. (2013). Investigating discrepancies in heat, $CO_2$ fluxes, and $O_3$ deposition velocity over maize as measured by the eddy-covariance and the aerodynamic gradient methods. *Agricultural and Forest Meteorology*, *169*, 35–50. https://dx.doi.org/10.1016/j.agrformet.2012.09.010

MacPherson, J. I., Desjardins, R. L., Schuepp, P. H., & Pearson, R. Jr. (1995). Aircraft-measured ozone deposition in the San Joaquin Valley of California. *Atmospheric Environment*, *29*(21), 3133–3145.

Mahrt, L., Lenschow, D. H., Sun, J., Weil, J. C., MacPherson, J. I., & Desjardins, R. L. (1995). Ozone fluxes over a patchy cultivated surface. *Journal of Geophysical Research*, *100*(D11), 23,125–23,131. https://doi.org/10.1029/95JD02599

Maier-Maercker, U., & Koch, W. (1991). Experiments on the control capacity of stomata of *Picea abies (l) karst* after fumigation with ozone and in environmentally damaged material. *Plant, Cell & Environment*, *14*, 175–184.

Makar, P. A., Fuentes, J. D., Wang, D., Staebler, R. M., & Wiebe, H. A. (1999). Chemical processing of biogenic hydrocarbons within and above a temperate deciduous forest. *Journal of Geophysical Research*, *104*(D3), 3581–3603. https://doi.org/10.1029/1998JD100065

Manes, F., Donato, E., & Vitale, M. (2001). Physiological response of *Pinus halepensis* needles under ozone and water stress conditions. *Physiologia Plantarum*, *113*, 249–257.

Manes, F., Vitale, M., Donato, E., & Paoletti, E. (1998). $O_3$ and $O_3$ + $CO_2$ effects on a Mediterranean evergreen broadleaf tree, holm oak (*Quercus ilex L.*). *Chemosphere*, *36*, 801–806.

Martin, M. J., Host, G. E., Lenz, K. E., & Isebrands, J. G. (2001). Simulating the growth response of aspen to elevated ozone: A mechanistic approach to scaling a leaf-level model of ozone effects on photosynthesis to a complex canopy architecture. *Environmental Pollution*, *115*(3), 425–436.

Massman, W. J. (1993). Partitioning ozone fluxes to sparse grass and soil and the inferred resistances to dry deposition. *Atmospheric Environment*, *27A*(2), 167–174.

Massman, W. J. (1998). A review of the molecular diffusivities of $H_2O$, $CO_2$, $CH_4$, CO, $O_3$, $SO_2$, $NH_3$, $N_2O$, NO, and $NO_2$ in air, $O_2$ and $N_2$ near STP. *Atmospheric Environment*, *32*(6), 1111–1127.

Massman, W. J. (1999). A model study of $kBH^{-1}$ for vegetated surfaces using 'localized near-field' Lagrangian theory. *Journal of Hydrology*, *223*(1-2), 27–43.

Massman, W. J. (2004). Toward an ozone standard to protect vegetation based on effective dose: A review of deposition resistances and a possible metric. *Atmospheric Environment*, *38*, 2323–2337.

Massman, W. J., Musselman, R. C., & Lefohn, A. S. (2000). A conceptual ozone dose-response model to develop a standard to protect vegetation. *Atmospheric Environment*, *34*(5), 745–759.

Massman, W. J., Pederson, J., Delany, A., Grantz, D., Den Hartog, G., Neumann, H. H., et al. (1994). An evaluation of the regional acid deposition model surface module for ozone uptake at three sites in the San Joaquin Valley of California. *Journal of Geophysical Research*, *99*(D4), 8281–8294. https://doi.org/10.1029/93JD03267

Matichuk, R., Tonnesen, G., Luecken, D., Gilliam, R., Napelenok, S. L., Baker, K. R., et al. (2017). Evaluation of the Community Multiscale Air Quality Model for simulating winter ozone formation in the Uinta Basin. *Journal of Geophysical Research: Atmospheres*, *122*, 13,545–13,572. https://doi.org/10.1002/2017JD027057

Matsuda, K., Watanabe, I., Wingpud, V., Theramongkol, P., Khummongkol, P., Wangwongwatana, S., & Totsuka, T. (2005). Ozone dry deposition above a tropical forest in the dry season in northern Thailand. *Atmospheric Environment*, *39*(14), 2571–2577.

Matsuda, K., Watanabe, I., Wingpud, V., Theramongkol, P., & Ohizumi, T. (2006). Deposition velocity of $O_3$ and $SO_2$ in the dry and wet season above a tropical forest in northern Thailand. *Atmospheric Environment*, *40*(39), 7557–7564.

Matyssek, R., Sandermann, H., Wieser, G., Booker, F., Cieslik, S., Musselman, R., & Ernst, D. (2008). The challenge of making ozone risk assessment for forest trees more mechanistic. *Environmental Pollution*, *156*(3), 567–582.

Matyssek, R., Wieser, G., Nunn, A. J., Kozovits, A. R., Reiter, I. M., Heerdt, C., et al. (2004). Comparison between AOT40 and ozone uptake in forest trees of different species, age and site conditions. *Atmospheric Environment*, *38*(15), 2271–2281. https://doi.org/10.1016/j.atmosenv.2003.09.078

Mayer, J.-C., Bargsten, A., Rummel, U., Meixner, F. X., & Foken, T. (2011). Distributed Modified Bowen Ratio method for surface layer fluxes of reactive and non-reactive trace gases. *Agricultural and Forest Meteorology*, *151*(6), 655–668.

McCabe, J., & Abbatt, J. P. D. (2009). Heterogeneous loss of gas-phase ozone on n-hexane soot surfaces: Similar kinetics to loss on other chemically unsaturated solid surfaces. *The Journal of Physical Chemistry C*, *113*(6), 2120–2127. https://doi.org/10.1021/jp806771q

McLaughlin, S. B., Wullschleger, S. D., Sun, G., & Nosal, M. (2007). Interactive effects of ozone and climate on water use, soil moisture content and streamflow in a southern Appalachian forest in the USA. *New Phytologist*, *174*, 125–136.

Medlyn, B. E., Duursma, R. A., Eamus, D., Ellsworth, D. S., Prentice, I. C., Barton, C. V., et al. (2011). Reconciling the optimal and empirical approaches to modelling stomatal conductance. *Global Change Biology*, *17*(6), 2134–2144.

Meixner, F., Fickinger, T., Marufu, L., Serca, D., Nathaus, F., Makina, E., et al. (1997). Preliminary results on nitric oxide emission from a southern African savanna ecosystem. *Nutrient Cycling in Agroecosystems*, *48*, 123–138.

Mészáros, R., Horváth, L., Weidinger, T., Neftel, A., Nemitz, E., Dammgen, U., et al. (2009). Measurement and modelling ozone fluxes over a cut and fertilized grassland. *Biogeosciences*, *6*(10), 1987–1999.

Mészáros, R., Zsély, I. G., Szinyei, D., Vincze, C., & Lagzi, I. (2009). Sensitivity analysis of an ozone deposition model. *Atmospheric Environment*, *43*(3), 663–672. https://doi.org/10.1016/j.atmosenv.2008.09.058

Meyers, T. P., & Baldocchi, D. D. (1993). Trace gas exchange above the floor of a deciduous forest: 2. $SO_2$ and $O_3$ deposition. *Journal of Geophysical Research*, *98*(D7), 12,631–12,638. https://doi.org/10.1029/93JD00720

Meyers, T. P., & Baldocchi, D. D. (2005). Current micrometeorological flux methodologies with applications in agriculture. Publications, Agencies and Staff of the U.S. Department of Commerce (500).

Meyers, T. P., Finkelstein, P., Clarke, J., Ellestad, T. G., & Sims, P. F. (1998). A multilayer model for inferring dry deposition using standard meteorological measurements. *Journal of Geophysical Research*, *103*(D17), 22,645–22,661. https://doi.org/10.1029/98JD01564

Michou, M., Laville, P., Serça, D., Fotiadi, A., Bouchou, P., & Peuch, V. H. (2005). Measured and modeled dry deposition velocities over the ESCOMPTE area. *Atmospheric Research*, *74*(1-4), 89–116.

Mikkelsen, T. N., Ro-Poulsen, H., Hovmand, M. F., Jensen, N. O., Pilegaard, K., & Egeløv, A. H. (2004). Five-year measurements of ozone fluxes to a Danish Norway spruce canopy. *Atmospheric Environment*, *38*(15), 2361–2371. https://doi.org/10.1016/j.atmosenv.2003.12.036

Mikkelsen, T. N., Ro-Poulsen, H., Pilegaard, K., Hovmand, M. F., Jensen, N. O., Christensen, C. S., & Hummgelshoej, P. (2000). Ozone uptake by an evergreen forest canopy: Temporal variation and possible mechanisms. *Environmental Pollution*, *109*, 423–429.

Mills, G., Hayes, F., & Wilkinson, S. (2009). Chronic exposure to increasing background ozone impairs stomatal functioning in grassland species. *Global Change Biology*, *15*(6), 1522–1533. https://doi.org/10.1111/j.1365-2486.2008.01798.x

Mills, G., Pleijel, H., Malley, C. S., Sinha, B., Cooper, O. R., Schultz, M. G., et al. (2018). Tropospheric Ozone Assessment Report: Present-day tropospheric ozone distribution and trends relevant to vegetation. *Elementa: Science of the Anthropocene*, *6*(1), 47. https://doi.org/10.1525/elementa.302

Min, K. E., Pusede, S. E., Browne, E. C., LaFranchi, B. W., & Cohen, R. C. (2014). Eddy covariance fluxes and vertical concentration gradient measurements of NO and $NO_2$ over a ponderosa pine ecosystem: Observational evidence for within-canopy chemical removal of $NO_x$. *Atmospheric Chemistry and Physics*, *14*(11), 5495–5512.

Min, K. E., Pusede, S. E., Browne, E. C., LaFranchi, B. W., Wooldridge, P. J., Wolfe, G. M., et al. (2012). Observations of atmosphere-biosphere exchange of total and speciated peroxynitrates: Nitrogen fluxes and biogenic sources of peroxynitrates. *Atmospheric Chemistry and Physics*, *12*(20), 9763–9773.

Miner, G. L., Bauerle, W. L., & Baldocchi, D. D. (2017). Estimating the sensitivity of stomatal conductance to photosynthesis: A review. *Plant, Cell & Environment*, *40*(7), 1214–1238.

Morrison, G. C., & Nazaroff, W. W. (2002). The rate of ozone uptake on carpet: mathematical modeling. *Atmospheric Environment*, *36*, 1749–1756.

Muller, J. B. A., Coyle, M., Fowler, D., Gallagher, M. W., Nemitz, E. G., & Percival, C. J. (2009). Comparison of ozone fluxes over grassland by gradient and eddy covariance technique. *Atmospheric Science Letters*, *10*(3), 164–169. https://doi.org/10.1002/asl.226

Muller, J. B. A., Percival, C. J., Gallagher, M. W., Fowler, D., Coyle, M., & Nemitz, E. (2010). Sources of uncertainty in eddy covariance ozone flux measurements made by dry chemiluminescence fast response analysers. *Atmospheric Measurement Techniques*, *3*(1), 163–176.

Munger, J. W., Wofsy, S. C., Bakwin, P. S., Fan, S.-M., Goulden, M. L., Daube, B. C., et al. (1996). Atmospheric deposition of reactive nitrogen oxides and ozone in a temperate deciduous forest and a subarctic woodland 1. Measurements and mechanisms. *Journal of Geophysical Research*, *101*(D7), 12,639–12,657. https://doi.org/10.1029/96JD00230

Murray, K. A., Kramer, L. J., Doskey, P. V., Ganzeveld, L., Seok, B., Van Dam, B., & Helmig, D. (2015). Dynamics of ozone and nitrogen oxides at Summit, Greenland. II. Simulating snowpack chemistry during a spring high ozone event with a 1-D process-scale model. *Atmospheric Environment*, *117*, 110–123. https://doi.org/10.1016/j.atmosenv.2015.07.004

Musselman, R. C., Lefohn, A. S., Massman, W. J., & Heath, R. L. (2006). A critical review and analysis of the use of exposure-and flux-based ozone indices for predicting vegetation effects. *Atmospheric Environment*, *40*(10), 1869–1888.

National Academies of Sciences, Engineering, and Medicine (NASEM) (2016). *The future of atmospheric chemistry research: Remembering yesterday, understanding today, anticipating tomorrow*. Washington, DC: National Academies Press. https://doi.org/10.17226/23573

Neirynck, J., Gielen, B., Janssens, I. A., & Ceulemans, R. (2012). Insights into ozone deposition patterns from decade-long ozone flux measurements over a mixed temperate forest. *Journal of Environmental Monitoring*, *14*(6), 1684–1695.

Neirynck, J., & Verstraeten, A. (2018). Variability of ozone deposition velocity over a mixed suburban temperate forest. *Frontiers in Environmental Science*, *6*. https://doi.org/10.3389/fenvs.2018.00082

Nicolini, G., Aubinet, M., Feigenwinter, C., Heinesch, B., Lindroth, A., Mamadou, O., et al. (2018). Impact of $CO_2$ storage flux sampling uncertainty on net ecosystem exchange measured by eddy covariance. *Agricultural and Forest Meteorology*, *248*, 228–239. https://doi.org/10.1016/j.agrformet.2017.09.025

Noormets, A., Sôber, A., Pell, E. J., Dickson, R. E., Podila, G. K., Sôber, J., et al. (2001). Stomatal and non-stomatal limitation to photosynthesis in two trembling aspen (*Populus tremuloides michx.*) clones exposed to elevated $CO_2$ and/or $O_3$. *Plant, Cell & Environment*, *24*, 327–336.

Nunn, A. J., Cieslik, S., Metzger, U., Wieser, G., & Matyssek, R. (2010). Combining sap flow and eddy covariance approaches to derive stomatal and non-stomatal $O_3$ fluxes in a forest stand. *Environmental Pollution*, *158*(6), 2014–2022. https://doi.org/10.1016/j.envpol.2009.11.034

Oliver, R. J., Mercado, L. M., Sitch, S., Simpson, D. M., Medlyn, B. E., Lin, Y., & Folberth, G. A. (2018). Large but decreasing effect of ozone on the European carbon sink. *Biogeosciences*, *15*(13), 4245–4269.

Omasa, K., Tobe, K., Hosomi, M., & Kobayashi, M. (2000). Absorption of ozone and seven organic pollutants by *Populus nigra* and *Camellia sasanqua*. *Environmental Science & Technology*, *34*(12), 2498–2500.

Padro, J. (1993). Seasonal contrasts in modeled and observed dry deposition velocities of $O_3$, $SO_2$ and $NO_2$ over 3 surfaces. *Atmospheric Environment*, *27*(6), 807–814. https://doi.org/10.1016/0960-1686(93)90002-G

Padro, J. (1994). Observed characteristics of the dry deposition velocity of $O_3$ and $SO_2$ above a wet deciduous forest. *Science of the Total Environment*, *146*, 395–400.

Padro, J. (1996). Summary of ozone dry deposition velocity measurements and model estimates over vineyard, cotton, grass and deciduous forest in summer. *Atmospheric Environment*, *30*(13), 2363–2369.

Padro, J., Den Hartog, G., & Neumann, H. H. (1991). An investigation of the ADOM dry deposition module using summertime $O_3$ measurements above a deciduous forest. *Atmospheric Environment. Part A. General Topics*, *25*(8), 1689–1704.

Padro, J., Massman, W. J., Den Hartog, G., & Neumann, H. H. (1994). Dry deposition velocity of $O_3$ over a vineyard obtained from models and observations: The 1991 California ozone deposition experiment. *Water, Air, and Soil Pollution*, *75*(3-4), 307–323.

Padro, J., Massman, W. J., Shaw, R. H., Delany, A., & Oncley, S. P. (1994). A comparison of some aerodynamic resistance methods using measurements over cotton and grass from the 1991 California ozone deposition experiment. *Boundary-Layer Meteorology*, *71*(4), 327–339.

Padro, J., Neumann, H. H., & Den Hartog, G. (1992). Modelled and observed dry deposition velocity of $O_3$ above a deciduous forest in the winter. *Atmospheric Environment. Part A. General Topics*, *26*(5), 775–784.

Paoletti, E. (2005). Ozone slows stomatal response to light and leaf wounding in a Mediterranean evergreen broadleaf, *Arbutus unedo*. *Environmental Pollution*, *134*(3), 439–445. https://doi.org/10.1016/j.envpol.2004.09.011

Paoletti, E., & Grulke, N. E. (2005). Does living in elevated $CO_2$ ameliorate tree response to ozone? A review on stomatal responses. *Environmental Pollution*, *137*(3), 483–493.

Paoletti, E., & Grulke, N. E. (2010). Ozone exposure and stomatal sluggishness in different plant physiognomic classes. *Environmental Pollution*, *158*(8), 2664–2671.

Pape, L., Ammann, C., Nyfelder-Brunner, A., Spirig, C., Hans, K., & Meixner, F. X. (2009). An automated dynamic chamber system for surface exchange measurement of non-reactive and reactive trace gases of grassland ecosystem. *Biogeosciences*, *6*, 405–429.

Park, R. J., Hong, S. K., Kwon, H. A., Kim, S., Guenther, A., Woo, J. H., & Loughner, C. P. (2014). An evaluation of ozone dry deposition simulations in East Asia. *Atmospheric Chemistry and Physics*, *14*(15), 7929–7940.

Patton, E. G., Davis, K. J., Barth, M. C., & Sullivan, P. P. (2001). Decaying scalars emitted by a forest canopy: A numerical study. *Boundary-Layer Meteorology*, *100*, 91–129.

Patton, E. G., & Finnigan, J. J. (2013). Canopy turbulence. In H. J. S. Fernando (Ed.), *Handbook of environmental fluid dynamics* (Vol. 1, pp. 311–327). Boca Raton: CRC Press/Taylor & Francis Group.

Patton, E. G., Horst, T. W., Sullivan, P. P., Lenschow, D. H., Oncley, S. P., Brown, W. O., et al. (2011). The canopy horizontal array turbulence study. *Bulletin of the American Meteorological Society*, *92*(5), 593–611. https://doi.org/10.1175/2010BAMS2614.1

Patton, E. G., Sullivan, P. P., Shaw, R. H., Finnigan, J. J., & Weil, J. C. (2016). Atmospheric stability influences on coupled boundary layer and canopy turbulence. *Journal of the Atmospheric Sciences*, *73*, 1621–1647.

Paulot, F., Malyshev, S., Nguyen, T., Crounse, J. D., Shevliakova, E., & Horowitz, L. W. (2018). Representing sub-grid scale variations in nitrogen deposition associated with land use in a global Earth system model: Implications for present and future nitrogen deposition fluxes over North America. *Atmospheric Chemistry and Physics*, *18*(24), 17,963–17,978.

Paw U, K. T., & Meyers, T. P. (1989). Investigations with a higher-order canopy turbulence model into mean source-sink levels and bulk canopy resistances. *Agricultural and Forest Meteorology*, *47*, 259–271.

Pearson, R. (1990). Measuring ambient ozone with high-sensitivity and bandwidth. *Review of Scientific Instruments*, *61*(2), 907–916.

Peterson, M. C., & Honrath, R. E. (2001). Observations of rapid photochemical destruction of ozone in snowpack interstitial air. *Geophysical Research Letters*, *28*, 511–514.

Pilegaard, K. (2001). Air-soil exchange of NO, $NO_2$ and $O_3$ in forests. *Water, Soil, and Air Pollution: Focus*, *1*, 79–88.

Pilegaard, K., Hummelshøj, P., & Jensen, N. O. (1998). Fluxes of ozone and nitrogen dioxide measured by eddy correlation over a harvested wheat field. *Atmospheric Environment*, *32*(7), 1167–1177.

Pilegaard, K., Jensen, N. O., & Hummelshøj, P. (1995). Seasonal and diurnal variation in the deposition velocity of ozone over a spruce forest in Denmark. *Water, Air, and Soil Pollution*, *85*(4), 2223–2228.

Pio, C. A., & Feliciano, M. S. (1996). Dry deposition of ozone and sulphur dioxide over low vegetation in moderate southern European weather conditions. Measurements and modelling. *Physics and Chemistry of the Earth*, *21*(5-6), 373–377.

Pio, C. A., Feliciano, M. S., Vermeulen, A. T., & Sousa, E. C. (2000). Seasonal variability of ozone dry deposition under southern European climate conditions, in Portugal. *Atmospheric Environment*, *34*(2), 195–205.

Plake, D., Sörgel, M., Stella, P., Held, A., & Trebs, I. (2015). Influence of meteorology and anthropogenic pollution on chemical flux divergence of the NO–$NO_2$-$O_3$ triad above and within a natural grassland canopy. *Biogeosciences*, *12*(4), 945–959.

Plake, D., Stella, P., Moravek, A., Mayer, J.-C., Amman, C., Held, A., & Trebs, I. (2015). Comparison of ozone deposition measured with the dynamic chamber and the eddy covariance method. *Agricultural and Forest Meteorology*, *206*, 97–112. https://doi.org/10.1016/j.agrformet.2015.02.014

Plake, D., & Trebs, I. (2013). An automated system for selective and continuous measurements of vertical thoron profiles for the determination of transport times near the ground. *Atmospheric Measurement Techniques*, *6*(4), 1017–1030. https://doi.org/10.5194/amt-6-1017-2013

Pleijel, H., Pihl Karlsson, G., Danielsson, H., & Selldén, G. (1995). Surface wetness enhances ozone deposition to a pasture canopy. *Atmospheric Environment*, *29*(22), 3391–3393.

Pleim, J., & Ran, L. (2011). Surface flux modeling for air quality applications. *Atmosphere*, *2*(3), 271–302. https://doi.org/10.3390/atmos2030271

Pleim, J. E., Xiu, A., Finkelstein, P. L., & Otte, T. L. (2001). A coupled land-surface and dry deposition model and comparison to field measurements of surface heat, moisture, and ozone fluxes. *Water, Air, & Soil Pollution: Focus*, *1*(5-6), 243–252.

Plöchl, M., Lyons, T., Ollerenshaw, J., & Barnes, J. (2000). Simulating ozone detoxification in the leaf apoplast through the direct reaction with ascorbate. *Planta*, *210*(3), 454–467.

Popek, R., Gawrońska, H., Wrochna, M., Gawroński, S. W., & Sæbø, A. (2013). Particulate matter on foliage of 13 woody species: Deposition on surfaces and phytostabilisation in waxes—A 3-year study. *International Journal of Phytoremediation*. https://doi.org/10.1080/15226514.2012.694498

Pöschl, U., & Shiraiwa, M. (2015). Multiphase chemistry at the atmosphere-biosphere interface influencing climate and public health in the Anthropocene. *Chemical Reviews*, *115*(10), 4440–4475. https://doi.org/10.1021/cr500487s

Potier, E., Loubet, B., Durand, B., Flura, D., Bourdat-Deschamps, M., Ciuraru, R., & Ogée, J. (2017). Chemical reaction rates of ozone in water infusions of wheat, beech, oak and pine leaves of different ages. *Atmospheric Environment*, *151*, 176–187. https://doi.org/10.1016/j.atmosenv.2016.11.069

Potier, E., Ogée, J., Jouanguy, J., Lamaud, E., Stella, P., Personne, E., et al. (2015). Multilayer modelling of ozone fluxes on winter wheat reveals large deposition on wet senescing leaves. *Agricultural and Forest Meteorology*, *211-212*, 58–71. https://doi.org/10.1016/j.agrformet.2015.05.006

Poyatos, R., Granda, V., Molowny-Horas, R., Mencuccini, M., Steppe, K., & Martínez-Vilalta, J. (2016). SAPFLUXNET: Towards a global database of sap flow measurements. *Tree Physiology*, *36*(12), 1449–1455. https://doi.org/10.1093/treephys/tpw110

Pyles, R. D., Weare, B. C., & Paw U, K. T. (2000). The UCD advanced canopy-atmosphere-soil algorithm: Comparisons with observations from different climate and vegetation regimes. *Quarterly Journal of the Royal Meteorological Society*, *126*, 2951–2980.

Ran, L., Pleim, J., Song, C., Band, L., Walker, J. T., & Binkowski, F. S. (2017). A photosynthesis-based two-leaf canopy stomatal conductance model for meteorology and air quality modeling with WRF/CMAQ PX LSM. *Journal of Geophysical Research: Atmospheres*, *122*, 1930–1952. https://doi.org/10.1002/2016JD025583

Rannik, Ü., Altimir, N., Mammarella, I., Bäck, J., Rinne, J., Ruuskanen, T. M., et al. (2012). Ozone deposition into a boreal forest over a decade of observations: Evaluating deposition partitioning and driving variables. *Atmospheric Chemistry and Physics*, *12*(24), 12,165–12,182. https://doi.org/10.5194/acp-12-12165-2012

Rannik, Ü., Mammarella, I., Keronen, P., & Vesala, T. (2009). Vertical advection and nocturnal deposition of ozone over a boreal pine forest. *Atmospheric Chemistry and Physics*, *9*, 2089–2095.

Raoult, N. M., Jupp, T. E., Cox, P. M., & Luke, C. M. (2016). Land-surface parameter optimisation using data assimilation techniques: The adJULES system V1.0. *Geoscientific Model Development*, *9*(8), 2833–2852. https://doi.org/10.5194/gmd-9-2833-2016

Raupach, M. R. (1979). Anomalies in flux-gradient relationships over forest. *Boundary-Layer Meteorology*, *16*(3), 467–486.

Raupach, M. R. (1989). Applying Lagrangian fluid mechanics to infer scalar source distributions from concentration profiles in plant canopies. *Agricultural and Forest Meteorology*, *47*, 85–108.

Raupach, M. R., & Finnigan, J. J. (1987). 'Single-layer models of evaporation from plant canopies are incorrect but useful, whereas multilayer models are correct but useless': Discuss. *Australian Journal of Plant Physiology*, *15*, 705–716.

Raupach, M. R., Finnigan, J. J., & Brunet, Y. (1996). Coherent eddies and turbulence in vegetation canopies: The mixing-layer analogy. *Boundary-Layer Meteorology*, *78*, 351–382.

Ray, J. D., Stedman, D. H., & Wendel, G. J. (1986). Fast chemiluminescent method for measurement of ambient ozone. *Analytical Chemistry*, *58*(3), 598–600.

Regener, V. H. (1957). The vertical flux of atmospheric ozone. *Journal of Geophysical Research*, *62*(2), 221–228. https://doi.org/10.1029/JZ062i002p00221
Reich, P. B. (1987). Quantifying plant response to ozone: A unifying theory. *Tree Physiology*, *3*(1), 63–91.
Remde, A., Ludwig, J., Meixner, F. X., & Conrad, R. (1993). A study to explain the emission of nitric oxide from a marsh soil. *Journal of Atmospheric Chemistry*, *17*, 249–275.
Rich, S. (1964). Ozone damage to plants. *Annual Review of Phytopathology*, *2*, 253–266.
Rich, S., Waggoner, P. E., & Tomlinson, H. (1970). Ozone update by bean leaves. *Science*, *169*(3940), 79–80. https://doi.org/10.1126/science.169.3940.79
Rischbieter, E., Stein, H., & Schumpe, A. (2000). Ozone solubilities in water and aqueous salt solutions. *Journal of Chemical and Engineering Data*, *45*(2), 338–340.
Rondón, A. (1993). Atmosphere-surface exchange of nitrogen oxides and ozone (Doctoral dissertation. Stockholm, Sweden: Stockholm University.
Rondón, A., Johansson, C., & Granat, L. (1993). Dry deposition of nitrogen dioxide and ozone to coniferous forests. *Journal of Geophysical Research*, *98*(D3), 5159–5172. https://doi.org/10.1029/92JD02335
Ro-Poulsen, H., Mikkelsen, T. N., Hovamand, M. F., Hummelshøj, P., & Jensen, N. O. (1998). Ozone deposition in relation to canopy physiology in a mixed conifer forest in Denmark. *Chemosphere*, *36*(4-5), 669–674.
Rummel, U., Ammann, C., Gut, A., Meixner, F. X., & Andreae, M. O. (2002). Eddy covariance measurements of nitric oxide flux within an Amazonian rain forest. *Journal of Geophysical Research*, *107*(D20), 8050. https://doi.org/10.1029/2001JD000520
Rummel, U., Ammann, C., Kirkman, G. A., Moura, M. A. L., Foken, T., Andreae, M. O., & Meixner, F. X. (2007). Seasonal variation of ozone deposition to a tropical rain forest in southwest Amazonia. *Atmospheric Chemistry and Physics*, *7*(20), 5415–5435. https://doi.org/10.5194/acp-7-5415-2007
Rydsaa, J. H., Stordal, F., Gerosa, G., Finco, A., & Hodnebrog, Ø. (2016). Evaluating stomatal ozone fluxes in WRF-Chem: Comparing ozone uptake in Mediterranean ecosystems. *Atmospheric Environment*, *143*, 237–248.
Sadiq, M., Tai, A. P. K., Lombardozzi, D., & Val Martin, M. (2017). Effects of ozone-vegetation coupling on surface ozone air quality via biogeochemical and meteorological feedbacks. *Atmospheric Chemistry and Physics*, *17*(4), 3055–3066. https://doi.org/10.5194/acp-17-3055-2017
Sæbø, A., Popek, R., Nawrot, B., Hanslin, H. M., Gawronska, H., & Gawronski, S. W. (2012). Plant species differences in particulate matter accumulation on leaf surfaces. *The Science of the Total Environment*. https://doi.org/10.1016/j.scitotenv.2012.03.084
Sánchez, M. L., Rodríguez, R., & López, A. (1997). Ozone dry deposition in a semi-arid steppe and in a coniferous forest in Southern Europe. *Journal of the Air & Waste Management Association*, *47*(7), 792–799. https://doi.org/10.1080/10473289.1997.10463939
Sander, R. (1999). Modeling atmospheric chemistry: Interactions between gas-phase species and liquid phase cloud/aerosol particles. *Surveys in Geophysics*, *20*, 2–31.
Sander, R. (2015). Compilation of Henry's law constants (version 4.0) for water as solvent. *Atmospheric Chemistry and Physics*, *15*(8), 4399–4981. https://doi.org/10.5194/acp-15-4399-2015
Savi, F., & Fares, S. (2014). Ozone dynamics in a Mediterranean Holm oak forest: Comparison among transition periods characterized by different amounts of precipitation. *Annals of Silvicultural Research*, *38*(1), 1–6.
Schobesberger, S., Lopez-Hilfiker, F. D., Taipale, D., Millet, D. B., D'Ambro, E. L., Rantala, P., et al. (2016). High upward fluxes of formic acid from a boreal forest canopy. *Geophysical Research Letters*, *43*(17), 9342–9351. https://doi.org/10.1002/2016GL069599
Schuepp, P. H. (1993). Tansley Review No. 69. Leaf boundary layers. *New Phytologist*, *125*(3), 477–507.
Schwede, D., Zhang, L., Vet, R., & Lear, G. (2011). An intercomparison of the deposition models used in the CASTNET and CAPMoN networks. *Atmospheric Environment*, *45*(6), 1337–1346. https://doi.org/10.1016/j.atmosenv.2010.11.050
Schwede, D. B., Leduc, S. K., & Otte, T. L. (2001). Using meteorological model output as a surrogate for on-site observations to predict deposition velocity. *Water, Air, & Soil Pollution: Focus*, *1*, 59–66.
Seinfeld, J. H., & Pandis, S. N. (2006). *Atmospheric chemistry and physics*. Hoboken, NJ: Wiley.
Seok, B., Helmig, D., Liptzin, D., Williams, M. W., & Vogel, C. S. (2015). Snowpack-atmosphere gas exchanges of carbon dioxide, ozone, and nitrogen oxides at a hardwood forest site in northern Michigan. *Elementa-Science of the Anthropocene*, *3*, 1–20. https://doi.org/10.12952/journal.elementa.000040
Shen, J., & Gao, Z. (2018). Ozone removal on building material surface: A literature review. *Building and Environment*. https://doi.org/10.1016/j.buildenv.2018.02.046
Shu, Y., & Atkinson, R. (1994). Rate constants for the gas-phase reactions of $O_3$ with a series of terpenes and OH radical formation from the $O_3$ reactions with sesquiterpenes at 296 $\pm$ 2 K. *International Journal of Chemical Kinetics*, *26*, 1192–1205.
Silva, S., & Heald, C. (2018). Investigating dry deposition of ozone to vegetation. *Journal of Geophysical Research-Atmospheres*, *123*, 559–573. https://doi.org/10.1002/2017JD027278
Silva, S. J., Heald, C. L., Ravela, S., Mammarella, I., & Munger, J. W. (2019). A deep learning parameterization for ozone dry deposition velocities. *Geophysical Research Letters*, *46*(2), 983–989. https://doi.org/10.1029/2018GL081049
Simpson, D., Tuovinen, J. P., Emberson, L., & Ashmore, M. R. (2001). Characteristics of an ozone deposition module. *Water, Air, & Soil Pollution: Focus*, *1*(5-6), 253–262.
Simpson, D., Tuovinen, J. P., Emberson, L., & Ashmore, M. R. (2003). Characteristics of an ozone deposition module II: Sensitivity analysis. *Water, Air, and Soil Pollution*, *143*(1-4), 123–137.
Sitch, S., Cox, P. M., Collins, W. J., & Huntingford, C. (2007). Indirect radiative forcing of climate change through ozone effects on the land-carbon sink. *Nature*. https://doi.org/10.1038/nature06059
Solberg, S., Hov, Ø., Søvdee, A., Isaksen, I. S. A., Coddevillee, P., De Backer, H., et al. (2008). European surface ozone in the extreme summer 2003. *Journal of Geophysical Research*, *113*, D07307. https://doi.org/10.1029/2007JD009098
Sorimachi, A., & Sakamoto, K. (2007). Laboratory measurement of dry deposition of ozone onto northern Chinese soil samples. In P. Brimblecombe, H. Hara, D. Houle, & M. Novak (Eds.), *Acid rain—Deposition to recovery* (pp. 181–186). Dordrecht: Springer. https://doi.org/10.1007/978-1-4020-5885-1_20
Sorimachi, A., Sakamoto, K., Ishihara, H., Fukuyama, T., Utiyama, M., Liu, H., et al. (2003). Measurements of sulfur dioxide and ozone dry deposition over short vegetation in northern China—A preliminary study. *Atmospheric Environment*, *37*(22), 3157–3166. https://doi.org/10.1016/S1352-2310(03)00180-8
Sperry, J. S., Venturas, M. D., Anderegg, W. R., Mencuccini, M., Mackay, D. S., Wang, Y., & Love, D. M. (2017). Predicting stomatal responses to the environment from the optimization of photosynthetic gain and hydraulic cost. *Plant, Cell & Environment*, *40*(6), 816–830.

Stedman, D. H., Daby, E., Stuhl, F., & Niki, H. (1972). Analysis of ozone and nitric oxide by a chemiluminescent method. *Journal of the Air Pollution Control Association*, *22*, 260–263.

Steiner, A. L., Pressley, S. N., Botros, A., Jones, E., Chung, S. H., & Edburg, S. L. (2011). Analysis of coherent structures and atmosphere-canopy coupling strength during the CABINEX field campaign. *Atmospheric Chemistry and Physics*, *11*, 11,921–11,936. https://doi.org/10.5194/acp-11-11921-2011

Stella, P., Loubet, B., de Berranger, C., Charrier, X., Ceschia, E., Gerosa, G., et al. (2019). Soil ozone deposition: Dependence of soil resistance to soil texture. *Atmospheric Environment*, *119*, 202–209. https://doi.org/10.1016/j.atmosenv.2018.11.036

Stella, P., Loubet, B., Lamaud, E., Laville, P., & Cellier, P. (2011). Ozone deposition onto bare soil: A new parameterisation. *Agricultural and Forest Meteorology*, *151*(6), 669–681. https://doi.org/10.1016/j.agrformet.2011.01.015

Stella, P., Loubet, B., Laville, P., Lamaud, E., Cazaunau, M., Laufs, S., et al. (2012). Comparison of methods for the determination of NO-$O_3$-$NO_2$ fluxes and chemical interactions over a bare soil. *Atmospheric Measurement Techniques*, *5*(6), 1241–1257.

Stella, P., Personne, E., Lamaud, E., Loubet, B., Trebs, I., & Cellier, P. (2013). Assessment of the total, stomatal, cuticular, and soil 2 year ozone budgets of an agricultural field with winter wheat and maize crops. *Journal of Geophysical Research: Biogeosciences*, *118*, 1120–1132. https://doi.org/10.1002/jgrg.20094

Stella, P., Personne, E., Loubet, B., Lamaud, E., Ceschia, E., Béziat, P., et al. (2011). Predicting and partitioning ozone fluxes to maize crops from sowing to harvest: The Surfatm-$O_3$ model. *Biogeosciences*, *8*(10), 2869–2886. https://doi.org/10.5194/bg-8-2869-2011

Stevenson, D. S., Dentener, F. J., Schultz, M. G., Ellingsen, K., van Noije, T. P. C., Wild, O., et al. (2006). Multimodel ensemble simulations of present-day and near-future tropospheric ozone. *Journal of Geophysical Research*, *111*, D08301. https://doi.org/10.1029/2005JD006338

Stocker, D. W., Stedman, D. H., Zeller, K. F., Massman, W. J., & Fox, D. G. (1993). Fluxes of nitrogen oxides and ozone measured by eddy correlation over a shortgrass prairie. *Journal of Geophysical Research*, *98*(D7), 12,619–12,630. https://doi.org/10.1029/93JD00871

Stocker, D. W., Zeller, K. F., & Stedman, D. H. (1995). $O_3$ and $NO_2$ fluxes over snow measured by eddy-correlation. *Atmospheric Environment*, *29*, 1299–1305.

Stokes, V. J., Morecroft, M. D., & Morison, J. I. L. (2006). Boundary layer conductance for contrasting leaf shapes in a deciduous broad-leaved forest canopy. *Agricultural and Forest Meteorology*, *139*, 40–54.

Stoy, P. C., El-Madany, T., Fisher, J. B., Gentine, P., Gerken, T., Good, S. P., et al. (2019). Reviews and syntheses: Turning the challenges of partitioning ecosystem evaporation and transpiration into opportunities. *Biogeosciences*, *16*(19), 3747–3775. https://doi.org/10.5194/bg-16-3747-2019

Stroud, C., Makar, P., Karl, T., Guenther, A., Geron, C., Turnipseed, A., et al. (2005). Role of canopy-scale photochemistry in modifying biogenic-atmosphere exchange of reactive terpene species: Results from the CELTIC field study. *Journal of Geophysical Research*, *110*, D17303. https://doi.org/10.1029/2005JD005775

Stull, R. B. (1988). *An introduction to boundary layer meteorology*. Netherlands: Springer.

Subke, J.-A., Toet, S., D'Haese, D., Crossman, Z., Emberson, L. D., Barnes, J. D., et al. (2009). A new method using $^{18}O$ to trace ozone deposition. *Rapid Communications in Mass Spectrometry*, *23*(7), 980–984. https://doi.org/10.1002/rcm.3961

Sun, G., McLaughlin, S. B., Porter, J. H., Uddling, J., Mulholland, P. J., Adams, M. B., & Pederson, N. (2012). Interactive influences of ozone and climate on streamflow of forested watersheds. *Global Change Biology*, *18*(11), 3395–3409. https://doi.org/10.1111/j.1365-2486.2012.02787.x

Sun, S., Moravek, A., Trebs, I., Kesselmeier, J., & Sörgel, M. (2016). Investigation of the influence of liquid surface films on $O_3$ and PAN deposition to plant leaves coated with organic/inorganic solution. *Journal of Geophysical Research: Atmospheres*, *121*, 14,239–14,256. https://doi.org/10.1002/2016JD025519

Sun, S., Moravek, A., von der Heyden, L., Held, A., Sörgel, M., & Kesselmeier, J. (2016). Twin-cuvette measurement technique for investigation of dry deposition of $O_3$ and PAN to plant leaves under controlled humidity conditions. *Atmospheric Measurement Techniques*, *9*(2), 599–617. https://doi.org/10.5194/amt-9-599-2016

Super, I., Vilá-Guerau de Arellano, J., & Krol, M. C. (2015). Cumulative ozone effect on canopy stomatal resistance and the impact on boundary layer dynamics and $CO_2$ assimilation at the diurnal scale: A case study for grassland in the Netherlands. *Journal of Geophysical Research: Biogeosciences*, *120*, 1348–1365. https://doi.org/10.1002/2015JG002996

Tang, W., Cohan, D. S., Morris, G. A., Byun, D. W., & Luke, W. T. (2011). Influence of vertical mixing uncertainties on ozone simulation in CMAQ. *Atmospheric Environment*, *45*(17), 2898–2909. https://doi.org/10.1016/j.atmosenv.2011.01.057

Tao, F., Feng, Z., Tang, H., Chen, Y., & Kobayashi, K. (2017). Effects of climate change, $CO_2$ and $O_3$ on wheat productivity in Eastern China, singly and in combination. *Atmospheric Environment*, *153*, 182–193.

Thom, A. S. (1975). Momentum, mass, and heat exchange of plant communities. In J. L. Monteith (Ed.), *Vegetation and the atmosphere* (pp. 57–109). London: Academic Press.

Thomas, C., & Foken, T. (2007). Flux contribution of coherent structures and its implications for the exchange of energy and matter in a tall spruce canopy. *Boundary-Layer Meteorology*, *123*(2), 317–337.

Thomas, J. L., Stutz, J., Lefer, B., Huey, L. G., Toyota, K., Dibb, J. E., & von Glasow, R. (2011). Modeling chemistry in and above snow at Summit, Greenland - Part 1: Model description and results. *Atmospheric Chemistry and Physics*, *11*(10), 4899–4914. https://doi.org/10.5194/acp-11-4899-2011

Toet, S., Subke, J.-A., D'Haese, D., Ashmore, M. R., Emberson, L. D., Crossman, Z., et al. (2009). A new stable isotope approach identifies the fate of ozone in plant-soil systems. *New Phytologist*, *182*, 85–90.

Tong, L., Wang, X., Geng, C., Wang, W., Lu, F., Song, W., et al. (2011). Diurnal and phenological variations of $O_3$ and $CO_2$ fluxes of rice canopy exposed to different $O_3$ concentrations. *Atmospheric Environment*, *45*(31), 5621–5631. https://doi.org/10.1016/j.atmosenv.2011.03.070

Torsethaugen, G., Pell, E., & Assmann, S. (1999). Ozone inhibits guard cell K+ channels implicated in stomatal opening. *Proceedings of the National Academy of Sciences*, *96*(23), 13,577–13,582. https://doi.org/10.1073/pnas.96.23.13577

Toyota, K., Dastoor, A. P., & Ryzhkov, A. (2016). Parameterization of gaseous dry deposition in atmospheric chemistry models: Sensitivity to aerodynamic resistance formulations under statically stable conditions. *Atmospheric Environment*, *147*, 409–422. https://doi.org/10.1016/j.atmosenv.2016.09.055

Travis, K. R., & Jacob, D. J. (2019). Systematic bias in evaluating chemical transport models with maximum daily 8 h average (MDA8) surface ozone for air quality applications: A case study with GEOS-Chem v9.02. *Geoscientific Model Development*, *12*(8), 3641–3648. https://doi.org/10.5194/gmd-12-3641-2019

Tuovinen, J.-P., Ashmore, M. R., Emberson, L. D., & Simpson, D. (2004). Testing and improving the EMEP ozone deposition module. *Atmospheric Environment*, *38*(15), 2373–2385.

Tuovinen, J.-P., Aurela, M., & Laurila, T. (1998). Resistances to ozone deposition to a flark fen in the Northern Aapa Mire Zone. *Journal of Geophysical Research*, *103*(D14), 16,953–16,966. https://doi.org/10.1029/98JD01165

Tuovinen, J.-P., Emberson, L., & Simpson, D. (2009). Modelling ozone fluxes to forests for risk assessment: Status and prospects. *Annals of Forest Science*, *66*(4), 401. https://doi.org/10.1051/forest/2009024

Tuovinen, J.-P., Simpson, D., Mikkelsen, T. N., Emberson, L. D., Ashmore, M. R., Aurela, M., et al. (2001). Comparisons of measured and modelled ozone deposition to forests in Northern Europe. *Water, Air, & Soil Pollution: Focus*, *1*(5/6), 263–274. https://doi.org/10.1023/A:1013131927678

Turner, N. C., Rich, S., & Waggoner, P. E. (1973). Removal of ozone by soil. *Journal of Environmental Quality*, *2*(2), 259–263.

Turner, N. C., Waggoner, P. E., & Rich, S. (1974). Removal of ozone from the atmosphere by soil and vegetation. *Nature*, *250*, 486–489.

Turnipseed, A. A., Burns, S. P., Moore, D. J., Hu, J., Guenther, A. B., & Monson, R. K. (2009). Controls over ozone deposition to a high elevation subalpine forest. *Agricultural and Forest Meteorology*, *149*(9), 1447–1459. https://doi.org/10.1016/j.agrformet.2009.04.001

Turnipseed, A. A., Huey, L. G., Nemitz, E., Stickel, R., Higgs, J., Tanner, D. J., et al. (2006). Eddy covariance fluxes of peroxyacetyl nitrates (PANs) and $NO_y$ to a coniferous forest. *Journal of Geophysical Research*, *111*, D09304. https://doi.org/10.1029/2005JD006631

Tuzet, A., Perrier, A., Loubet, B., & Cellier, P. (2011). Modeling ozone deposition fluxes: The relative roles of deposition and detoxification processes. *Agricultural and Forest Meteorology*, *151*(4), 480–492. https://doi.org/10.1016/j.agrformet.2010.12.004

U.S. Environmental Protection Agency (EPA). (2006). Air quality criteria for ozone and related photochemical oxidants, Vol. 1.

Uddling, J., Matyssek, R., Pettersson, J. B. C., & Wieser, G. (2012). To what extent do molecular collisions arising from water vapour efflux impede stomatal $O_3$ influx? *Environmental Pollution*, *170*, 39–42.

Unsworth, M., Heagle, A., & Heck, W. (1984). Gas exchange in open-top field chambers—I. Measurement and analysis of atmospheric resistances to gas exchange. *Atmospheric Environment*, *18*, 373–380.

Val Martin, M., Heald, C. L., & Arnold, S. R. (2014). Coupling dry deposition to vegetation phenology in the Community Earth System Model: Implications for the simulation of surface $O_3$. *Geophysical Research Letters*, *41*(8), 2988–2996. https://doi.org/10.1002/2014GL059651

Van Aalst, R. M. (1982). Air pollution by nitrogen oxides dry deposition of $NO_x$. *Studies in Environmental Science*. https://doi.org/10.1016/B978-0-444-42127-2.50028-2

Van Dam, B., Helmig, D., Doskey, P. V., & Oltmans, S. J. (2016). Summertime surface $O_3$ behavior and deposition to tundra in the Alaskan Arctic. *Journal of Geophysical Research: Atmospheres*, *121*, 8055–8066. https://doi.org/10.1002/2015JD023914

Van Dam, B., Helmig, D., Honrath, R., Hueber, J., Seok, B., Toro, C., et al. (2010). Exchange of ozone at the atmosphere-snowpack interface at Summit, Greenland. 2010 State of the Arctic Meeting, 16-19 March, Miami, Florida, Poster Presentation.

Van Dam, B., Helmig, D., Toro, C., Doskey, P., Kramer, L., Murray, K., et al. (2015). Dynamics of ozone and nitrogen oxides at Summit, Greenland: I. Multi-year observations in the snowpack. *Atmospheric Environment*, *123*, 268–284. http://doi.org/10.1016/j.atmosenv.2015.09.060

Van Pul, W. A. J., & Jacobs, A. F. G. (1994). The conductance of a maize crop and the underlying soil to ozone under various environmental conditions. *Boundary-Layer Meteorology*, *69*(1-2), 83–99.

Vautard, R., Honore, C., Beekmann, M., & Rouil, L. (2005). Simulation of ozone during the August 2003 heat wave and emission control scenarios. *Atmospheric Environment*, *39*(16), 2957–2967.

Verhoef, A., & Egea, G. (2014). Modeling plant transpiration under limited soil water: Comparison of different plant and soil hydraulic parameterizations and preliminary implications for their use in land surface models. *Agricultural and Forest Meteorology*, *191*, 22–32. http://doi.org/10.1016/j.agrformet.2014.02.009

Vieno, M., Dore, A. J., Stevenson, D. S., Doherty, R., Heal, M. R., Reis, S., et al. (2010). Modelling surface ozone during the 2003 heat-wave in the UK. *Atmospheric Chemistry and Physics*, *10*(16), 7963–7978. https://doi.org/10.5194/acp-10-7963-2010

Vilá-Guerau de Arellano, J. (2003). Bridging the gap between atmospheric physics and chemistry in studies of small-scale turbulence. *Bulletin of the American Meteorological Society*, 51–56.

Vilá-Guerau de Arellano, J., & Duynkerke, P. G. (1992). Influence of chemistry on the flux-gradient relationships for the $NO_2$-$O_3$-NO system. *Boundary-Layer Meteorology*, *61*, 375–387.

Vilá-Guerau de Arellano, J., Duynkerke, P. G., & Builtjes, P. J. H. (1993). The divergence of the turbulent diffusion flux in the surface layer due to chemical reactions: The NO-$O_3$-$NO_2$ system. *Tellus Series B: Chemical and Physical Meteorology*, *45*(1), 23–33. https://doi.org/10.3402/tellusb.v45i1.15576

Vitale, M., Gerosa, G., Ballarin-Denti, A., & Manes, F. (2005). Ozone uptake by an evergreen Mediterranean forest (*Quercus ilex L.*) in Italy—Part II: Flux modelling. Upscaling leaf to canopy ozone uptake by a process-based model. *Atmospheric Environment*, *39*(18), 3267–3278.

Vuolo, R. M., Loubet, B., Mascher, N., Gueudet, J. C., Durand, B., Laville, P., et al. (2017). Nitrogen oxides and ozone fluxes from an oilseed-rape management cycle: The influence of cattle slurry application. *Biogeosciences*, *14*(8), 2225–2244. https://doi.org/10.5194/bg-14-2225-2017

Walker, T. W. (2014). Applications of adjoint modelling in chemical composition: Studies of tropospheric ozone at middle and high northern latitudes (Doctoral dissertation). Retrieved from University of Toronto. (https://tspace.library.utoronto.ca). Toronto, Canada: University of Toronto.

Walton, S., Gallagher, M. W., Choularton, T. W., & Duyzer, J. (1997). Ozone and $NO_2$ exchange to fruit orchards. *Atmospheric Environment*, *31*(17), 2767–2776.

Walton, S., Gallagher, M. W., & Duyzer, J. H. (1997). Use of a detailed model to study the exchange of $NO_x$ and $O_3$ above and below a deciduous canopy. *Atmospheric Environment*, *31*(18), 2915–2931.

Wang, D., Hinckley, T. M., Cumming, A. B., & Braatne, J. (1995). A comparison of measured and modeled ozone uptake into plant leaves. *Environmental Pollution*, *89*(3), 347–254.

Warrick, A. W., & Nielsen, D. R. (1980). Spatial variability of soil physical properties in the field. In D. Hillel (Ed.), *Applications of soil physics* (pp. 319–344). New York: Academic Press.

Wehr, R., Commane, R., Munger, J. W., McManus, J. B., Nelson, D. D., Zahniser, M. S., et al. (2017). Dynamics of canopy stomatal conductance, transpiration, and evaporation in a temperate deciduous forest, validated by carbonyl sulfide uptake. *Biogeosciences*, *14*(2), 389–401. https://doi.org/10.5194/bg-14-389-2017

Wehr, R., Munger, J. W., McManus, J. B., Nelson, D. D., Zahniser, M. S., Davidson, E. A., et al. (2016). Seasonality of temperate forest photosynthesis and daytime respiration. *Nature*, *534*, 680–683.

Wehr, R., & Saleska, S. R. (2015). An improved isotopic method for partitioning net ecosystem-atmosphere $CO_2$ exchange. *Agricultural and Forest Meteorology*, *214-215*, 515–531. https://doi.org/10.1016/j.agrformet.2015.09.009

Weinheimer, A. J. (2006). Chemical methods: Chemiluminescence, chemical amplification, electrochemistry, and derivatization. In D. E. Heard (Ed.), *Analytical Techniques for Atmospheric Measurement* (pp. 311–354). Oxford, UK: Blackwell Publishing Ltd.

Wesely, M. L. (1989). Parameterization of surface resistances to gaseous dry deposition in regional-scale numerical models. *Atmospheric Environment*, *23*(6), 1293–1304.

Wesely, M. L., Cook, D. R., & Williams, R. M. (1981). Field measurements of small ozone fluxes to snow, wet bare soil, and lake water. *Boundary-Layer Meteorology*, *20*, 459–471.

Wesely, M. L., Eastman, J. A., Cook, D. R., & Hicks, B. B. (1978). Daytime variations of ozone eddy fluxes to maize. *Boundary-Layer Meteorology*, *15*(3), 361–373. https://doi.org/10.1007/bf02652608

Wesely, M. L., & Hicks, B. B. (1977). Some factors that affect the deposition rates of sulfur dioxide and similar gases on vegetation. *Journal of the Air Pollution Control Association*, *27*(11), 1110–1116.

Wesely, M. L., & Hicks, B. B. (2000). A review of the current status of knowledge on dry deposition. *Atmospheric Environment*, *34*, 2261–2282.

Whelan, M. E., Lennartz, S. T., Gimeno, T. E., Wehr, R., Wohlfahrt, G., Wang, Y., et al. (2018). Reviews and syntheses: Carbonyl sulfide as a multi-scale tracer for carbon and water cycles. *Biogeosciences*, *15*(12), 3625–3657. https://doi.org/10.5194/bg-15-3625-2018

Wieser, G., Luis, V. C., & Cuevas, E. (2006). Quantification of ozone uptake at the stand level in a Pinus canariensis forest in Tenerife, Canary Islands: An approach based on sap flow measurements. *Environmental Pollution*, *140*(3), 383–386. https://doi.org/10.1016/j.envpol.2005.12.003

Wieser, G., Matyssek, R., Götz, B., & Grünhage, L. (2012). Branch cuvettes as means of ozone risk assessment in adult forest tree crowns: Combining experimental and modelling capacities. *Trees*, *26*(6), 1703–1712.

Wieser, G., Matyssek, R., Köstner, B., & Oberhuber, W. (2003). Quantifying ozone uptake at the canopy level of spruce, pine and larch trees at the alpine timberline: An approach based on sap flow measurement. *Environmental Pollution*, *126*, 5–8.

Wild, O. (2007). Modelling the tropospheric ozone budget: Exploring the variability in current models. *Atmospheric Chemistry and Physics*, *7*, 2643–2660.

Wilson, K. B., & Baldocchi, D. D. (2000). Seasonal and interannual variability of energy fluxes over a broadleaved temperate deciduous forest in North America. *Agricultural and Forest Meteorology*, *100*, 1–18.

Wofsy, S., Goulden, M., Munger, J. W., Fan, S., Bakwin, P., Daube, B., et al. (1993). Net exchange of $CO_2$ in a mid-latitude forest. *Science*, *260*, 1314–1317.

Wohlfahrt, G., Haslwanter, A., Hörtnagl, L., Jasoni, R. L., Fenstermaker, L. F., Arnone, J. A. III, & Hammerle, A. (2009). On the consequences of the energy imbalance for calculating surface conductance to water vapor. *Agricultural and Forest Meteorology*, *149*(9), 1556–1559. https://doi.org/10.1016/j.agrformet.2009.03.015

Wohlfahrt, G., Hörtnagl, L., Hammerle, A., Graus, M., & Hansel, A. (2009). Measuring eddy covariance fluxes of ozone with a slow-response analyser. *Atmospheric Environment*, *43*(30), 4570–4576. https://doi.org/10.1016/j.atmosenv.2009.06.031

Wolf, A., Anderegg, W. R., & Pacala, S. W. (2016). Optimal stomatal behavior with competition for water and risk of hydraulic impairment. *Proceedings of the National Academy of Sciences*, *113*(46), E7222–E7230.

Wolfe, G. M., Hanisco, T. F., Arkinson, H. L., Bui, T. P., Crounse, J. D., Dean-Day, J., et al. (2015). Quantifying sources and sinks of reactive gases in the lower atmosphere using airborne flux observations. *Geophysical Research Letters*, *42*, 8231–8240. https://doi.org/10.1002/2015GL065839

Wolfe, G. M., & Thornton, J. A. (2011). The Chemistry of Atmosphere-Forest Exchange (CAFE) Model—Part 1: Model description and characterization. *Atmospheric Chemistry and Physics*, *11*, 77–101.

Wolfe, G. M., Thornton, J. A., McKay, M., & Goldstein, A. H. (2011). Forest-atmosphere exchange of ozone: Sensitivity to very reactive biogenic VOC emissions and implications for in-canopy photochemistry. *Atmospheric Chemistry and Physics*, *11*(15), 7875–7891. https://doi.org/10.5194/acp-11-7875-2011

Wolfe, G. M., Thornton, J. A., Yatavelli, R. L. N., McKay, M., Goldstein, A. H., LaFranchi, B., et al. (2009). Eddy covariance fluxes of acyl peroxy nitrates (PAN, PPN and MPAN) above a Ponderosa pine forest. *Atmospheric Chemistry and Physics*, *9*(2), 615–634. https://doi.org/10.5194/acp-9-615-2009

Wong, A. Y. H., Geddes, J. A., Tai, A. P. K., & Silva, S. J. (2019). Importance of dry deposition parameterization choice in global simulations of surface ozone. *Atmospheric Chemistry and Physics*, *19*(22), 14,365–14,385. https://doi.org/10.5194/acp-19-14365-2019

Wong, S. C., Cowan, I. R., & Farquhar, G. D. (1979). Stomatal conductance correlates with photosynthetic capacity. *Nature*, *282*, 424–426.

Wu, Y., Brashers, B., Finkelstein, P. L., & Pleim, J. E. (2003). A multilayer biochemical dry deposition model 2. Model evaluation. *Journal of Geophysical Research*, *108*(D1), 4014. https://doi.org/10.1029/2002JD002306

Wu, Z., Schwede, D. B., Vet, R., Walker, J. T., Shaw, M., Staebler, R., & Zhang, L. (2018). Evaluation and intercomparison of five North American dry deposition algorithms at a mixed forest site. *Journal of Advances in Modeling Earth Systems*, *10*(7), 1571–1586. https://doi.org/10.1029/2017MS001231

Wu, Z., Staebler, R., Vet, R., & Zhang, L. (2016). Dry deposition of $O_3$ and $SO_2$ estimated from gradient measurements above a temperate mixed forest. *Environmental Pollution*, *210*, 202–210. https://doi.org/10.1016/j.envpol.2015.11.052

Wu, Z., Wang, X., Chen, F., Turnipseed, A. A., Guenther, A. B., Niyogi, D., et al. (2011). Evaluating the calculated dry deposition velocities of reactive nitrogen oxides and ozone from two community models over a temperate deciduous forest. *Atmospheric Environment*, *45*(16), 2663–2674. https://doi.org/10.1016/j.atmosenv.2011.02.063

Wu, Z. Y., Zhang, L., Wang, X. M., & Munger, J. W. (2015). A modified micrometeorological gradient method for estimating $O_3$ dry depositions over a forest canopy. *Atmospheric Chemistry and Physics*. https://doi.org/10.5194/acp-15-7487-2015

Xu, X., Zhang, Z., Bao, L., Mo, L., Yu, X., Fan, D., & Lun, X. (2017). Influence of rainfall duration and intensity on particulate matter removal from plant leaves. *Science of the Total Environment*, *609*, 11–16.

Yeats, T. H., & Rose, J. K. (2013). The formation and function of plant cuticles. *Plant Physiology*, *163*(1), 5–20.

Yee, L. D., Isaacman-VanWertz, G., Wernis, R. A., Meng, M., Rivera, V., Kreisberg, N. M., et al. (2018). Observations of sesquiterpenes and their oxidation products in central Amazonia during the wet and dry seasons. *Atmospheric Chemistry and Physics*, *18*(14), 10,433–10,457. https://doi.org/10.5194/acp-18-10433-2018

Young, P. J., Archibald, A. T., Bowman, K. W., Lamarque, J.-F., Naik, V., Stevenson, D. S., et al. (2013). Pre-industrial to end 21$^{st}$ century projections of tropospheric ozone from the Atmospheric Chemistry and Climate Model Intercomparison Project (ACCMIP). *Atmospheric Chemistry and Physics*, *13*(4), 2063–2090. https://doi.org/10.5194/acp-13-2063-2013

Young, P. J., Naik, V., Fiore, A. M., Gaudel, A., Guo, J., Lin, M. L., et al. (2018). Tropospheric Ozone Assessment Report: Assessment of global-scale model performance for global and regional ozone distributions, variability, and trends. *Elementa: Science of the Anthropocene*, *6*(1), 10. https://doi.org/10.1525/elementa.265

Yue, X., & Unger, N. (2014). Ozone vegetation damage effects on gross primary productivity in the United States. *Atmospheric Chemistry and Physics*, *14*(17), 9137–9153. https://doi.org/10.5194/acp-14-9137-2014

Zahn, A., Weppner, J., Widmann, H., Schlote-Holubek, K., Burger, B., Kuehner, T., & Franke, H. (2012). A fast and precise chemiluminescence ozone detector for eddy flux and airborne application. *Atmospheric Measurement Techniques*, *5*(2), 363–375.

Zapletal, M., Cudlín, P., Chroust, P., Urban, O., Pokorný, R., Edwards-Jonášová, M., et al. (2011). Ozone flux over a Norway spruce forest and correlation with net ecosystem production. *Environmental Pollution*, *159*(5), 1024–1034. https://doi.org/10.1016/j.envpol.2010.11.037

Zeller, K. (2000). Wintertime ozone fluxes and profiles above a subalpine spruce–fir forest. *Journal of Applied Meteorology*, *39*(1), 92–101.

Zeller, K., & Hehn, T. (1995). Ozone deposition in a snow-covered subalpine spruce-fir forest environment. In *Biogeochemistry of seasonally snow-covered catchments*, *International Association of Hydrological Sciences Publication No*, (Vol. 228, pp. 17–22). Boulder, CO.

Zeller, K., & Hehn, T. (1996). Measurements of upward turbulent ozone fluxes above a subalpine spruce-fir forest. *Geophysical Research Letters*, *23*(8), 841–844. https://doi.org/10.1029/96GL00786

Zeller, K. F., & Nikolov, N. T. (2000). Quantifying simultaneous fluxes of ozone, carbon dioxide and water vapor above a subalpine forest ecosystem. *Environmental Pollution*, *107*, 1–20.

Zenone, T., Hendriks, C., Brilli, F., Fransen, E., Gioli, B., Portillo-Estrada, M., et al. (2016). Interaction between isoprene and ozone fluxes in a poplar plantation and its impact on air quality at the European level. *Scientific Reports*, *6*(1), 32676. https://doi.org/10.1038/srep32676

Zhang, L., Brook, J. R., & Vet, R. (2002). On ozone dry deposition—With emphasis on non-stomatal uptake and wet canopies. *Atmospheric Environment*, *36*, 4787–4799.

Zhang, L., Brook, J. R., & Vet, R. (2003). A revised parameterization for gaseous dry deposition in air-quality models. *Atmospheric Chemistry and Physics*, *3*(2), 1777–1804. https://doi.org/10.5194/acpd-3-1777-2003

Zhang, L., Brook, J. R., Vet, R., Shaw, M., & Finkelstein, P. L. (2001). Evaluation and improvement of a dry deposition model using $SO_2$ and $O_3$ measurements over a mixed forest. *Water, Air, & Soil Pollution: Focus*, *1*, 67–78.

Zhang, L., Vet, R., Brook, J. R., Legge, A., & H. (2006). Factors affecting stomatal uptake of ozone by different canopies and a comparison between dose and exposure. *Science of the Total Environment*, *370*, 117–132.

Zhang, L., Zhang, Z., Chen, L., & McNulty, S. (2019). An investigation on the leaf accumulation-removal efficiency of atmospheric particulate matter for five urban plant species under different rainfall regimes. *Atmospheric Environment*. https://doi.org/10.1016/j.atmosenv.2019.04.010

Zhang, S., Chen, X., Hara, H., Horie, K., Aoki, M., Matsuda, K., et al. (2005). Diurnal and seasonal variations of the $O_3$ dry deposition velocity on a red pine forest and its relationship with microclimate factors. *Journal of Agricultural Meteorology*, *60*(5), 1053–1056. https://doi.org/10.2480/agrmet.1053

Zhou, P. T., Ganzeveld, L., Rannik, Ü., Zhou, L. X., Gierens, R., Taipale, D., et al. (2017). Simulating ozone dry deposition at a boreal forest with a multi-layer canopy deposition model. *Atmospheric Chemistry and Physics*, *17*, 1361–1379. https://doi.org/10.5194/acp-17-1361-2017

Zhou, S., Duursma, R. A., Medlyn, B. E., Kelly, J. W., & Prentice, I. C. (2013). How should we model plant responses to drought? An analysis of stomatal and non-stomatal responses to water stress. *Agricultural and Forest Meteorology*, *182*, 204–214. https://doi.org/10.1016/j.agrformet.2013.05.009

Zhou, S. S., Tai, A. P., Sun, S., Sadiq, M., Heald, C. L., & Geddes, J. A. (2018). Coupling between surface ozone and leaf area index in a chemical transport model: Strength of feedback and implications for ozone air quality and vegetation health. *Atmospheric Chemistry and Physics*, *18*(19), 14,133–14,148.

Zhu, Z. (2019). Effects of environmental factors on ozone flux over a wheat field modeled with an artificial neural network. *Advances in Meteorology*. https://doi.org/10.1155/2019/1257910

Zhu, Z., Sun, X., Dong, Y., Zhao, F., & Meixner, F. X. (2014). Diurnal variation of ozone flux over corn field in Northwestern Shandong Plain of China. *Science China Earth Sciences*, *57*(3), 503–511.

Zhu, Z., Zhao, F., Voss, L., Xu, L., Sun, X., Yu, G., & Meixner, F. X. (2015). The effects of different calibration and frequency response correction methods on eddy covariance ozone flux measured with a dry chemiluminescence analyzer. *Agricultural and Forest Meteorology*, *213*, 114–125.

Zona, D., Gioli, B., Fares, S., De Groote, T., Pilegaard, K., Ibrom, A., & Ceulemans, R. (2014). Environmental controls on ozone fluxes in a poplar plantation in Western Europe. *Environmental Pollution*, *184*, 201–210.